

Investigation of the role of UBE4B ubiquitin ligase in p53  
regulation in response to DNA damage in ATM-proficient and  
ATM-deficient cells

by

Habib Al Yousef

A thesis submitted in partial fulfillment of the requirements for the degree of

Doctor of Philosophy

Medical Sciences-Laboratory Medicine and Pathology  
University of Alberta

© Habib Al Yousef, 2017

## ABSTRACT

The tumour suppressor protein p53 maintains genomic integrity by coordinating the DNA damage response, which includes growth arrest, DNA damage repair, and apoptotic cell death. p53 is mutated in more than 50% of human cancer, which reflects its importance. The complex mechanism that controls the regulation of p53 remains only partially understood. p53 is mainly regulated by post-translational modifications such as phosphorylation and ubiquitination. Following exposure to DNA-damaging agents, protein kinases such as ATM and ATR activate and stabilize p53 via phosphorylation. In unstressed cells, ubiquitin ligases bind and assist to degrade p53, keeping p53 at the basal level to enable the cell's normal function. The MDM2 ubiquitin ligase represents the most extensively studied negative regulator of p53. Previous studies with unstressed cells have shown that UBE4B, a p53 ubiquitin ligase, is essential for MDM2-mediated p53 polyubiquitination and degradation both *in vitro* and *in vivo*. However, the role of UBE4B in regulating p53 in response to DNA damage remains unknown.

This dissertation hypothesized that ATM or ATR phosphorylates p53, thus affecting its level and disrupting UBE4B-p53 interactions in response to DNA damage. Also, UBE4B constitutes a critical p53 negative regulator in the ATM- or ATR-dependent pathway. To test this hypotheses, the main objectives of this study aimed to (i) determine the levels of UBE4B, MDM2, and p53 following DNA damage; (ii) explore the phosphorylation status of p53 following DNA damage; (iii) examine the interactions of UBE4B and MDM2 with p53; (iv) determine the effects of UBE4B and MDM2 on p53 degradation and (v) analyze the cytoplasmic as well as nuclear localization of p53,

UBE4B, and MDM2. Most experiments involved human cells that express wild-type p53, with a few experiments including p53-null cells.

Non-cancerous ATM-proficient and ATM-deficient EBV-transformed lymphoblastoid cell lines that grow in suspension were employed. In addition, some studies were performed with cancerous (MCF7 and H1299) and non-cancerous (MCF10) cell lines that grow as adherent cultures. Western blot analysis was performed to detect the protein levels and co-immunoprecipitation was utilized to explore the protein-protein interactions. Moreover, DNA extraction and transformation were used to prepare various constructs. Cellular fractionation analysis was utilized to investigate the subcellular localization of proteins and flow cytometric analysis was used to examine cell cycle distributions.

The findings with lymphoblastoid cells suggested that induced UBE4B levels and interactions with p53 are ATM-independent. However, it is unknown whether ATR signalling or some other protein kinase p53 activator may constitute the predominant pathway operating in AT cells. Consistent with previous reports, the data in this study revealed that UBE4B binds to and promotes the degradation of phosphorylated forms of p53, such as Ser15 or Ser392, after exposure to ionizing radiation (IR); furthermore, this investigation found that this downregulation remains independent of MDM2.

In conclusion, these research findings provide new insights into the potential role of UBE4B in p53 regulation via the ATM or ATR pathway following response to DNA damage. Collectively, the data revealed that the pattern of UBE4B induction or its interactions with p53 in ATM positive wild-type cells differs from that in AT cells, supporting the previous studies which reported that UBE4B may negatively regulate

phosphorylated p53 in response to ionizing radiation. Further investigations are needed to explore the role of UBE4B in p53 regulation, especially within various contexts of the DNA damage response. Such studies will assist to better understand the ever-expanding complexity of p53 regulation, which eventually may contribute towards developing novel p53-based therapeutic cancer approaches.

I dedicate this thesis to my beloved wife Amira and lovely children Jinan, Fatimah, Ali and Hussain for their endless love, patience and support during my study. May Allah bless them, grant them his guidance and fulfil their wishes and hopes in their whole lifetime

## ACKNOWLEDGMENT

At this point in time, after all of the highs and lows I have been through during my Ph.D. program, I would like to take a deep breath, rest, and sincerely express my deep gratitude and honour to all of those individuals to whom I am indebted and without whom I could not have accomplished this research.

First of all, I would like to thank my supervisor, Dr. Roger Leng, who always provided me with not only academic knowledge but also assistance, guidance, and support, making it easy for me to overcome all the hurdles I faced during different phases of my research project. He paved the way to my current final success.

Likewise, my committee members, Dr. Michael Weinfeld and Dr. Consolato Sergi, have been extremely supportive. Dr. Weinfeld, besides your precious guidance and advice, I very much appreciated your help when you allowed me to use your laboratory facilities during a stage of my project, which made it easy for me to complete an essential part of my research.

Dr. Sergi, I greatly appreciate your inspiring support and guidance throughout my entire project.

Furthermore, I want to give special gratitude to Dr. Mirzayans from the department of experimental oncology at the University of Alberta for his generous assistance with the EBV-transformed LCLs and his invaluable knowledge during my required course, which enlightened my scientific vision and allowed me to better appreciate our field of study.

Also, I would like to thank my fellows in Dr. Leng's lab, especially Dr. Cheng Du, for his assistance in overcoming some technical difficulties in Co-IP experiments, developing various mutant p53 constructs, and providing me with necessary technical guidance.

Additionally, I would like to express my gratitude to Dr. Benfan Wang for his technical guidance in localization studies and flow cytometric analysis. I also want to provide special thanks to my colleague, Ph.D student Mr. Yasser Abuetabh, for his spiritual support, especially during the last stage of my thesis.

In addition, I want to acknowledge the contributions of Dr. Anne Galloway and Mr. Ray Rowland, lab technicians, at the Cross Cancer Institute, University of Alberta, for their assistance in using the gamma cell irradiator facility during the period of my experiments. Also, I am very thankful to Bonnie Andrais, a lab technician in Razmik's lab, who helped me to maintain a continuous supply of LCL cells.

I must also acknowledge my beloved wife, Amira as well as my four lovely children, Jinan, Fatimah, Ali, and Hussain, who endured all imaginable hardships and showed incredible support and patience without which I would not have been able to continue all the way to the end of this project.

Likewise, I must acknowledge my great parents, my mother Ameena and my father Saleh; Allah bless them and grant them health and wealth. Their faithful prayers were incredibly invaluable and paved the way to my current successes. All the words in this world fail to articulate my gratitude for their constant love and support.

Finally, I would like to thank my sponsor, the Ministry of Higher Education in Saudi Arabia, which granted me a full scholarship and financially supported me during most of my academic studies. In addition, I extend my appreciation to the staff at the Department of Lab Medicine and Pathology at University of Alberta, especially Cheryl Titus, who was always there to promptly answer my administrative inquires and guide me through the process of my research.

## TABLE OF CONTENTS

|   |           |
|---|-----------|
| <b>Introduction</b> .....   | <b>2</b>  |
| p53 Structure.....  | 2         |
| p53 regulation in ATM proficient cells .....  | 5         |
| <i>p53 regulation by ubiquitin ligases</i> .....  | 5         |
| <i>MDM2, a main p53 ubiquitin ligase</i> .....  | 13        |
| <i>ATM-p53-MDM2 model of p53 stabilization</i> .....  | 15        |
| <i>UBE4B, an emerging p53 ubiquitin ligase</i> .....  | 16        |
| <i>p53 dynamics: More complex regulation</i> .....  | 18        |
| <i>Role of WIP1 in negative regulation of p53</i> .....   | 22        |
| <i>Role of p21 in negative regulation of p53</i> .....  | 23        |
| Wild type p53 signalling in ATM-proficient cell lines .....   | 26        |
| <i>Transcriptional activation by wild-type p53</i> .....  | 26        |
| <i>Transcriptional repression by wild-type p53</i> .....  | 27        |
| <i>Protein-protein interactions</i> .....   | 27        |
| <i>The role of p53 in DNA damage Response Network: A History</i> .....  | 27        |
| <i>The role of WIP1 in p53 signalling pathway</i> .....   | 36        |
| <i>The role of p21 in p53 signalling pathway</i> .....  | 38        |
| <i>The relationship between p53 protein level and apoptosis</i> .....   | 39        |
| p53 regulation in ATM-deficient cells.....  | 41        |
| Hypothesis, objectives, and main findings .....   | 43        |
| <b>Materials and Methods</b> .....  | <b>48</b> |
| Cell Cultures .....   | 48        |
| Gamma irradiation treatment.....  | 49        |
| UV light treatment .....  | 49        |
| Protein Analysis.....   | 49        |
| <i>Cell harvesting</i> .....  | 49        |
| <i>Protein Quantification</i> .....   | 50        |
| <i>Sodium Dodecyl Sulphate Poly-acrylamide Gel Electrophoresis (SDS-PAGE) Analysis and Transfer</i> .....           | 50        |
| <i>Western Blot Analysis</i> .....  | 51        |
| Antibodies.....   | 52        |
| Immunoprecipitation Analysis.....   | 53        |
| Cell viability assay .....  | 53        |
| DNA transfection, plasmids, reagents and antibodies.....  | 54        |
| Subcellular fractionation .....   | 54        |
| Densitometry analysis .....   | 54        |
| Flow cytometric analysis .....  | 55        |
| <b>Results</b> .....  | <b>58</b> |
| Characterization of LCL cells: Radiation -induced loss of cell viability in normal and AT lymphoblastoid cells..... | 59        |
| MDM2 and UBE4B are upregulated in response to DNA damage.....   | 62        |

|   |            |
|---|------------|
| p53 phosphorylation at Serine 15 and Serine 392 in LCLs is dose-independent and ATM-independent.....  | 69         |
| UBE4B induction in response to UV light and 5-FU drug is ATM-independent.....   | 82         |
| p53 interacts with MDM2 and UBE4B and its affinity with MDM2 and UBE4B is augmented post-irradiation in ATM deficient-lymphoblastoid cells .....                                  | 94         |
| MCF7 Cells: UBE4B bound p53 at Ser15 and Ser392 phosphorylated residues and interactions between UBE4B and MDM2 was diminished in response to DNA damage.....                     | 101        |
| UBE4B enhances the degradation of phospho-p53 (Serine 15) and phospho-p53 (Serine 392) .....  | 108        |
| Subcellular localization: UBE4B is mainly localized in cytoplasm post-exposure to DNA damage .....  | 110        |
| Cell cycle analysis in wild-type and mutant LCL cells .....   | 113        |
| <b>Discussion .....</b>   | <b>117</b> |
| p53 dynamics in lymphoblastoid cells .....  | 119        |
| ATR signalling might be the predominant pathway in ATM-deficient cells .....  | 119        |
| ATM is not essential for p53 interactions with MDM2 and UBE4B ubiquitin ligases in lymphoblastoid cells.....  | 123        |
| UBE4B, a potential role in regulating p53 at Ser15 and Ser392 in response to DNA damage.....  | 125        |
| Subcellular localization of p53, MDM2 and UBE4B in response to DNA damage: Possible connection with UBE4B role and suggestive of a new insight on p53 trafficking regulation..... | 130        |
| UBE4B role in DNA damage and a suggested model.....   | 134        |
| <b>Future Directions.....</b>   | <b>139</b> |
| Short-term directions.....  | 139        |
| Long-term directions.....   | 140        |
| <b>References .....</b>   | <b>142</b> |

## LIST OF FIGURES

|  |     |
|--|-----|
| Figure 1. Post-translational modifications on p53  | 4   |
| Figure 2. Schematic representation of ubiquitination pathway   | 7   |
| Figure 3. Domains of E3 ligases  | 10  |
| Figure 4. Overview of Lahav's model (2004)   | 21  |
| Figure 5. Communication between p53, p21, p14 <sup>ARF</sup> and MDM2  | 25  |
| Figure 6. Kastan's Model explaining p53 signaling (1993)   | 30  |
| Figure 7. Enoch Norbury model explaining signaling (1995)  | 32  |
| Figure 8. Current knowledge or radiation-induced responses   | 35  |
| Figure 9. Regulation of wild-type p53 proteins   | 45  |
| Figure 10. AT LCLs show normal cell viability  | 61  |
| Figure 11. Induction of ubiquitin ligases (MDM2 and UBE4B) post-irradiation in LCL cells (6 Gy, 2 Gy)                  | 66  |
| Figure 12. Induction of ubiquitin ligases (MDM2 and UBE4B) post-irradiation with 6 Gy in human breast cell lines       | 68  |
| Figure 13. p53 phosphorylation post-irradiation in human breast cell lines   | 70  |
| Figure 14. p53 phosphorylation in LCL cells (6 Gy, 2 Gy)   | 77  |
| Figure 15 A-C. Induction of ATM and ATR post-irradiation (6 Gy) in LCLs  | 79  |
| Figure 15 D-F. Induction of ATM and ATR post irradiation (2 Gy) in LCLs  | 81  |
| Figure 16 A-D. UV dose-dependnent inductions of ubiquitin ligases (MDM2, UBE4B) and Ser15.                             | 87  |
| Figure 16 E,,F. Time-course assay for induction of ubiquitin ligases (MDM2, UBE4B) and Ser15 post-exposure to UV light | 89  |
| Figure 17 A,B. Induction of ubiquitin ligases (MDM2, UBE4B) and Ser15 post-exposure to various doses of 5-FU drug      | 91  |
| Figure 17 C,D. Induction of ubiquitin ligases (MDM2, UBE4B) and Ser15 post-exposure to 5-FU                            | 93  |
| Figure 18A. MDM2 and UBE4B interact with p53 in wild-type LCL cells at 3 h post-irradiation                            | 96  |
| Figure 18B. MDM2 and UBE4B interact with p53 in wild-type LCL cells at 24 h post-irradiation                           | 97  |
| Figure 18C. MDM2 and UBE4B interact with p53 in mutant AT LCL cells at 3 h post-irradiation                            | 98  |
| Figure 18D. MDM2 and UBE4B interact with p53 in mutant cells at 24 h post-irradiation                                  | 99  |
| Figure 18E. MDM2 and UBE4B interact with p53 in mutant VKE AT LCL cells at 3 h post-irradiation                        | 100 |
| Figure 19 A,B. UBE4B binds phosphorylated residues of p53 at Ser15 and Ser392 post-irradiation                         | 103 |
| Figure 19C. UBE4B dissociates from MDM2 post-irradiation   | 104 |
| Figure 20. UBE4B binds phosphorylated residues of p53 at Ser15 and Ser392 post-irradiation                             | 107 |

*Figure 21. Phosphorylated residues of p453 at Ser15 and Ser392 are targets for UBE4B-mediated p53 degradation ----- 109*

*Figure 22. Subcellular localization of ubiquitin ligases in response to DNA damage-- 112*

*Figure 23. Cell cycle analysis in response to ionizing radiation in wild-type Vs. mutant LCLs----- 115*

*Figure 24. Role of UBE4B in regulation of wild-type p53 protein; a proposed model - 135*

## **ABBREVIATIONS**

|        |   |  |
|--------|---|--|
| AMPK   | = | Adenosine monophosphate-activated protein kinase |
| ARF    | = | Alternate reading frame                          |
| ASK-1  | = | Apoptosis signal-regulating kinase 1             |
| ATM    | = | Ataxia telangiectasia mutated                    |
| ATR    | = | Ataxia telangiectasia and RAD3 related           |
| BCL-2  | = | B-cell lymphoma 2                                |
| CARPs  | = | Caspase 8/10- associated RING proteins           |
| CBP    | = | CREB-binding protein                             |
| CDK    | = | Cyclin-dependent kinase                          |
| COP1   | = | Constitutively photomorphogenic 1                |
| CHIP   | = | C-terminus of Hsc70 Interacting Protein          |
| Chk1   | = | Checkpoint kinase 1                              |
| Chk2   | = | Checkpoint kinase 2                              |
| CREB   | = | cAMP-response element-binding                    |
| DAXX   | = | Death domain associated protein                  |
| DNA-PK | = | DNA dependent-protein kinase                     |
| DSBs   | = | Double strand breaks                             |
| EBV    | = | Epstein Barr virus                               |
| ECS    | = | Elongin B/C-Cul2/5-SOCS-box protein              |
| FEZ1   | = | Fasciculation and elongation protein zeta-1      |

|        |   |  |
|--------|---|--|
| GADD45 | = | Growth arrest and DNA-damage-inducible 45                      |
| Gy     | = | Gray   |
| HA     | = | Hemagglutinin  |
| hADA3  | = | Human homologue of yeast alteration/deficiency in activation 3 |
| HDS    | = | High density survival  |
| HECT   | = | Homologous to the E6AP carboxyl terminus                       |
| HPV    | = | Human papillomavirus   |
| IR     | = | Ionizing radiation   |
| KAP1   | = | KRAB-associated protein-1                                      |
| LCLs   | = | Lymphoblastoid cell lines                                      |
| MAPK   | = | Mitogen-activated protein kinase                               |
| MCL-1  | = | Myeloid cell leukemia-1  |
| MDM2   | = | Mouse double minute 2  |
| MDM4   | = | Mouse double minute 4  |
| MDR-1  | = | Multi drug resistance protein 1                                |
| NES    | = | Nuclear export signal  |
| NLS    | = | Nuclear localization signal                                    |
| P/CAF  | = | p300/CBP-associated factor                                     |
| PIRH2  | = | p53-induced protein with a RING-H2 domain                      |
| PUMA   | = | p53 upregulated modulator of apoptosis.                        |
| RING   | = | Really Interesting New Gene1                                   |

SIPS = Stress-induced premature senescence

# *Chapter 1*

## *Introduction*

# Introduction

## p53 Structure

The human p53 protein is encoded by the *TP53* gene, which is located on the third band of the first region in the short arm of chromosome 17 (17p13) [1,2]. The gene, which spans 20 kb, consists of 11 exons. In vertebrates, the *TP53* coding sequence encompasses five highly conserved regions, mainly in exons 2, 5, 6, 7 and 8, which correspond to amino acid residues 13-23, 117-142, 171-181, 234-250, and 270-286, respectively [3]. The wild-type p53 protein comprises a polypeptide chain of 393 amino acids with a molecular mass of 53 kDa. p53 is a tetrameric transcription factor, which is organized in the following domains (Figure 1): the N-terminal transactivation domain, the proline-rich domain, the DNA binding domain, the tetramerization (also called oligomerization) domain, and the regulatory domain in the C-terminus [4].

More than 80% of the mutations commonly found in human cancers constitute missense mutations that are localized in the DNA-binding domain, especially residues 93-292 [5]. Depending upon the type of affected residues, these mutations are divided into two categories: mutations that directly contact the DNA (R248 or R273) or cause structural alterations of the p53 protein folding, thus impeding its ability to bind DNA (R175, G245, R249 and R282) [6].

Since p53 needs to form tetramers in order to conduct DNA binding and transcriptional activity, mutations in the DNA binding domain and/or the tetramerization domain impact p53 tumour suppression function. In addition, mutations in regions that reside outside of these domains may also profoundly influence the function of p53, even

in a heterozygous state, where cells express both wild type and mutant p53. In these cells, the mutations in other domains result in mutant p53, which occurs from the dominant negative effect of inactive p53 monomers on the wild-type monomers. Under these conditions, the functions of wild-type p53 monomers become disrupted when they combine with mutant p53 monomers containing defective DNA-binding/tetramerization domains. This alteration results in the formation of non-functional heterogeneous p53 tetramers, which may ultimately promote carcinogenesis.

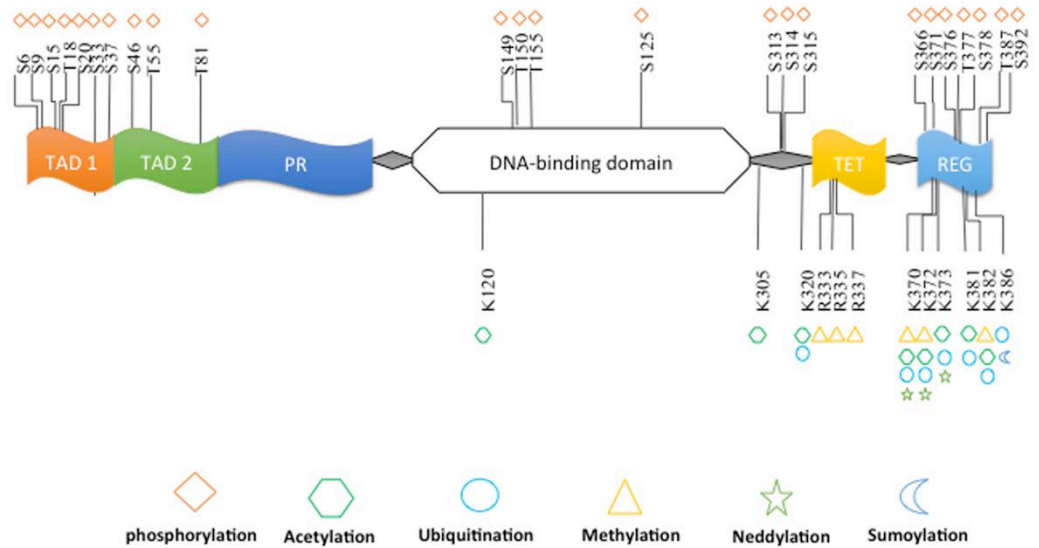


**Figure 1. Post-translational modifications on p53**

Schematic representation of the structure of human p53 showing its different domains along with the sites of post-translational modifications including phosphorylation, acetylation, ubiquitination, methylation, neddylation, and sumoylation. Abbreviations: N-terminal transactivation domain (TAD); proline-rich domain (PR); Tetramerization domain; (TET); C-terminal regulatory domain (REG). [R, arginine; K, lysine; S, serine; T, threonine.]

## **p53 regulation in ATM proficient cells**

The wild-type p53 protein, described as the “guardian of the genome,” fulfills an essential role in maintaining a homeostatic state in single cells and in the entire organism by preserving genomic integrity and preventing mutations [7].

In stressed cells, p53 initiates and coordinates a complex network of signalling pathways that determine the final fate of the cell [8]. Interestingly, p53 experiences inactivation in more than 80% of all human cancers, with the most frequently observed alteration in cancer cells constituting *TP53* mutations [9-11]. Hence, the strict regulation of p53 in both normal and abnormal cells is crucial for preventing and treating tumourigenesis. In the absence of genotoxic stress, the p53 protein remains at a minimal level through the process of rapid turnover, which prevents undesirable effects from occurring to the cell [12]. Exposure to various genomic stressors, such as DNA-damaging agents, provokes several types of post-translational modifications involving p53, resulting in an increase of its stability, accumulation in the nucleus, and change from a latent to active form [13,14].

## **p53 regulation by ubiquitin ligases**

The p53 protein expression, activity, and sub-cellular localization mostly undergo regulation via posttranslational modifications, such as ubiquitination, phosphorylation, summolyation, and acetylation [15,16]. One of the most crucial regulatory mechanisms of p53 involves ubiquitination. In the absence of genotoxic stress, ubiquitination maintains a rapid turnover based on the extremely short half-life of the p53 tumour suppressor protein. In ubiquitination, an abundant and essential 8.5 kDa protein called ubiquitin [17]

tags cellular proteins and thus signals them for final proteasome degradation. Ubiquitination results in the ligation between the C-terminus of ubiquitin (G76) and the amino group of a substrate lysine residue. This process occurs through successive enzymatic reactions by several enzymes. First, E1s, known as ubiquitin-activating enzymes, stimulate the C-terminus of ubiquitin by forming a thiol ester with its carboxyl group at G76. Secondly, E2s, ubiquitin-conjugating enzymes, receive the activated ubiquitin, which is temporarily transferred as a thioester conjugate. The E3s, or ubiquitin-protein ligases, simultaneously associate with the substrate and transfer the activated ubiquitin from E2s, thus serving as a scaffold connecting the activated ubiquitin moieties to lysine residues of substrates or previously-linked ubiquitin [18,19]. Finally, E4s, polyubiquitin chain assembly factors, attach additional ubiquitin molecules to the previously ubiquitinated substrate, creating a polyubiquitin chain. A schematic representation of ubiquitination occurs in Figure 2.

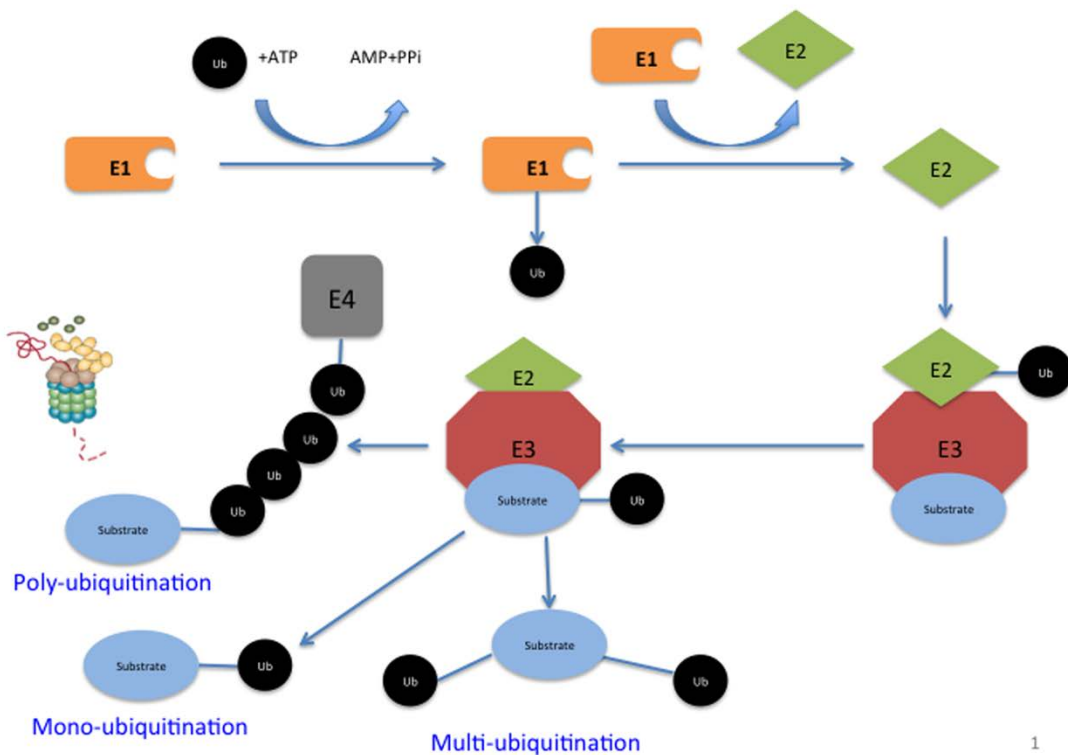


**Figure 2. Schematic representation of ubiquitination pathway**

Ubiquitination is an enzymatic process in which several enzymes are sequentially involved to eventually tag a particular substrate for proteasomal degradation. Marking substrates includes the addition of ubiquitin protein moieties. Adding a single (mono) or multiple separated unchained (multiple) or multiple chained (poly) units of ubiquitin determines the fate of the tagged substrates.

Following ubiquitination, the fate of the p53 protein depends on the type of ubiquitination that has occurred. While monoubiquitination and multiple monoubiquitination result in p53 translocation from the nucleus to the cytoplasm, polyubiquitination leads to a complete degradation of p53 via proteasome 26S. Previous reports have confirmed that the covalent linkage of the Lysine 48 residue to p53 results in polyubiquitination, while the association of the Lysine 63 residue to p53 causes monoubiquitination [20,21]. More specifically, the type of conjugated lysine residue of ubiquitin controls the fate of the substrate. While the attachment of Lysine 48 leads to the proteolytic degradation of the substrate, the linkage of Lysine 63 results in non-proteolytic consequences [20,21].

E3 ubiquitin ligases have been structurally and functionally categorized according to their distinctive catalytic domains into two major classes: Really Interesting New Gene (RING) finger domain E3 ligases and Homologous to the E6-AP Carboxyl Terminus (HECT) domain E3 ligases [18]. In 2001, U-box ubiquitin ligases were suggested as a special type of E3 ligases, based on the finding that some mammalian U-box proteins had the ability to polyubiquitinate and proteosomally degrade substrates independently of other known E3 ligases [22]. Moreover, unlike RING and HECT ubiquitin ligases, which target lysine 48 residues, U-box ligases employ other residues, such as lysine 29, as signals to polyubiquitinate and thus lead to the degradation of substrates [23]. Recently, studies have proposed a new class of E3 ligases, namely “The RING between RING” (RBR) [24]. Since they bind diverse substrates and link these substrates to ubiquitin, E3 ubiquitin ligases constitute the major determinants in specifying the ubiquitination

pathway. Hence, despite the existence of only two E1 ligases and few dozen E2 ligases, approximately six hundred E3 ligases were identified [25]. The mechanisms of various E3 ligases classes differ based on how they conjugate ubiquitin to the substrate. The functional differences among E3 ligases vary according to the type of ubiquitin conjugation to the substrates (Figure 3). While HECT domains attach ubiquitin directly to the substrates, RING domain ligases operate as scaffolds, indirectly connecting ubiquitin to the substrates [25]. Although RBR E3 ligases consisting of multiple RING domains initially comprised a subclass of RING E3 ligases, researchers subsequently likened the operation of these ligases to those of HECT E3 [26].

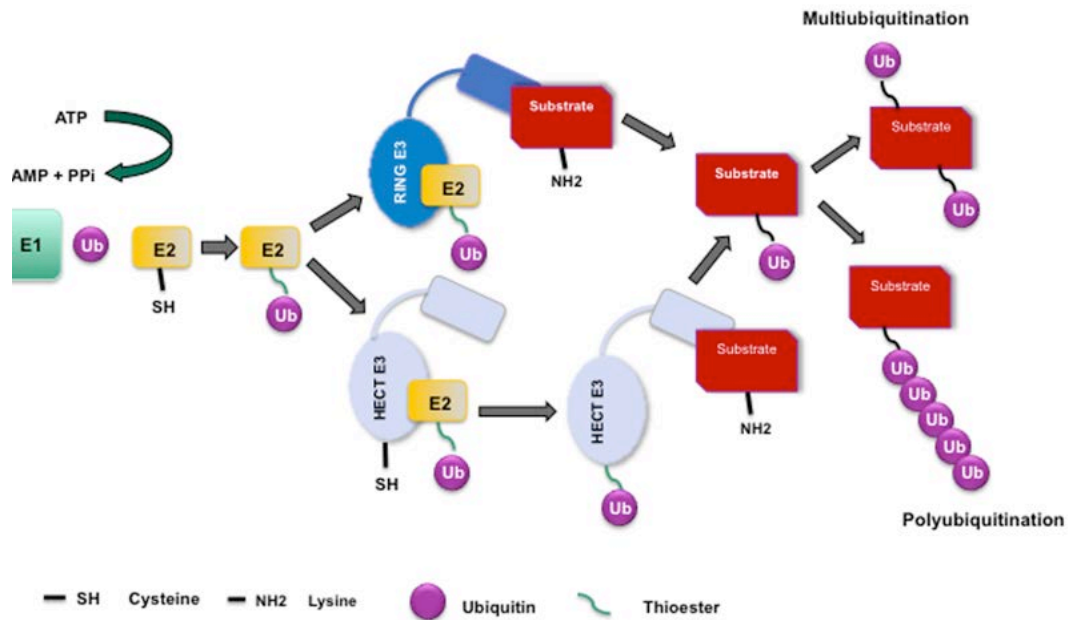


**Figure 3. Domains of E3 ligases**

E3 ligases have different structural and functional domains, namely; RING (blue oval shapes) vs HECT (gray oval shape) domains. Unlike RING domains that catalyze indirect attachment of the ubiquitin (violet circles) to the substrates, HECT domains catalyze direct attachment of ubiquitin to substrates. Incorporating ubiquitin moieties by either way eventually leads to mono-ubiquitination, multi-ubiquitination or poly-ubiquitination.

The functions of p53 in different contexts involve biological diversity, such as the significant involvement in various signalling pathways that maintain cellular genomic integrity as well as the need for regulating many isoforms of p53, such as p63 and p73, along with regulating the mutant p53 (Reviewed in [27]). Consequently, several E3 and E4 ubiquitin ligases have been found to ubiquitinate, thus leading to p53 proteasomal degradation. Examples of well-identified p53 E3 ligases include MDM2, MDM4, PIRH-2, and COP1 [28,29]. (See Table 1)

| Ligase     | Type  | Ub        | p53 lysine residue                 | p53 status                    |
|------------|-------|-----------|------------------------------------|-------------------------------|
| UBE4B      | U-box | Mono/Poly | K370,K372,K373<br>K381, K382, K386 | Degradation                   |
| MDM2       | RING  | Mono/Poly | K370,K372,K373<br>K381, K382, K386 | Degradation                   |
| PIRH2      | RING  | Poly      | -                                  | Degradation                   |
| COP1       | RING  | Poly      | -                                  | Degradation                   |
| TRIM24     | RING  | Poly      | -                                  | Degradation                   |
| ARF-BP1    | HECT  | Poly      | -                                  | Degradation                   |
| CARP1/2    | RING  | Poly      | -                                  | Degradation                   |
| TOPORS     | RING  | Poly      | -                                  | Degradation                   |
| Synoviolin | RING  | Poly      | -                                  | Degradation                   |
| CHIP       | U-box | Poly      | -                                  | Degradation                   |
| JFK        | RING  | Poly      | -                                  | Degradation                   |
| MKRN1      | RING  | -         | K291,K292                          | Degradation                   |
| ICPO       | RING  | Poly      | -                                  | Translocation to nuclear foci |
| MSL2       | RING  | Poly      | K351,K357                          | Nuclear Export                |
| WWP1       | HECT  | Mono/Poly | -                                  | Nuclear Export                |

**Table 1.** List of E3 ubiquitin ligases associated with p53 tumour suppressor regulation, including the type of domains that they possess, the type of ubiquitination they conduct, targeted p53 lysine residues, and variable fates of p53 inflicted by each ligase.

In addition, other ubiquitin ligases destabilize p53 indirectly. For example, DAXX augments the intrinsic ligase MDM2 activity towards p53 and hence assists in p53 degradation [30]. Contrastingly, the p14 ARF tumour suppressor binds MDM2, indirectly stabilizing p53 by preventing MDM2 - p53 interaction and the consequent MDM2-mediated p53 degradation [31,32]. The protein expression of these substances, direct and indirect negative regulators of p53, is mediated by p53 transcriptional activity in a negative auto-regulatory feedback loop.

### **MDM2, a main p53 ubiquitin ligase**

Mdm2, the human homolog of which comprises Hdm2 or MDM2, constitutes a crucial p53 negative regulator and a RING E3 ligase. MDM2 knockout mouse develops an embryonic lethal phenotype [33,34], which is rescued by deleting the p53 gene. This activity highlights the critical importance of MDM2-mediated down-regulatory role in the early stages of development [33,34]. MDM2 ubiquitinates p53 and hence promotes its degradation via the ubiquitin proteasome system [35,36]. Complete p53 degradation lacks feasibility unless the proteasome system adequately recognizes the polyubiquitin chains [37]. MDM2 can conduct either mono or multiple ubiquitination of p53 *in vitro* and *in vivo* [38,39]. However, research has not yet determined whether MDM2 catalyzes the formation of polyubiquitin chain signals on p53 or whether other factors mediate this crucial step. Thus, several investigators have proposed that MDM2-mediated p53 ubiquitination may be modulated by other proteins, such as p300 [40], YY1 [41], Gankyrin [42], KAP1 [43], and Siva1 [44]. Conversely, other studies suggested that

MDM2 levels constitute a major determinant for the type of p53 ubiquitination (mono Vs. polyubiquitination) [39,45] .

Furthermore, recently, *in vitro* and tissue culture analysis revealed that many ubiquitin ligases efficiently enhance p53 degradation independent of MDM2, including PIRH2 [46] and COP1 [47] . However, the role of these agents in p53 regulation in response to stress remains unknown.

MDM2-mediated p53 regulation contains more complexity than originally believed. MDM2 not only affects the level of p53 but also influences its transcriptional activity and subcellular localization. Specifically, MDM2 binds to the p53 transactivation domain at the N-terminal region, blocking its transcriptional activity [48-50] . Also, this regulator promotes the nuclear export of p53 by adding a single ubiquitin molecule onto one or more lysine residues within the C-terminal region of p53, a process referred to as “mono-ubiquitination.” Recently, studies reported that MDM2 also negatively regulates other p53-induced target genes, such as p21 [51] .

Following exposure to DNA-damaging agents such as ionizing radiation, the wild-type p53 protein undergoes post-translational modifications at multiple sites (Figure 1), which lead to the stabilization and nuclear localization of p53 and the activation of its biological functions. Among the many different types of p53 modifications, phosphorylation, along with ubiquitination, represent the most extensively studied biochemical and genetic changes. In response to DNA damage, p53 undergoes rapid phosphorylation at several amino acid residues within the N-terminal transcriptional activation region [52,53] , including Ser15 (Ser17 in mice) [53] , Thr18 and Ser20 (Ser23 in mice) [54] , and the C-terminal regulatory region of p53. These

phosphorylations are mediated by several protein kinases, including members of the phosphatidylinositol 3-kinase-related (PI3KK) family of protein kinases, such as ATM (ataxia-telangiectasia-mutated), ATR (ataxia-telangiectasia and RAD3 related) [55,56] , DNA-PK, Checkpoint kinase 1 (Chk1) and Checkpoint Kinase 2 (Chk2) [57-59] . However, the precise contribution of these phosphorylations remains unknown.

### **ATM-p53-MDM2 model of p53 stabilization**

One of the earlier accepted paradigms of p53 stabilization involves the ATM-p53-MDM2 model. This model proposes that after exposure to ionizing radiation, ATM phosphorylates both p53 and MDM2 at their binding sites, which leads to the interruption of their interactions and hence stabilizes p53. In particular, Ser15, Thr18 and Ser20 constitute crucial phosphorylation sites for p53 protein stabilization. The phosphorylation of Ser15 initiates the subsequent phosphorylation of Thr18 and Ser20, which are located close to each other in the binding site of MDM2. Consequently, these phosphorylations prevent p53-MDM2 interactions and thus weaken the suppressive effect of MDM2 on p53.

Some controversy exists regarding the role of DNA damage-induced phosphorylation of p53 for stabilization and activation. While researchers generally agree that the phosphorylation of p53 in its binding sites with MDM2 fulfills a crucial role in disrupting MDM2-p53 interactions, and hence contributes to the stability and activation of p53 [58,60-63] , several genetic and biochemical studies argue against its significance. Compared to cells extracted from wild-type mice, murine embryonic fibroblasts, extracted from individual mutant knock-in mouse models at Ser15 (Ser18) [64,65] and Ser20 (Ser23), demonstrated a lack of reduction in p53 stabilization in response to

ionizing radiation [66] . Interestingly, however, the results for double mutant mice revealed the significance of phosphorylation at these residues in specific tissues, especially for DNA damage-induced apoptosis [67] . These findings imply that the requirement of phosphorylation for p53 stability may demonstrate context-dependent behaviour. Moreover, several studies have confirmed the dispensability of p53 phosphorylation status for its activation [68-71] . For instance, some studies focus on acetylation as a major determinant of p53 stability [72] . Notably, studies have confirmed that the phosphorylation of Ser15, Thr18, and Ser20 is accompanied by the acetylation of a group of lysine residues at the C-terminal of p53. The acetylation of such residues, identified as normal targets for ubiquitination [73] , ultimately enhance p53 stability. Several agents, including p300, CBP, P/CAF [74,75] , acetylate p53.

Taken together, accumulated evidence suggests that in addition to phosphorylation, other modifications may contribute towards p53 stabilization. Instead of a single modification, a more complex regulatory network is needed to stabilize and activate p53. Broadly speaking, the coordination between phosphorylation and other modifications is essential for modulating p53 activity.

### **UBE4B, an emerging p53 ubiquitin ligase**

UBE4B constitutes a human homolog of the *Saccharomyces cerevisiae* protein UFD2. Yeast UFD2 is encoded by a single-copy gene and involved in the ubiquitin fusion degradation (UFD) pathway [22,23]. As the earliest identified E4 ubiquitination factor, UFD2 is required for enzymatic activity in the ubiquitin chain assembly [23]. UFD2-related genes have been identified in *Mus musculus* (Ube4a and Ube4b or Ufd2a)

and *Homo sapiens* (UBE4A and UBE4B) [76,77]. UBE4B and its homologs share a U-box conserved domain that consists of approximately 70 amino acids. This protein may exhibit E3 and/or E4 activity [78]. Studies have reported that UBE4B, as an E4 ligase, participates in the degradation of some substrates, such as the pathological form of ataxin-3 [79], and the ubiquitination of substrates, such as FEZ1 [80]. Following cisplatin treatment, Ube4b, a mouse homolog, promotes the proteasomal degradation of p73 but without involving the ubiquitination pathway [81]. In addition, Ube4b reportedly diminishes the transcriptional activity and apoptotic-mediated function of p73 [81]. Unlike non-lethal effect of UFD2 knockout in yeast, Ube4b deletion in mice was lethal with marked apoptosis [82]. However, investigators failed to confirm if this lethality is attributed to p53 level and activity.

Several E4 ligases have reportedly engaged in p53-mediated ubiquitination and degradation. According to Avantaggiati et al., p300 binds and acetylates p53, resulting in p53 stabilization [83]. However, Grossman et al. subsequently showed that p300 functions as an E4 ligase by mediating p53 polyubiquitination [40]. Likewise, CBP, which demonstrates E3 ligase activity via its N-terminus [84], displayed E4 activity and directly polyubiquitinates p53 *in vivo* in an MDM2-independent manner [84]. Also, Yin Yang (YY1) functions as a molecular clamp that mediates p53 polyubiquitination [41]. Esser et al. reported that CHIP indirectly promotes the polyubiquitination of both mutant and wild type p53 through binding with the molecular chaperones Hsp90 and Hsc70 [85].

Our group of researchers, Leng et al., initially conducted *in vivo* studies and showed that UBE4B affects p53 ubiquitination as mediated by MDM2 and UBE4B is required for

MDM2-mediated p53 degradation. Hence, these findings suggest that the E4 activity of UBE4B is essential for MDM2 to promote p53 polyubiquitination and degradation [86]. In addition, the consistent observations of UBE4B protein overexpression and gene amplification in human brain tumours may provide a new model for better understanding the previously unexplained p53 inactivation in brain malignancies [86]. The ability of UBE4B to induce the same effect in other cell lines or in different contexts, such as in response to DNA damage stress, remains known. Thus, studies require investigation into the role of UBE4B as an active E4 ligase in promoting MDM2-mediated p53 degradation pathways in response to DNA damage. Such studies would enable researchers to exploit UBE4B as a potential target in p53-based anti-cancer therapy.

### **p53 dynamics: More complex regulation**

The preservation of genomic integrity assumes more complex levels of regulation; thus, in addition to the role of ubiquitin ligases, p53 regulation occurs through the functioning of other proteins. In recent years, two p53-induced proteins, WIP1 and p21, emerged as major p53 negative regulators, hence necessitating the coordination and integration between different regulators. Therefore, in order for phosphorylated p53 to represent a suitable target for MDM2 ubiquitination and subsequent degradation, it first requires dephosphorylation. According to recent literature, this important function is mediated by factors such as WIP1, the wild type p53-induced phosphatase 1. Since 2008, the Lahav group has shown the significant role of WIP1 in p53 signaling. Specifically, p53 transcriptionally activates WIP1, which subsequently inactivates p53 by dephosphorylating p53 and other upstream kinases such as ATM. Although the

involvement of MDM2 has been principally implicated in this pathway, the contribution of UBE4B to WIP1-mediated p53 inactivation remains unknown.

In recent years, studies have shown that the regulation of p53 after exposure to DNA damaging agents such as ionizing radiation and UV light contains more complexity than originally believed. Several groups have recently revealed that exposure of human cells to these agents induces different “pulses” of p53 induction. For example, mathematical models had predicted multiple p53 pulses after ionizing radiation and suggested that different pulses were responsible for different biological effects [87]. The laboratory of Lahav first reported experimental evidence for different p53 pulses [88-90]. Using MCF7 breast cancer cell lines, these researchers showed that ionizing radiation induces two pulses of p53 during the 10 h following radiation exposure: the first pulse occurred at ~2 h and the second pulse at ~7 h after irradiation. The amplitude or level of induction, duration, and frequency of individual p53 pulses in response to ionizing radiation are fixed and lack dependency on the radiation dose in MCF7 cells [88,91].

In their initial reports, Lahav’s group focused on MDM2 as an important regulator of p53 at different pulses [88]. They identified another p53 regulator, WIP1, which also fulfills an important function in p53 regulation [89]. The suggested models for both ionizing radiation and UV light are reproduced in Figure 4. According to these models, ionizing radiation activates p53 through ATM, and p53 transcriptionally activates both MDM2 and WIP1; thus, these two proteins negatively regulate p53 (Figure 4, left). The UV-induced response model (Figure 4, right) resembles that of ionizing radiation. However, in the presence of UV light, ATR fulfills a role in p53 activation rather than ATM, which serves the same function in the case of ionizing radiation. Although research

has assumed that ionizing radiation and UV light activate the ATM and ATR pathways respectively, recent evidence shows that ATR functions downstream in the ATM pathway upon exposure to ionizing radiation [92] .

As mentioned, p53 regulation involves an extremely complex process involving a large number of proteins. Thus, further work is needed to identify additional p53 regulators that contribute to p53 pulses at different times after exposure to different DNA-damaging agents, such as ionizing radiation and chemotherapeutic agents in different human cell types, such as cancerous versus normal cells. One such candidate, based on studies reported from this laboratory, constitutes UBE4B [86] .

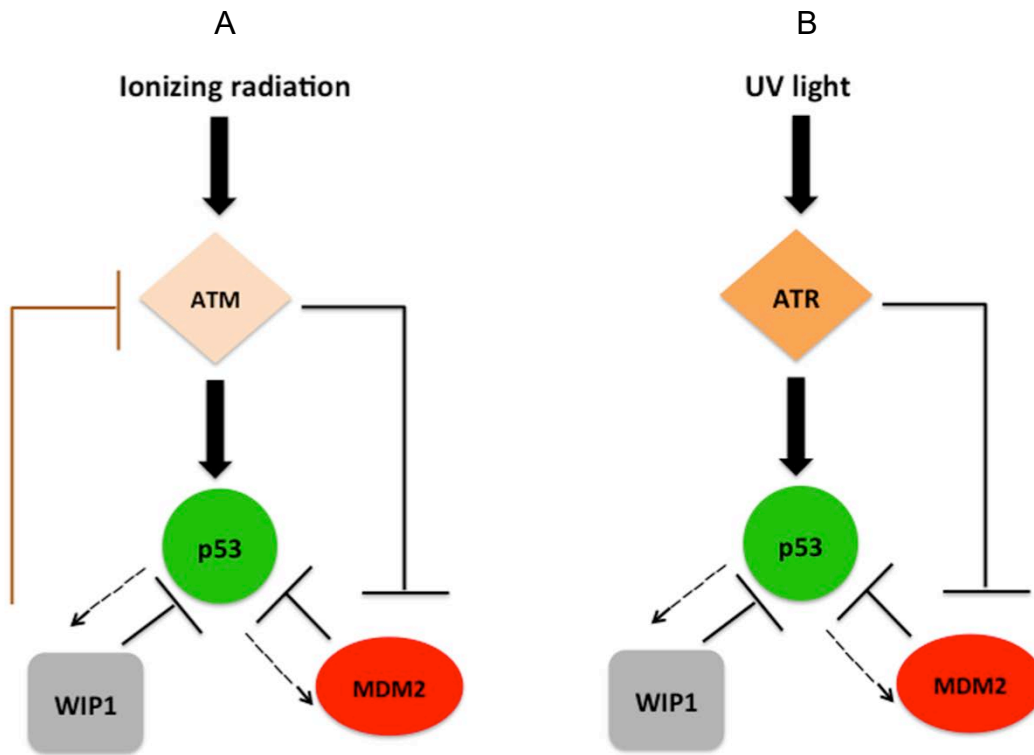


**Figure 4. Overview of Lahav's model (2004)**

This model proposes WIP1 and MDM2 as major players in the p53 signaling pathways in response to ionizing radiation (IR) (Left, A) or ultra violet light (UV) (Right, B). Arrows indicate activations. T-shape lines indicate inhibition.

## **Role of WIP1 in negative regulation of p53**

DNA damage response involves an essential means by which cells cope with stressors, such as ionizing radiation, through an intricate network of signal transductions, including the transmission of signals via post-translational modifications. In order to maintain cell homeostasis and resume normal growth, cells need to inhibit the DNA damage response mechanism upon repair of the genomic injury. This crucial function occurs through the efforts of WIP1, the wild-type p53 inducible protein 1 (WIP1) phosphatase, the product of the PPMID gene and a type 2C serine/threonine phosphatase [93]. WIP1 encodes a 605-amino acid nuclear protein that is sub-categorized into two main domains: a highly conserved N-terminal phosphatase domain spanning amino acids 1-375 and a less conserved non-catalytic domain spanning amino acids 376-605. The latter contains two putative nuclear localization signals [93]. Initially, WIP1 was identified as a nuclear phosphatase, which is exclusively expressed in a p53-dependent manner post-irradiation [94]. Research has recently discovered that the promoter region of the PPMID gene-encoding WIP1 consists of binding motifs that can potentially bind a wide array of transcription factors. This finding suggests the existence of greater complexity in the regulation and role of WIP1, especially within the context of various types of stresses and tissues [95]. In this regard, experimental evidence has verified the role of several transcriptional factors in WIP1 regulation, including CREB [96], c-jun [97], and E2F [98].

Following exposure to ionizing irradiation, WIP1 deactivates p53 through several mechanisms. First, WIP1 dephosphorylates p53 at the Ser15 residue [99]. Additionally, WIP1 indirectly diminishes p53 function by deactivating numerous upstream kinases,

such as ATM, ATR, Chk1, Chk2, and p38 MAPK, thus reducing p53 phosphorylation at various sites, including Ser15, Ser20, Ser33 and Ser46 [99-102] . Interestingly, WIP1 also affects p53-MDM2 interactions. Specifically, WIP1 simultaneously inhibits p53 phosphorylation at Ser20 and dephosphorylates MDM2 at Ser395; these functions result in the restoration of the p53-MDM2 interaction, which subsequently leads to MDM2-mediated destabilization of p53 [103] .

### **Role of p21 in negative regulation of p53**

The protein p21 is also known as CDK-interacting protein 1 (CIP1), wild type p53-activated fragment 1 (WAF1), and senescent cell-derived inhibitor 1 (SDI1). This protein functions as a main p53-induced downstream target effector. Research has long established the notion of p21 as a negative regulator of p53. Hence, the elevated protein expression of p53 occurs in p21 knockout cells, such as HCT116 p21 <sup>-/-</sup> cells without external stimuli [104] . The negative regulation of p53 via p21 occurs indirectly through the engagement of ARF (p14<sup>ARF</sup>) and MDM2. As depicted in Figure 5, when activated, p53 transcriptionally activates p21 and MDM2. MDM2 associates with both p53 [105] and p21 [51] , promoting their proteasomal degradation. In the nucleus, the physical interaction of p14<sup>ARF</sup> with MDM2 hinders the ability of MDM2 to associate and ubiquitinate, thus degrading target proteins such as p53 and p21 [31,32]. The inhibition of p14<sup>ARF</sup> action by p21 results in the interruption of the p14<sup>ARF</sup>/MDM2/p53 regulatory loop [106] . Consequently, the restoration of MDM2 ubiquitinating activity negatively affects p53 stability. These research findings used HCT116 wild type and p21 knockout colon carcinoma cell lines [104] . Subsequently, other groups confirmed these data using

HCT116 and HT1080 human fibrosarcoma without implicating MDM2 [107] . This mechanism, along with other factors, facilitates p21-mediated suppression of apoptosis. As discussed in subsequent sections, p21 represents a well-established anti-apoptotic agent through several mechanisms.

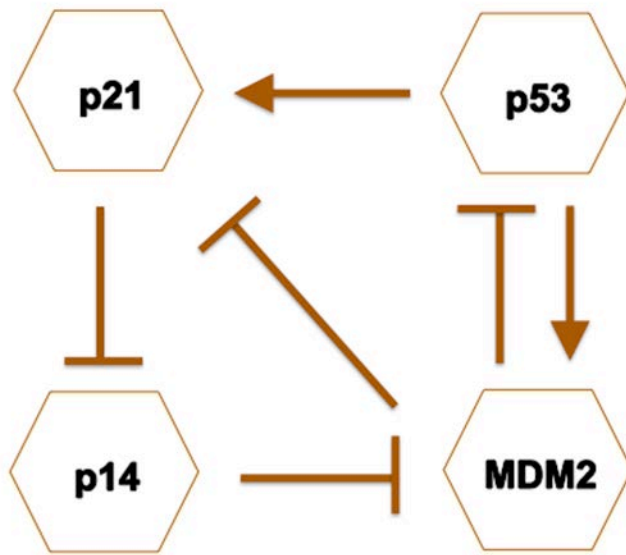


**Figure 5. Communication between p53, p21, p14<sup>ARF</sup> and MDM2**

Schematic representation illustrating the indirect role of p21 as a negative regulator of p53. Stimulation is indicated by Arrows. T-shape lines indicate inhibition.

## **Wild type p53 signalling in ATM-proficient cell lines**

The wild type p53 protein exerts its tumour suppressor functions via several mechanisms, including transcriptional activation of several genes, transcriptional suppression of several genes, and interactions with other proteins. The following subsections will discuss some proteins that play important roles in p53-mediated responses.

### **Transcriptional activation by wild-type p53**

The positive regulation of transcription represents the most extensively studied function of p53. Although many genes constitute transcriptional targets of p53 [108] , this tendency does not apply to all p53 target genes, cell types, and manners of genotoxic stress. As Lane emphasizes, *in vivo* studies have established the critical importance of three genes: encoding p21, PUMA and NOXA [29]. Levine and Feng identified four genes commonly associated with the transcriptional upregulation of p53 under different experimental conditions: encoding p21, MDM2, GADD45 and Cyclin G [108] . In terms of the DNA damage response, research has universally identified p21 as undergoing transcriptional activation by p53. This activation occurs rapidly (within hours) after DNA damage and occurs for different genotoxic agents both *in vitro* (cultured cell lines) and *in vivo* (various tissues). The importance of this observation becomes apparent when considering that p21 constitutes a multifunctional protein that controls not only p53 and its upstream kinase ATM but also different biological end points, such as cell cycle progression, apoptosis, and growth arrest [109-111] .

## **Transcriptional repression by wild-type p53**

As previously mentioned, the transcriptional activation of p53 target genes is associated with the DNA binding property of p53 tetramers. In addition to this property, p53 monomers negatively regulate the transcription of several genes, including those that encode BCL-2, MCL-1, survivin, and MDR-1 [reviewed by Mirzayans et al. [110] ]. The transcription repression property of p53 is associated with its proline-rich domain, which lies between the DNA binding and transactivation regions. Moreover, repression by p53 occurs indirectly through repressor proteins [29,112] . Löhr et al. identified p21 as the key repressor protein in the p53 pathway [112] .

## **Protein-protein interactions**

The p53 protein can independently and directly influence some biological functions via protein-protein interactions in a transcription-independent manner [113] . For example, p53 interacts with proteins involved in different DNA repair pathways [114] . This protein-protein interaction increases the rate of repair of DNA lesions. In general, p53 plays an auxiliary role in these processes; while it accelerates the process of repair, the repair process can occur without the presence of p53.

## **The role of p53 in DNA damage Response Network: A History**

In the mid 1990s, several authors suggested a two-arm model of the DNA damage response. This model demonstrated the activation of the p53 pathway by ionizing radiation, such as activated cell cycle checkpoints at the G1/S and G2/M borders,

suggesting that these events facilitate DNA repair before the cells resumed cycling. The second arm of the model involved the induction of p53-mediated apoptosis for eliminating cells with high levels of genomic injury, such as DNA damage and chromosome aberrations, from the proliferating population. This model remains widely popular [115,116] . However, as discussed below, neither the original observations reported in the early 1990s nor the subsequent investigations support the concept of an apoptotic arm for most cell types, including human skin fibroblasts and solid tumor-derived cells.

### **Original observations**

In the early 1990's, Kastan and associates initially addressed the role of p53 in determining the response of human cells to ionizing radiation. In the first instance, in 1991, they employed human hematopoietic cells, such as ML-1 leukemia cells and proliferating normal bone marrow myeloid progenitor cells. Subsequently, they concluded that DNA damage “causes a transient inhibition of replicative DNA synthesis via both G1 and G2 arrests.” [117] . These responses were later referred to as G1-S and G2-M checkpoints. In 1992, these authors confirmed their findings with other cell types, including human colorectal cancer cell lines and normal skin fibroblasts [118] . In 1993, these researchers extended their studies to include apoptosis and demonstrated the cell-type specific biological effect of p53 upregulation, which includes cell cycle checkpoints and apoptosis [119] .

The model that Kastan's group presented in their 1993 paper is reproduced below (Figure 6). In that paper, these authors concluded that the “induction of p53 by ionizing

radiation leads to a G1 arrest in certain cell types (e.g., fibroblasts) and to apoptosis in other cell types (e.g., hematopoietic cells). Loss of p53 function would lead to radio-resistance in cell types utilizing the apoptosis part of the pathway” [119] . Subsequent studies revealed the complexity of the cellular response to ionizing radiation, shown in the diagram below. Research also highlighted that due to the presence of p53-independent apoptotic pathways, the absence of wild type p53 function is not necessarily associated with radio resistance resulting from decreased p53-mediated apoptosis.

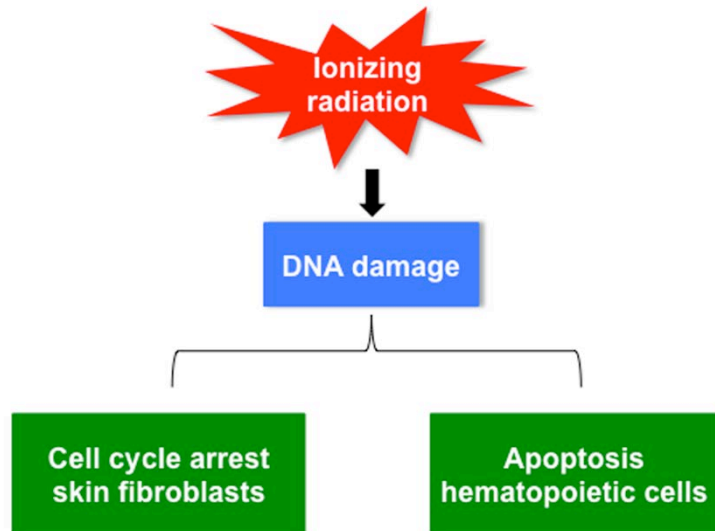


**Figure 6. Kastan's Model explaining p53 signaling (1993)**

This model highlights the cell-specific variable behaviours of p53 role in response to DNA damage (checkpoint activation “cell cycle arrest” vs programmed cell death (apoptosis)).

### **The widely-cited 1995 model**

Efforts to uncover the role of upstream ATM in the p53 pathway triggered the proposal of several models in the mid-1990s. The models specifically contradict Kastan's aforementioned notion that p53-mediated apoptosis response may lack generalization to all cell types. The 1995 model proposed by Enoch and Norbury [120] is reproduced in Figure 7. This theory, along with similar models [121], debated the extent to which the level of inflicted DNA damage was significant in determining the type of response, which involved a consideration of cell cycle checkpoints versus apoptosis. Currently, experimental evidence supports the notion that low levels of DNA damage lead to the activation of checkpoints to provide time for repair and thus promote survival. However, the assumption that high levels of DNA damage induce p53-mediated apoptosis lacks experimental evidence for many cell types. Such early models largely relied on studies that employed cell lines, such as SV40-transformed fibroblasts, in which wild type p53 is suppressed if not totally eliminated. Other cell lines in these research models included leukemia cell lines or mouse cell lines, all of which are prone to undergo apoptosis in response to different stimuli.

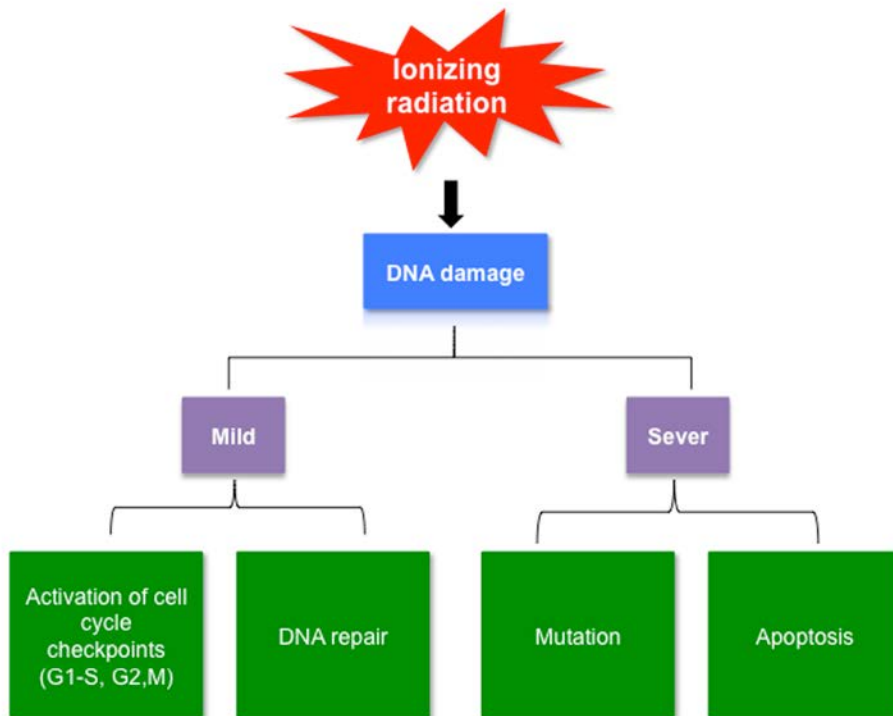


**Figure 7. Enoch Norbury model explaining signaling (1995)**

This model highlights the degree of DNA damage (mild vs severe) as a major determinant of p53 role in response to DNA damage. If mild DNA damage is inflicted, checkpoints are activated to allow a time for DNA repair. Alternatively, if DNA damage is irreparable, programmed cell death apoptosis is initiated by p53 in normal scenarios.

## **Current knowledge & proposed model**

Current research widely accepts that triggering the p53 pathway by ionizing radiation and other DNA-damaging agents might suppress rather than trigger apoptosis in most human cell types. The contemporary views of ionizing radiation-mediated responses in human skin fibroblasts and solid tumour-derived cells have undergone recent review [110] (Figure 8). These perceptions involve early responses, such as DNA repair and transient cell cycle checkpoints, which are associated with the early p53 pulses as previously discussed, or late responses, such as apoptosis and growth arrest, some of which are associated with late p53 pulses that occur several days following exposure to radiation.

**Early DNA damage responses:** Exposure to moderate doses of ionizing radiation, such as 4 Gy, leads to the rapid ATM-dependent activation of many proteins, such as p53, WRN, and DNA-PKcs [122,123] ; these proteins fulfill essential roles in the repair of DNA double-strand breaks (DSBs). Furthermore, radiation exposure provokes the p53-mediated activation of p21 that inhibits apoptosis and activates transient or reversible cell cycle checkpoints. The appropriate induction of such early responses is needed to enable the cells to repair potentially cytotoxic and mutagenic lesions before the cells exit the checkpoints and resume DNA synthesis as well as chromosome segregation.

**Late DNA damage responses:** Following exposure to radiation, the existence of persistent genomic lesions for long periods of time, such as several days, initiates the continuous upregulation of p21 that prevents apoptosis and induces a senescence-like growth arrested phenomenon called Stress-Induced Premature Senescence (SIPS). Long-

term maintenance of the SIPS response occurs through one positive feedback loop between ATM and p53 as well as another loop between ATM and p21 [124,125].

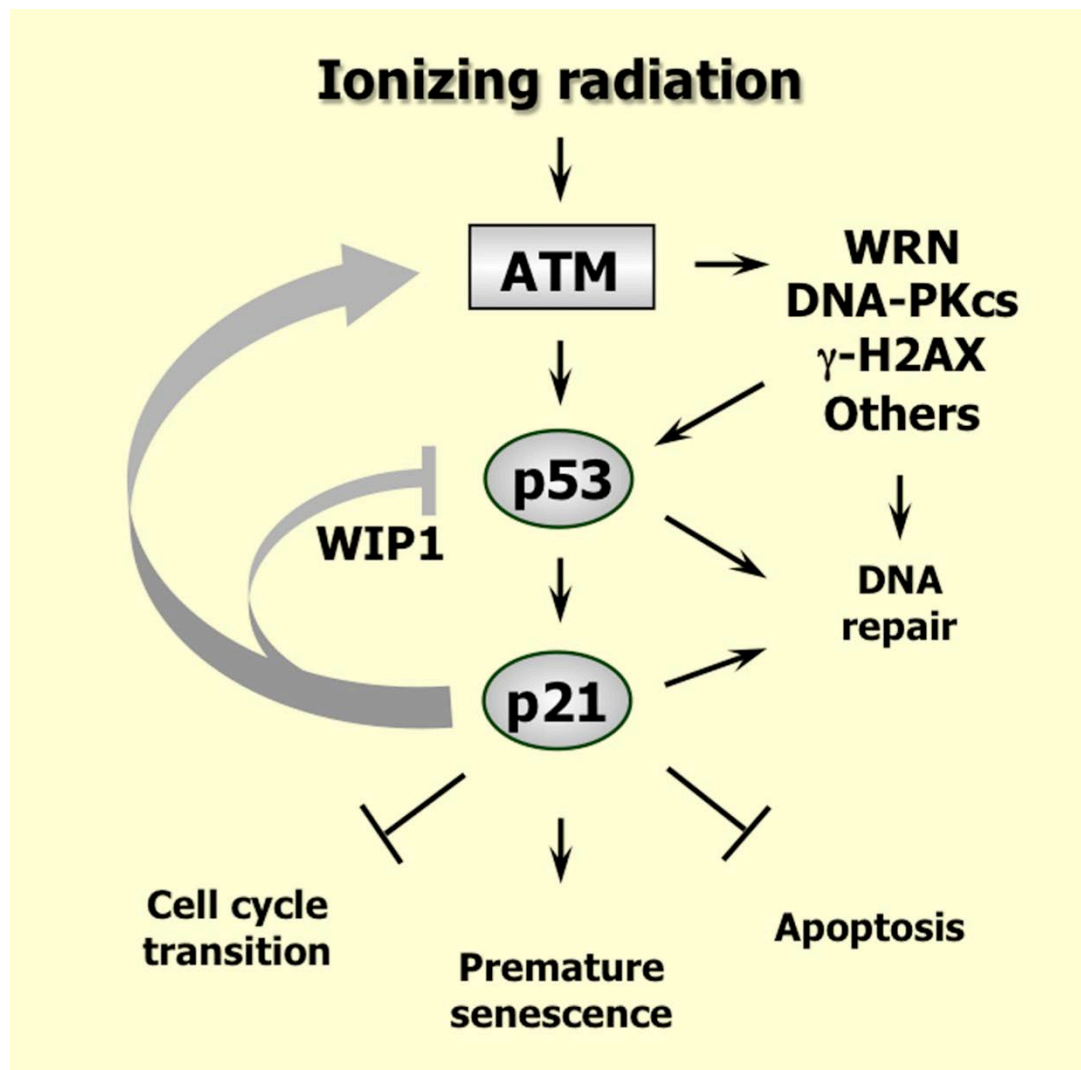


**Figure 8. Current knowledge of radiation-induced responses**

Responses induced by ionizing radiation in p53 wild-type human solid tumour-derived cell lines. Radiation exposure results in ATM-dependent activation of several proteins (e.g., p53, WRN, DNA-PKcs) that play important roles in DSB repair, as well as p53-mediated activation of p21 that suppresses apoptosis and activates cell cycle checkpoints. Proper activation of these events provides time for the repair of potentially cytotoxic and mutagenic lesions. Persistence of DNA damage leads to sustained induction of p21 which downregulates p53 (e.g., through WIP1), suppresses apoptosis and triggers SIPS. Positive feedback loops between ATM and p21 ensure the maintenance of the SIPS response for extended times (several months in culture). For further details, consult [126]. WRN, Werner's syndrome protein; DNA-PKcs, DNA-dependent protein kinase catalytic subunit;  $\gamma$ -H2AX, H2A variant histone H2AX phosphorylated on Ser139; WIP1, wild-type p53-induced phosphatase 1

Research evidence confirms that p21 fulfills a crucial role in determining the fate of a cell following DNA damage. Specifically, the p53-mediated suppression of apoptosis is a direct effect of the expression of p21. As previously indicated, p21-mediated inhibition of apoptosis occurs through various mechanisms, such as downregulating the MAPK cascade; suppressing the activation of two apoptotic enzymes, caspase-3 and caspase-9; and inhibiting the release of cytochrome c from mitochondria. Moreover, p21-mediated premature senescence occurs through various mechanisms, such as inhibiting the cyclin/CDK complexes, positively regulating the transcription of senescence-related genes, and negatively regulating the transcription of mitosis-related genes (reviewed by Mirzayans et al. [110] ). Also, studies have shown that the formation of a positive feedback loop between p21 and ATM represents a crucial process for maintaining the growth-arrested phenotype associated with premature senescence. The latter conclusion is based on the finding that the inhibition of either ATM or p21 causes senescent colon, breast, and lung cancer cells to undergo cell death [125] .

### **The role of WIP1 in p53 signalling pathway**

In addition to its effects on p53 protein stability, WIP1 impacts p53 signalling in other ways. WIP1 inhibits the transcription of p53 target genes. Studies have suggested that MDM4 conducts this inhibition. Specifically, both MDM4 and MDM2 proteins bind p53 via their highly homologous N-terminal domain [39]. Although the interactions of these genes in regulating p53 contain complex mechanisms that lack full understanding [127] , research has established that unlike MDM2, MDM4 lacks the ability to exhibit intrinsic E3 ligase activity toward p53. However, MDM4 can halt p53 activity [127] .

Zhang et al. [128] report that ionizing radiation triggers WIP1-mediated dephosphorylation and stabilization of MDM4, which subsequently promotes suppression of the p53 transcriptional program. Studies have observed that WIP1 interferes with various tumour suppressors in mammalian cultured cells, which suggests that it serves an oncogenic function [129]. Additional investigations on different cancer mouse cell models verified WIP1-associated oncogenic effect. In particular, studies revealed that WIP1 not only inhibits the tumour suppressors such as p53 but also enhances and complements the effects of other oncogenes such as H-Ras [129]. Moreover, several studies reported the frequent amplifications of the genomic region that contains the WIP1 locus (17q23.2) in many human cancers that harbour fewer common p53 mutations, such as breast cancers, ovarian clear cell carcinomas, neuroblastomas, and pancreatic cancers [130-132].

Research has established that WIP1 constitutes a p53-inducible protein; hence p53 comprises a positive regulator of WIP1. A recent study showed that a p53-regulated microRNA (miR-16) could bind and degrade WIP1 following DNA damage [133,134]. Since WIP1 is considered a tumour-promoting agent and miR-16 a tumour suppressor, the p53-miRNA-WIP1 pathway may contribute to the prevention of tumorigenesis [135-139]. The crucial role of WIP1 in DNA damage response occurs through its ability to bind, dephosphorylate, and deactivate a cluster of activator proteins upstream of p53 as well as effector proteins downstream of p53. This activity promotes tumorigenesis and inhibits p53-driven genomic integrity mechanisms such as cell cycle arrest, DNA repair, and apoptosis.

Similar to p21, WIP1 prevents apoptosis through various routes depending on the type of genotoxic stress and the genetic background of the cell. For instance, studies found that following exposure to ionizing irradiation, WIP1 dephosphorylates and thus deactivates Chk2, which facilitates both p53-dependent and p53-independent apoptosis via its effect on E2F [140]. In particular, WIP1-mediated dephosphorylation of Chk2 at T68 reduces its kinase activity. This reduction was observed in WIP1 overexpressing cells post-irradiation, thus confirming the apoptotic inhibitory effect of WIP1 [101,141]. Moreover, research revealed that the depletion of WIP1 in doxorubicin-treated MCF7 breast cancer cells increases the level of apoptosis. Since active p53 and Bax demonstrated high expression in MCF7 cells, researchers concluded that induced apoptosis is likely driven by p53 [142]. Likewise, another study showed that in the absence of exogenous stress, WIP1 knockdown via siRNA in MCF7 cells increased p53-dependent apoptosis, indicating WIP1's role in promoting the survival of breast cancer cells through inhibiting the apoptotic function of p53 [143].

### **The role of p21 in p53 signalling pathway**

Initially, research proposed that p21 abrogated apoptosis only by activating cell cycle checkpoints, which provides sufficient time for repair and thus prevents DNA damage induced-apoptosis. Last decade, studies found that p21 employs several mechanisms to exert its anti-apoptotic response, which differs from its effect on the cell cycle [144,145]. The first mechanism involves the inhibition of cytochrome c release from mitochondria [146], while another route works by suppressing the activity of proteins, such as caspase 3, caspase 8, caspase 9, caspase 10, stress-activated protein

kinases (SAPKs), and apoptosis signal-regulating kinase 1 (Ask1 or MAP3K5), which directly induces apoptosis [146-148] . Finally, the last mechanism controls the transcription of several different downstream target genes that downregulate the pro-apoptotic genes [148] and upregulate the anti-apoptotic genes [147,148] .

In addition, p21 plays a major role in the p53-signalling pathway. This protein triggers the growth arrest state, known as Stress Induced Premature Senescence (SIPS). This activity occurs through the inhibition of CDKs [149] , the transcriptional activation of senescence-associated genes, and the simultaneous repression of mitotic genes [150,151] . The continued upregulation of p21 appears to fulfill an essential role in maintaining SIPS following exposure to therapeutic agents [124,125,146] . Intriguingly, this function can be achieved by the established p21-ATM positive regulatory loop [124,125] . Furthermore, the continuous p21-ATM interplay enhances the ability of cells that undergo SIPS to resist apoptosis. Experimental evidence of this phenomenon showed that cells undergoing SIPS experience apoptotic-induced cell death when either p21 or ATM is targeted [125] . In summary, research has established that WIP1 and p21 comprise anti-apoptotic factors functioning to block p53-mediated apoptosis in response to DNA damage through direct and indirect routes.

### **The relationship between p53 protein level and apoptosis**

During the last four decades, the phenomenon of p53-triggered programmed cell death, apoptosis, has constituted the focus of extensive studies. Several proposed scenarios explain the way in which various DNA-damaging agents affect p53 induction and hence lead to variable p53-mediated apoptotic responses.

First, ionizing radiation and moderate doses of other agents, such as UVC radiation, result in the activation of a p53-signaling pathway in which down-stream targets, such as WIP1 and p21, downregulate p53 and block apoptosis [152]. Natural UV irradiated light is classified according to its wavelength into short-wavelength (UVC range 200-290 nm), medium-wavelength (UVB range 290-320 nm) and long-wavelength (UVA range 320-400 nm) light. Based on this categorization, the biological activity and skin-penetrating capacity of irradiated light varies accordingly. Conventional experimental UVC (254 nm) induces bulky DNA lesions, known as pyrimidine dimers, which block the transcription of genes [153]. At moderate UVC doses, these bulky lesions are rapidly removed from the transcribed genes, such as WIP1 and p21, via specialized DNA repair machinery known as transcription-coupled nucleotide excision repair; consequently, intact p21 and WIP1 exert their anti-apoptotic effects. Thus, although ionizing irradiation (IR) itself does not induce bulky lesions, its effect on p53 signalling resembles moderate doses of UVC (below 30 J/m<sup>2</sup>) [126]. Both ionizing radiation and moderate doses of UVC activate the ATM-p53-p21-WIP1 or ATR-p53-p21-WIP1 pathways, which ultimately results in the down-regulation of p53, suppression of apoptosis, and growth arrest through SIPS [126].

On the other hand, the exposure to higher doses of UVC reveals a different course of action in p53 signalling. Following exposure to > 30 J/m<sup>2</sup>, the p53 protein becomes robustly upregulated, which severely diminishes the expression of its target genes. Hence, the consequent inability of the protein to express p53 negative regulators, such as p21, WIP1, and MDM2, causes cells to undergo apoptosis. This scenario is predictable because p53 triggers apoptosis through its proline rich region [154]. Therefore, high

doses of UVC trigger a p53 response that differs from that induced by moderate doses of other DNA-damaging agents, such as ionizing radiation or UVC radiation less than 30 J/m<sup>2</sup>.

In addition, the process of transfecting p53 null cells with a wild type p53 construct, in the absence of exogenous stresses such as irradiation, creates another scenario. In the absence of p53 activation by upstream factors, such as ATM and ATR, or down-regulation via WIP1 and MDM2, transfected cells will likely harbor a relatively high level of p53, triggering apoptosis via its proline region. Simultaneously, these cells will display an absence of p21-mediated cell cycle arrest.

## **p53 regulation in ATM-deficient cells**

The gene encoding ATM mutates in patients with the autosomal recessive disorder known as ataxia telangiectasia (AT), which is characterized by many clinical features, including susceptibility to cancer and a severe reaction to conventional radiotherapy [reviewed by Lavin et al. [155] ]. Furthermore, cells derived from AT patients demonstrate hypersensitivity to ionizing radiation based on evaluations using the clonogenic survival assay. Studies addressing the regulation of p53 following DNA damage in AT cells have lacked consistent results. According to Lu and Lane [156] , several skin fibroblast strains from different AT patients displayed a normal induction of p53 after exposure to ionizing radiation. Other groups, however, reported that an ionizing radiation-induced p53 upregulation appears reduced, delayed, or absent in different types of cells, such as skin fibroblast strains and lymphoblastoid cell lines, from different AT

patients [157-160] . In a recent study, immunofluorescence microscopy experiments have shown that AT fibroblasts exhibit upregulation and nuclear accumulation of p53 after ionizing radiation exposure; however, this effect represents an extremely delayed reaction rather than an earlier response to irradiation [160] .

Despite the thorough nature of the research on p53 regulation, several gaps still remain, especially questions concerning the regulation of p53 in different types of AT cells, such as fibroblasts and lymphoblasts, before and after exposure to ionizing radiation. While the availability of ATM has significantly increased the understanding of p53 regulation in normal cells, the mechanisms of p53 regulation in AT cells still remain unclear. Part of the challenge in studying the p53 response in AT cells involves the difficulty of growing and maintaining these cells in cultures. Skin fibroblasts from AT patients, for example, have a very short lifespan and experience a state of permanent growth arrest, known as replicative or cellular senescence, at early stages in a culture [160] . Due to the short lifespan of primary AT cell cultures, AT fibroblasts and lymphocytes undergo immortalization to facilitate their study. Two methods of immortalization that have led to the cloning of the ATM gene; the first method involves Simian virus 40 (SV40)-mediated transformation of the dermal fibroblasts in order to create SV40-transformed fibroblast cell lines. The second method entails Epstein-Barr virus (EBV)-mediated immortalization of the lymphocytes to create lymphoblastoid cell lines (LCL) cells. Subsequently, studies have demonstrated that the SV40 large T antigen binds to p53, increases its stability, and prevents its DNA binding capability [161] . Thus, SV40-transformed cells fail to constitute appropriate models for studying p53 regulation. Unlike SV40-transformation, EBV transformation refrains from interfering

with the p53 response in LCLs [162,163] . However, LCLs constitute difficult study models for two main reasons. First, these cells display a relatively slow rate of growth, particularly AT LCLs, which require a high concentration of serum (e.g., 20%). In addition, the clumping of LCLs enhances the difficulty of preparing single-cell suspensions that are required for many assays without causing physical damage to the cells; for instance, the vigorous pipetting motion of LCLs to break the clumps may destroy the cells.

## **Hypothesis, objectives, and main findings**

The laboratory of Dr. Roger Leng has contributed significantly towards providing understanding about the role of ubiquitin ligases in regulating the p53 tumour suppressor [86] . The focus of this present project, which has unfolded over the past five years, has aimed to determine the involvement of two such ligases, MDM2 and UBE4B, in p53 regulation, both before and after exposure to DNA-damaging agents in ATM-proficient (normal) and ATM-deficient (ataxia tenagictasia) human cells. In particular, the main research question seeks to understand whether UBE4B ubiquitin ligase contributes to the downregulation of wild type p53 protein in response to ionizing radiation. As shown in Figure 9, the hypothesis of the study conjectures that ATM or ATR phosphorylates p53, which affects its level and results in the disruption of UBE4B-p53 interactions in response to DNA damage. As a result of this hypothesis, the study also assumes that UBE4B constitutes a critical p53 negative regulator in an ATM or ATR dependent pathway following exposure to DNA damage.

In order to answer the research question and test the hypothesis, this study has established the following major objectives:

- i. To detect the induction levels of MDM2 and UBE4B ubiquitin ligases in wild type and ATM-deficient human cells after irradiation.
- ii. To investigate the phosphorylation status of p53 in wild type and ATM-deficient human cells following irradiation.
- iii. To explore any changes in the binding affinity between p53 and ubiquitin ligases MDM2 and UBE4B before and after exposure to ionizing radiation in wild type and ATM-deficient human cells.
- iv. To determine whether UBE4B promotes the proteasomal degradation of wild-type p53 in response to ionizing radiation in wild type ATM-proficient cells.
- v. To study the effect of irradiation on the subcellular localization of p53, MDM2, and UBE4B before and after irradiation in wild type ATM-proficient cells.

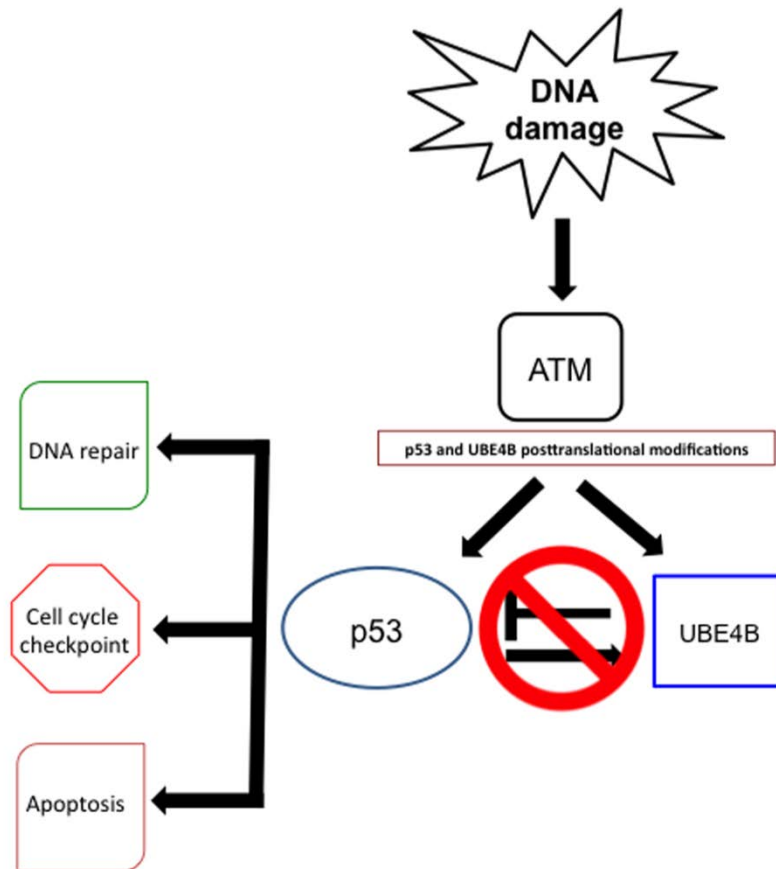


**Figure 9. Regulation of wild-type p53 proteins**

This model shows the plausible role of ATM, a p53-upstream protein kinase, in p53 regulation in response to ionizing radiation. In the absence of stress, UBE4B may contribute towards maintaining p53 at a basal level. After irradiation, both p53 and UBE4B might undergo phosphorylation at their interaction sites, which block their binding and thus stabilizes p53. Consequently, activated p53 induces its mediated DNA damage response, contributing to genomic integrity.

By the end of the study, the results revealed that along with MDM2, UBE4B experiences invariable induction and interacts with p53 in response to ionizing radiation in both ATM-proficient and ATM-deficient cells. In addition, consistent with other studies, UBE4B binds and degrades phosphorylated p53 in response to ionizing radiation in ATM-proficient cells. Interestingly, UBE4B co-localizes with p53 in the cytoplasm, which provides double insurance of its potential negative regulatory function. Several E3 and E4 ubiquitin ligases reportedly engage in p53 degradation pathways. UBE4B ubiquitin ligase has been proposed as a main contributor to MDM2-mediated p53 degradation *in vivo* and *in vitro*. The findings in this study support the UBE4B-related research that proposes UBE4B as a potential negative regulator of p53 in response to DNA damage. These results may springboard a wide range of future molecular biological studies that aim to uncover the previously unexamined potential role of UBE4B in various contexts of DNA damage response.

## *Chapter 2*

### *Materials and Methods*

# Materials and Methods

## Cell Cultures

Wild type EBV-transformed lymphoblastoid cell lines (GM03714) and two strains of ATM-deficient (AT) EBV-transformed lymphoblastoid cell lines (AT LCLs) (GM0719B and VKE) were generously supplied by Associate Clinical Professor Razmik Mirzayans (University of Alberta, Cross Cancer Institute, Edmonton, AB, Canada). Furthermore, human breast cancer (MCF7) and normal (MCF10A) cell lines, in addition to human H1299 (lung cancer) and HCT116 (colon cancer) adherent cells, were employed in the study. Wild-type LCL cells, breast cancer cells, H1299 cells, and HCT116 cells were cultured in Basic DMEM Non-GMP Formulation with Dulbecco's Modified Eagle medium, supplemented with 10% fetal bovine serum along with 1X nonessential amino acids and penicillin/streptomycin (Life Technologies Corporation, USA). AT cells were maintained in Basic RPMI media 1640 supplemented with 15% fetal bovine serum plus X non-essential amino acids and penicillin/streptomycin (Life Technologies Corporation, USA). Subsequently, cells were incubated in a humidified chamber at 37 °C with 5% CO<sub>2</sub>. Adherent cells were trypsinized in a Trypsin-EDTA solution (Sigma Life Science, USA) at a final concentration of 1.3X. Then, cells were re-cultivated according to the estimated growth rate of each cell type.

## **Gamma irradiation treatment**

Cells were subjected to 2 Gray and 6 Gray of gamma irradiation using a Gammacell Co-60 Self-Shield irradiator in the Department of Experimental Oncology, University of Alberta.

## **UV light treatment**

U.V treatment executed using Spectroline UV Crosslinker Select™ Series. UV wavelength was set to 254 nm in all experiments. For dose dependent assays, cells were treated and left for 3 h in incubator at 37°C followed by harvesting.

## **Protein Analysis**

### **Cell harvesting**

After irradiation, cells were maintained in a humidified environment before being harvested at different points over a 24 h period. Cell harvesting was conducted in a cold ice environment; the adherent cells were washed twice using 1X PBS (137 mM NaCl, 2.7 mM KCl, 10 mM Na<sub>2</sub>HPO<sub>4</sub>, and 2 mM K<sub>2</sub>HPO<sub>4</sub>). Subsequently, cells were scraped and transferred to a micro-centrifuge tube, where centrifugation occurred at room temperature. Pellets were then lysed using a lysis buffer containing 50 mmol/L Tris-HCl (pH 7.4), 1 mmol/L EDTA, 150 mmol/L NaCl, and 1% NP-40 mixed with a 10X protease inhibitor (Roch). Next, the pellets were vortexed, sonicated and finally centrifuged at 4° C; the cell lysate was then extracted. Likewise, EBV-transformed suspension cells were lysed in the same manner but without the initial scraping.

## **Protein Quantification**

Proteins were quantified using the Bio-Rad Protein Assay as per manufacturer instructions (Bio-Rad Protein Assay Dye Reagent Concentrate, BioRad Laboratories, Inc., USA).

## **Sodium Dodecyl Sulphate Poly-acrylamide Gel Electrophoresis (SDS-PAGE) Analysis and Transfer**

A SDS-PAGE analysis was conducted for both the western blot and Co-IP assays. Gel mixtures (10-11%) were prepared by mixing H<sub>2</sub>O and 40% Acrylamide/Bis-Acrylamide mix solution at a ratio of 37.5:1 (BioShop Canada Inc., Burlington, ON), 1.5 M Tris pH 8.8 (Tris hydroxymethyl aminomethane, USB Corporation, Cleveland, OH, USA), 10% Sodium Dodecyl Sulphate (SDS) (BioShop Canada Inc., Burlington, ON), 98% Ammonium persulfate for electrophoresis (APS) (SIGMA, USA), and 100% TEMED (N,N,N - Tetramethylethylene-diamine, Sigma, China). The mixture was then covered with Isopropanol and dried for 30-40 minutes. After undergoing rinsing, gels were stacked in a 5.1% solution containing 1 M Tris pH 6.8 as well as other ingredients used in gel preparation, including H<sub>2</sub>O, 40%, Acrylamide mix, 10% SDS, 10% APS, and 100% TEMED. Then, a running buffer consisting of Tris base, Glycine (BioShop, Burlington, ON), 10% SDS was used to electrophoretically separate the various proteins (30 mA per gel). **Approximately** 50 µg-80 µg concentrations of total protein lysate were loaded. 2X SDS was used as a loading buffer, which contained 100 mM Tris Cl (pH 6.8), 10% SDS prepared from the stock, 4% (W/V) SDS electrophoresis grade, 0.2% Bromophenol blue (Sigma-Aldrich, USA), and 20% (V/V) Glycerol (USB Corporation,

Cleveland OH, USA), added to 10% of the freshly prepared stock of 200 mM 2-Mercaptoethanol (Sigma Aldrich, Arkema Inc, USA). Gel proteins were then transferred to a Polyvinylidene difluoride (PVDF) membrane (Immunobilon, EMD Millipore Corporation, Billerica, MA, USA). A semi-dry gel transfer approach was employed using serial buffers that include three buffers. First, anode buffer I contained 0.3 M Tris base with Tris hydroxymethyl aminomethane ultrapure, MB Grade (USB Corporation, Cleveland, OH, USA) and 15% methanol (Fisher Scientific, Fair Lawn, New Jersey, USA) diluted in distilled water. Anode buffer II contained 0.025 M Tris base, 15% methanol, and distilled water, while cathode buffer III contained 0.025 M Tris base, 0.04 M 6-amino-n-caproic acid (BioShop Burlington, ON), 15% methanol, and distilled water. The transfer was executed applying 75 mA per gel. After the transfer of proteins to the PVDF membrane, the membranes remained dry at room temperature for 24 h and then kept at 4°C before further processing.

### **Western Blot Analysis**

Following the transfer of proteins to the PVDF membrane, the membranes remained dry at room temperature for 24 h before being kept at 4°C. The immunoblotting assay was initiated by blocking the membranes with 5% Tris buffered saline, milk, and Tween (TBSTM) (50 mM Tris HCl, 150 mM NaCl, 0.1% [v/v] Tween 20, and 5% milk) solution for 1 h. After blocking, membranes were washed 3 times for 10 minutes each time with Tris buffered saline and Tween (TBST). The membrane proteins were then incubated with designated primary antibodies for 1.5-2 h at room temperature. Subsequently, proteins were washed in TBST solution for 3 cycles of 10 minutes

washing/incubation per cycle; this process ensured the removal of unbound primary antibodies. Phospho-antibodies, which served to detect phosphorylated p53, were incubated overnight at 4°C. Membranes were further exposed to appropriate secondary antibodies for 1 h and then washed in TBST solution for 3 cycles of 10 min washing/incubation per cycle in order to remove unbound secondary antibodies. Finally, proteins were detected following one minute of exposure to an ECL detection kit (Western Lightning Plus-ECL, Enhanced Chemiluminescence Substrate, PerkinElmer, USA). Exposed films were developed in an OPIMAX X-Ray Film Processor (PROTEC GmbH & Co. KG, Germany)

## **Antibodies**

The immunoblot detection of various proteins was conducted using Anti-DO-1 or Anti-Pab 1801 or Anti-FL 393 for human p53, Anti-MDM2 (SMP14) and Anti-2A10 (EMD, Bioscience) for MDM2, and Anti-UFD2 for UBE4B (Santa Cruz Biotechnology, Inc., Dallas Texas, USA). The phosphorylation study was performed using Anti-human Ser15, Anti-human Ser20, Anti-human Ser392, and Anti-human Ser 37 (Phospho-p53 Antibody Sampler Kit, New England BioLabs Ltd., Whitby, Ontario, Cell Signaling Technology). In addition, ATM (D2E2) Rabbit mAb #2873 antibody, and ATR antibody #2790 (Cell Signaling Technology) were used to detect ATM and ATR respectively. Anti-Actin (Sigma) was employed for detecting the loading control (Beta Actin). Oct-1 (12F11; Santa Cruz Biotechnology) and tubulin (Sigma) were used for cell fractionation analysis. Finally, Myc-specific antibody (9E10), Roche, and HA (12CA5), were used in Co-IP analysis.

## **Immunoprecipitation Analysis**

Cell lysis was executed using a non-denaturing lysis buffer (50 mmol/L Tris-HCl pH 7.4, 1 mmol/L EDTA, 150 mmol/L NaCl, and 0.5% NP40) as well as a protease inhibitor tablet (Roch). Cell lysates were sonicated, centrifuged for clarification, quantified for protein, and immunoprecipitated with the designated antibodies. The immunocomplexes were captured with protein A Agarose beads (Protein A/G PLUS-Agarose, Santa Cruz Biotechnology), incubated overnight at 4°C, and washed three times with a lysis buffer. Unlike the previous buffer, this one contained an NP-40 concentration reduced to 0.2% and a protease inhibitor tablet (Roch). The immunocomplex was eluted using 2X SDS loading buffer that contained 100 mM Tris HCl [pH 6.8], 10% SDS prepared from 4% [W/V] SDS electrophoresis grade stock, 0.2% bromophenol blue [Sigma-Aldrich, USA], 20% [V/V] glycerol (USB Corporation, Cleveland OH, USA), and 10% freshly prepared 200 mM 2-mercaptoethanol stock (Sigma Aldrich, Arkema Inc., USA). The eluted immuocomplex was analyzed using SDS-PAGE followed by western blot analysis (as described above) .

## **Cell viability assay**

Cell viability was determined by the use of trypan blue vital stain (0.4%, Gibco, Life Technologies Corporation, USA). Following irradiation, cell suspensions of ATM-proficient and ATM-deficient LCL cells were diluted with 1X phosphate buffer saline (PBS) (137 mM NaCl, 2.7 mM KCl, 10 mM Na<sub>2</sub>HPO<sub>4</sub>, 2 mM K<sub>2</sub>HPO<sub>4</sub>) (1:1 or 1:2 ratio depending on the confluence of the cell suspension), and incubated with trypan blue dye (9:1 cells:dye ratio), for 1-3 min at room temperature. Trypan blue- positive (blue) cells

were manually examined and counted under a light microscope (Nikon ECLIPSE TS100, China) using a grid-counting chamber (0.100 mm deep, Neubauer Brightline, USA) according to manufacturer instructions.

## **DNA transfection, plasmids, reagents and antibodies**

Conventional calcium phosphate methodology was employed for both transient and stable transfection protocols, as described previously [86,164]. The various p53 mutants, including S15A, S392A and 2A, were made using a QuickChange site-directed mutagenesis kit (Stratagene, USA). Sequencing was used to verify all of the plasmids.

## **Subcellular fractionation**

Cell fractionation analysis was carried out according to the manufacturer's instructions (ProteoJET Cytoplasmic and Nuclear Protein Extraction Kit, Fermentas; or NE-PER Nuclear Protein Extraction Kit, Pierce; or Cytoplasmic and Nuclear Protein Enrichment Kit, Amresco).

## **Densitometry analysis**

All results are repeats of at least three independent experiments.  $\beta$ -actin was used as a loading control. Densitometry on Western blots or Co-IP was performed with ImageJ software (<http://rsb.info.nih.gov/ij/index.html>). The detailed method is outlined in the ImageJ documentation: <http://rsb.info.nih.gov/ij/docs/menus/analyze.html#gels>. In brief, a film was scanned at 300 dpi in TIFF file format. The image file is opened using File>open in ImageJ. A gray-scale image is converted to 8-bit. The relative p53 or

UBE4B or MDM2 band intensity normalized to  $\beta$ -actin for the Western blots or normalized to IgG heavy chain for the Co-IP experiments.

## **Flow cytometric analysis**

A flow cytometric assay was used to analyze cell cycle distribution by quantifying various fractions of cells that undergo G1, S, and G2/M phases. This procedure was conducted by using fixed cells stained with propidium iodide dye to label DNA. The amount of labeled DNA is proportional to the corresponding phase; specifically, the DNA content in G2/M cells is twice as much as that in G1 cells, while cells in the S phase have an intermediate amount of DNA.

Both wild-type GM03714 and mutant GM0719B LCL cells were subjected to the same treatment and analysis, which involved two repetitions. Cells were either treated with 6 Gy of IR or left untreated, harvested after 3 h, and re-suspended in cold (4°C) flow cytometry staining (FSC) wash buffer (0.5% FBS, 1 mM EDTA, and 0.05% sodium azide in PBS). The washing process underwent two repetitions. The cell number from each aliquot was estimated using a Bright Line Counting Chamber 3200 (Hausser Scientific, USA) with Trypan blue. The process used 1 mL of each aliquot containing equal number of cells (2 million cells/mL). Then, 7 mL of cold 70% ethanol, which was previously prepared and kept at -20°C, was used as a fixative. To fix the cells, cells were added to 70% ethanol drop-wise with a gentle shaking to minimize clumping and cell loss. The fixed cells were kept at -20°C overnight and subsequently centrifuged at 800 XG for 5 min before undergoing re-suspension in FCS wash buffer; the washing process was repeated twice. Afterwards, cellular DNA was stained by 1 mL of propidium iodide

dye, which contained 50  $\mu\text{g/ml}$  PI, 3.8 mM sodium citrate (Sigma Aldrich, USA) (Worthington Biochemicals, USA). In order to exclude unwanted RNA, 5  $\mu\text{L}$  of a working RNase A solution, (10  $\mu\text{g/ml}$  RNase A) stored at  $-20^{\circ}\text{C}$ , was added. A stock solution of RNase A (10 mg/ml) (Worthington Biochemicals, USA) was used to prepare the RNase working solution. Then, the mixture was covered in foil to reduce the light effect and ensure maximal dye staining efficiency as well as incubated at  $4^{\circ}\text{C}$  for 3 h before flow cytometry was conducted in the Flow Cytometry Core (Faculty of Medicine, University of Alberta). FlowJo 7.6.1 software (Tree Star, Ashland, OR) was used to analyze data readouts. The average PI absorbance for various cell populations (G1, S and G2/M) was calculated. Then, untreated cells were used as a control to assess the effect of the treatment (IR) on cell cycle arrest. Cell cycle arrest at G0/G1 was evaluated by calculating the G1/S ratio and statistical analysis was executed using SPSS, 7.0. Error bars represent the standard deviation and statistically significant difference between the averages of ratios, which was analyzed using an unpaired student's *t*-Test without assuming equal variance.

# *Chapter 3*

## *Results*

## Results

The investigation of p53 regulation in ATM-deficient cells requires the use of AT cells. In this study's experimental design, EBV-transformed LCL AT cells were selected among other proposed cell models because these cells possess technical advantages over other types of AT cells.

A major technical problem with studying AT cells involves the difficulty of growing and maintaining these cells in cultures. For example, skin fibroblasts from AT patients have a very short life span and enter a state of permanent growth arrest known as replicative or cellular senescence during early passages in culture [160]. Due to the short life span of primary AT cell cultures, AT fibroblasts and AT lymphocytes have undergone immortalization to facilitate their study. Two methods of immortalization facilitated the cloning of the ATM gene: SV40-mediated transformation of dermal fibroblasts to create SV40-transformed fibroblast cell lines, and EBV-mediated immortalization of lymphocytes, which give rise to LCLs. Subsequently, the investigation demonstrated that the SV40 large T antigen binds to p53, increases its stability, and prevents its DNA binding ability [161]. Unlike SV40-transformation, EBV transformation seems not to influence the p53 response in LCLs [162,163]. Since neither AT skin fibroblasts nor isogenic SV-40-transformed AT cells represented proper models, EBV-transformed LCLs AT cells were employed.

## **Characterization of LCL cells: Radiation -induced loss of cell viability in normal and AT lymphoblastoid cells**

The gene-encoding ATM undergoes mutation in patients with the autosomal recessive neurodegenerative disorder known as ataxia telangiectasia (AT). Clinical features of AT include a lack of muscle coordination (ataxia), dilatation of blood vessels around the eye (ocular telangiectasia), immunodeficiency, and increased vulnerability to cancer [155] . In the 1960s, studies showed that AT patients experienced a severe reaction to conventional cancer radiotherapy, known as hyper-radiosensitivity [165] , and in the 1970s, cultured cells derived from AT patients and carriers exhibited hypersensitivity when evaluated using the clonogenic survival assay [166,167] . The process of cloning the ATM gene and uncovering its pivotal role in the DNA damage response elucidated the molecular basis of AT pathogenesis and correlated ATM with clinical features. Research found that ATM activated several downstream effectors involved in DNA damage responses, such as cell cycle arrest, DNA repair, apoptosis, and SIPS. Thus, ATM mutations impair the activation of cell cycle checkpoints, hence hindering the ability to efficiently repair DNA double strand breaks and aberrant apoptosis/SIPS [126,159,168] . The final outputs of these events may assist in developing the main cellular and clinical features of the A-T illness, such as genomic instability, radiosensitivity, higher cancer susceptibility, and neurodegeneration [168] .

As noted above, AT cells are extremely radiosensitive in colony-forming assays [166,167] . This radiosensitivity undergoes detection several days after irradiation, which mainly reflects radiation-induced growth arrest rather than apoptosis [126,160] . Therefore, the expectations at the outset of this research project assumed that AT LCLs

were more radiosensitive than normal LCLs. To assess the cell viability of EBV-transformed AT LCLs, trypan blue-positive cells were counted in both wild type and AT LCLs in response to gamma irradiation. Surprisingly, the results found that trypan blue-positive cells demonstrated comparable levels in wild type and AT LCLs over a 24 h period following irradiation (Figure 10). Interestingly, these findings demonstrate consistency with previous 1996 studies, which reported that AT LCLs lacked radiosensitivity based on the loss of viability [169] . Most importantly, these data indicate the lack of significant difference in the loss of cell viability between normal and AT LCLs when measured within 24 h of irradiation. These results assist in the interpretation of the obtained data by excluding plausible interfering effects of excessive death from artefacts such as apoptosis-associated breaks in the AT cell models.

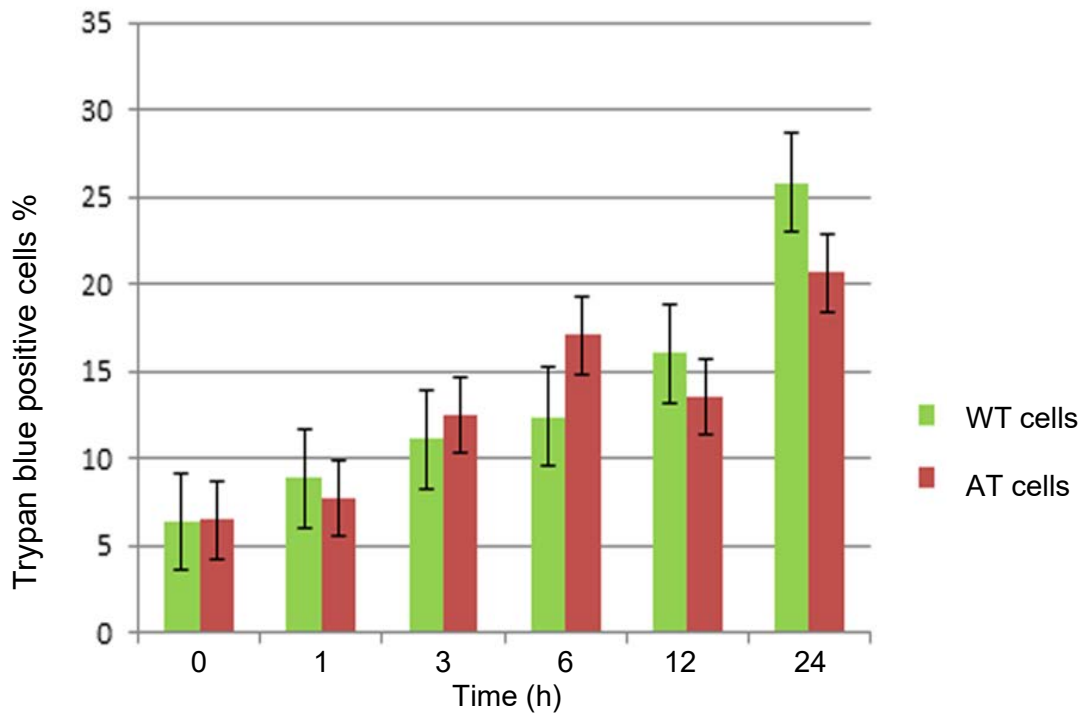


**Figure 10. AT LCLs show normal cell viability**

Wild-type (GM03714) and AT (VKE) cells were subjected to 6 Gy of IR. Cells were collected over the indicated time points. Loss of cell viability was assessed by the trypan blue assay. Ratios of number of trypan blue-positive (non-viable) versus total number of trypan blue-free (viable) and non-viable cells were recorded and compared.

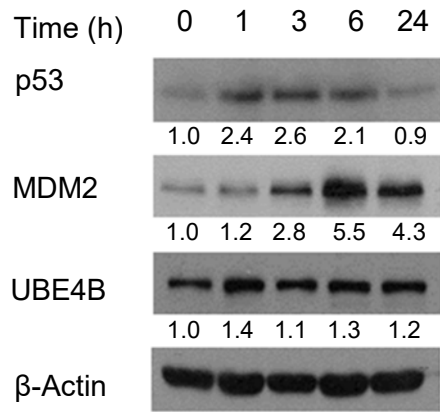
## **MDM2 and UBE4B are upregulated in response to DNA damage**

MDM2 and UBE4B constitute two essential p53 ubiquitin ligases. While research has extensively studied the role of MDM2 in ATM-dependent p53 regulatory pathways [156,170], the behaviour of MDM2 in ATM-independent p53 pathways remains largely unknown. Furthermore, investigations acknowledge the contribution of UBE4B in MDM2-mediated p53 ubiquitination and degradation *in vitro* and *in vivo* [86]; however, its role in regulating p53 in response to DNA damage has not been previously investigated in LCL cells. p53 is activated by gamma radiation [157], which undergoes routine utilization in cancer therapy. Specifically, fractionated doses such as 2 Gy and 6 Gy are employed in clinical radiotherapeutic modalities of cancer.

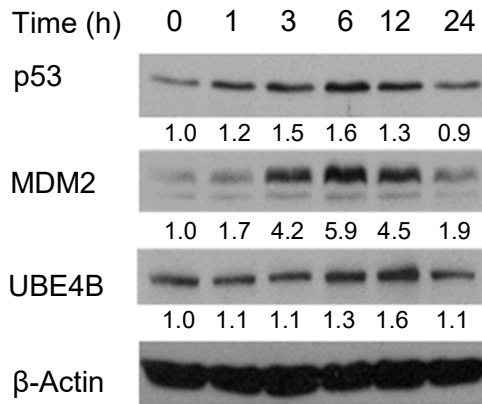
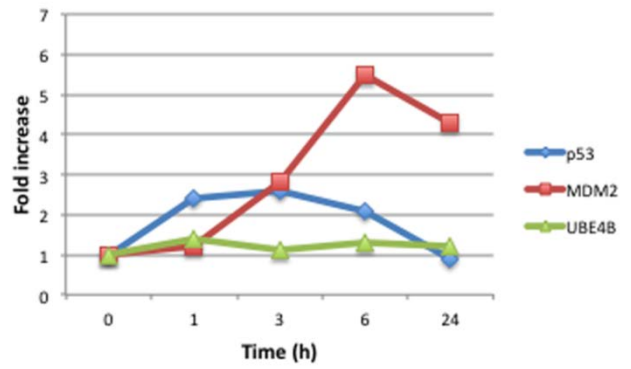
The protein levels of MDM2 and UBE4B in ATM-proficient and ATM-deficient cells were studied in response to p53 activation. Accordingly, wild type and AT EBV-transformed LCLs were subjected to IR (6 Gy and 2 Gy), harvested following indicated durations within 24 h and analyzed by immunoblotting. Initially, as in wild type cells, p53 induction occurred in the mutant cells (Figure 11), suggesting that p53 regulation in AT cells may not be exclusively ATM-dependent.

The induction of ubiquitin ligases in AT LCL cells (GM0719B, VKE cells) revealed that IR appears to upregulate MDM2 and UBE4B levels in a similar manner over time as in wild-type LCL cells (GM03714). Upregulation begins at 1 h and steadily continues until 6 h following exposure to either 6 Gy (Figure 11 A-C) or 2 Gy (Figure 11 D-F) of IR.

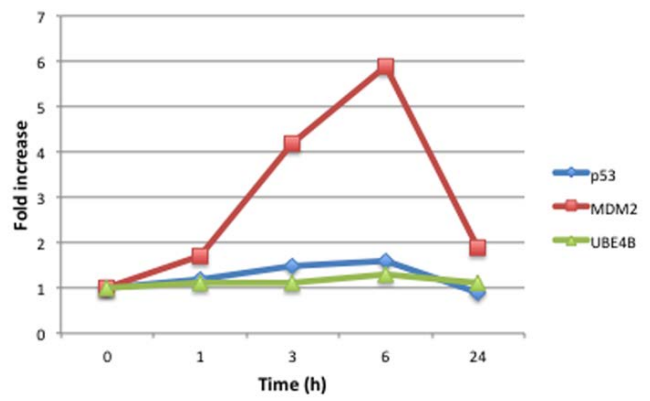
Densitometry analysis revealed that following exposure to 6 Gy, MDM2 clearly showed a gradual increase, reaching a peak of 5.5, 5.9, and 3.1 folds at 6 h in wild type, GM0719B, and VKE cells respectively followed by a decrease at later time points. In addition, UBE4B demonstrated a relatively overall lower fold increase over the tested time period with a peak at different time points (1.4 at 1 h in wild-type cells, 1.6 at 12 h in GM0719B cells, 2.5 at 3h in VKE cells). A drop in UBE4B induction at 24 h was noticed in all cells (Figure 11 A-C). Similarly, in response to 2 Gy, densitometry analysis showed a fold increase of MDM2 and UBE4B starting at 1 h and reach its peak at 6 h in wild-type and mutant cells (Figure 11 D-F).



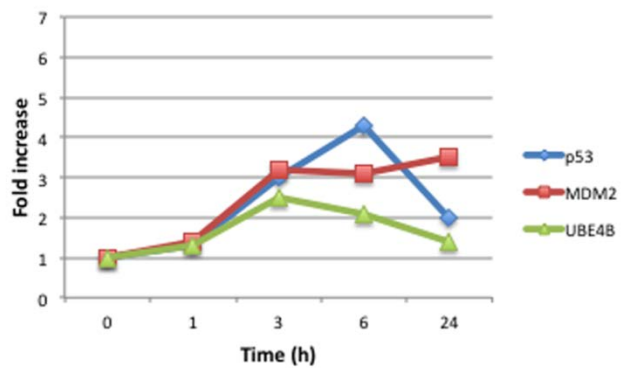
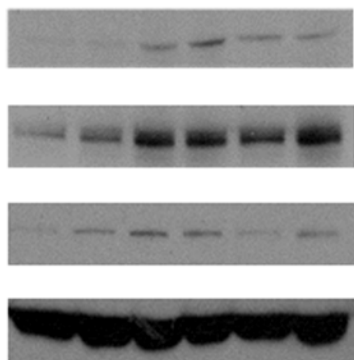
A

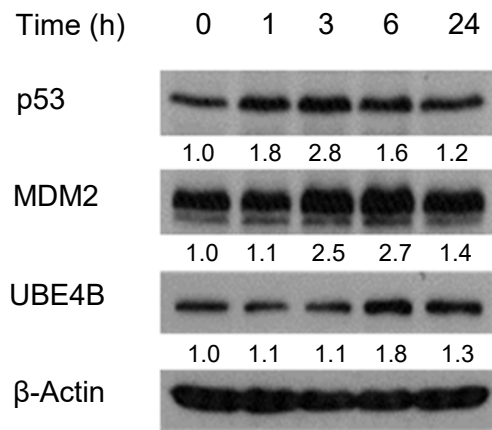


B

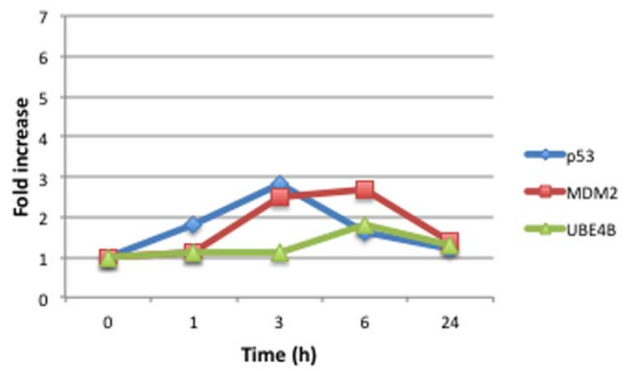


C

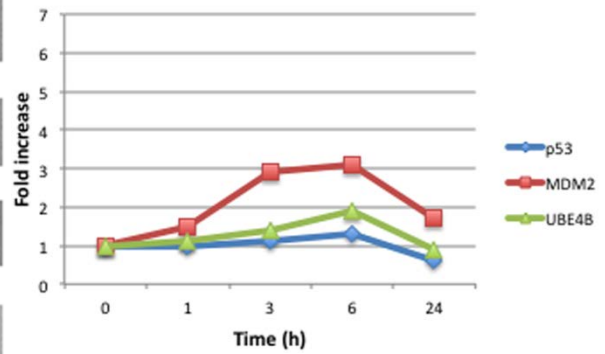
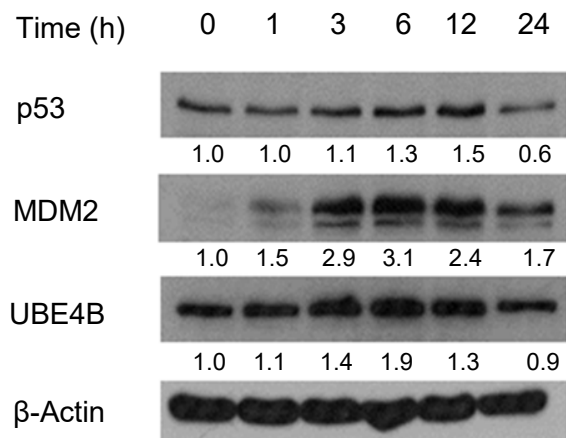




D



E



F

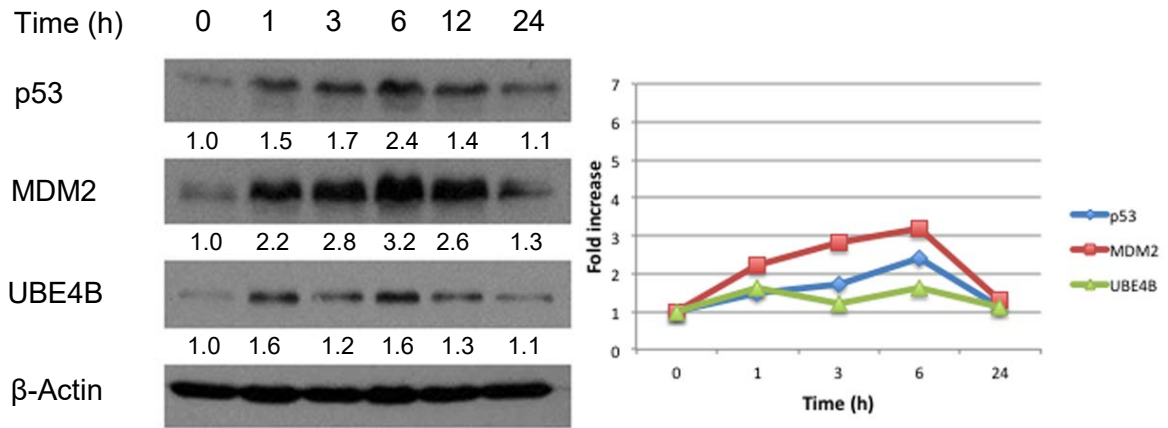


**Figure 11. Induction of ubiquitin ligases (MDM2 and UBE4B) post-irradiation in LCL cells (6 Gy, 2 Gy)**

Following treatment with 6 Gy of IR, cells were collected at different time points over a 24 h period and protein-induced ubiquitin ligases (MDM2 and UBE4B) were detected by western blotting in wild type cells (GM03714) (A), (B) in AT cells (GM0719B) and (C) in AT (VKE) LCL cells. Likewise, following treatment with 2 Gy of IR, cells were collected at different time points over a 24 h period and protein-induced ubiquitin ligases (MDM2 and UBE4B) were detected by western blotting in wild type cells (GM03714) (D), (E) in AT cells (GM0719B) and (F) in AT (VKE) LCL cells. In all cases,  $\beta$ -Actin was used as the loading control. Densitometry was performed with ImageJ software (NIH) and relative MDM2 or UBE4B band intensity was normalized to  $\beta$ -actin. Corresponding graphs demonstrate the densitometry analysis of the western blots, which represent a minimum of two replicates.

To gain further insight into the role of ligases in human cancer cells, the protein levels of MDM2 and UBE4B in response to IR were investigated in a wild type p53 human breast cancer cell line (MCF7) and normal human breast cell line (MCF10A). The exposure of both cells to 6 Gy of gamma radiation elevated the level of p53 and UBE4B at 2 h while the level of MDM2 increased at 3 h (Figure 12 A, B). A very low level of MDM2 occurred at 0 h, 1 h, and 2 h following DNA damage in MCF7 and MCF10A cells (Figure 12A and 12B). Strikingly, UBE4B decreased below the baseline level at later stages of post-irradiation (6 h) in normal human breast cells (Figure 12B).

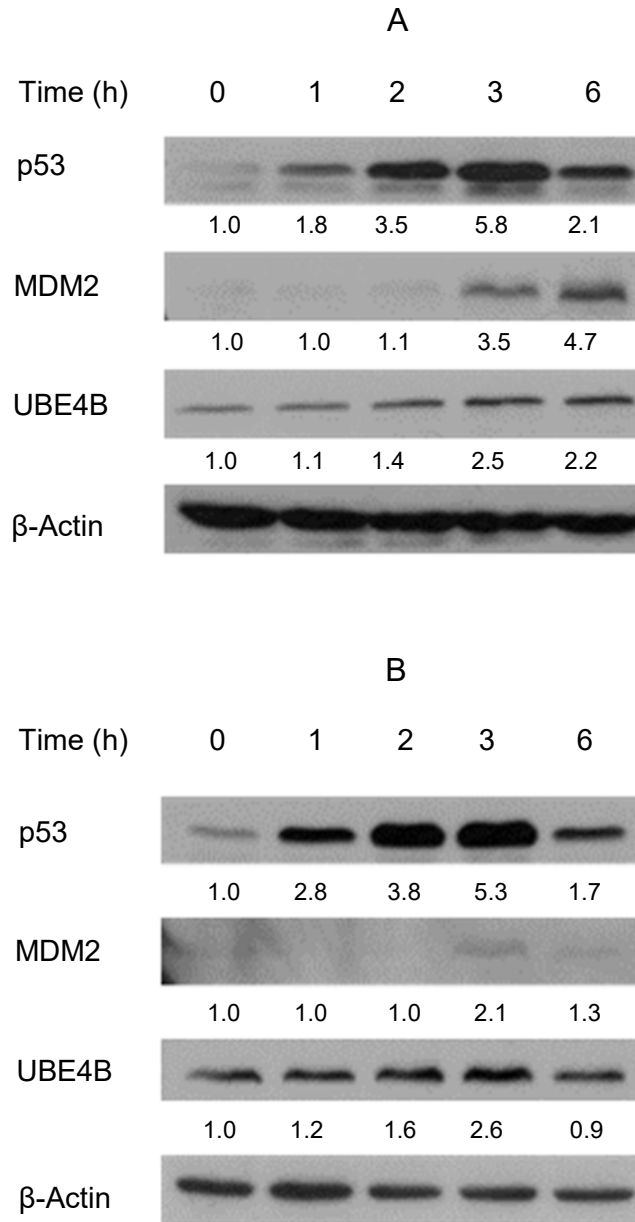


**Figure 12. Induction of ubiquitin ligases (MDM2 and UBE4B) post-irradiation with 6 Gy in human breast cell lines**

Following treatment with 6 Gy of IR, cells were collected at indicated time points and protein induced ubiquitin ligases (MDM2 and UBE4B) were detected by western blotting in MCF7 (**A**), and MCF10A cells (**B**). In all cases,  $\beta$ -Actin was used as the loading control. Densitometry was performed with ImageJ software (NIH) and relative p53 or MDM2 or UBE4B band intensity was normalized to  $\beta$ -actin. These blots represent a minimum of two replicates.

## **p53 phosphorylation at Serine 15 and Serine 392 in LCLs is dose-independent and ATM-independent**

Following exposure to DNA-damaging agents, Ser15, Thr18, and Ser20 constitute crucial phosphorylation sites for p53 protein stabilization [53,54]. These phosphorylation processes occur via a number of protein kinases, including ATM and ATR [55,56]. Thus, the determination of p53 phosphorylation status may reveal the prospective role of ATM in p53 regulation in AT LCL cells. By identifying the protein kinase, such as ATM or ATR, involved in p53 phosphorylation and correlating the kinase with detected ubiquitin ligases proteins, researchers can understand the role of p53 post-translational modifications in p53 stabilization for all studied cells.

The p53 phosphorylated proteins, Ser15, Ser20, Ser37 and Ser392, were elevated at 1.5 h and mostly reached their maximum levels at 3 h following 6 Gy of IR in MCF7 cells (Figure 13A). On the other hand, the maximum levels of p53 phosphorylated proteins, Ser15, Ser20, Ser37, and Ser392, were detected at 1.5 h in MCF10A cells (Figure 13B)

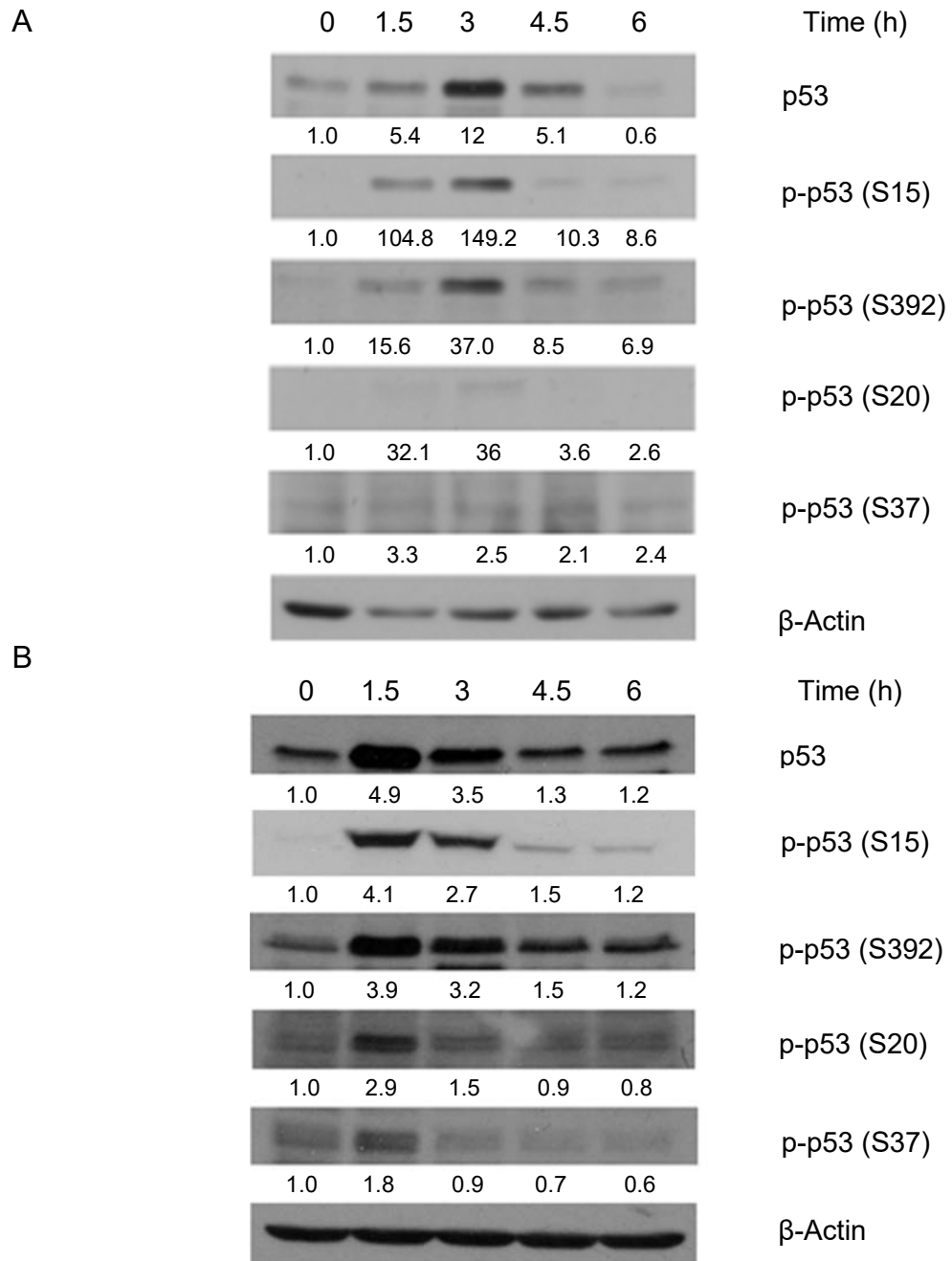


**Figure 13. p53 phosphorylation post-irradiation in human breast cell lines**

Following treatment with 6 Gy of IR, cells were collected at designated time points to detect p53 phosphorylated sites at Ser15, Ser392, Ser37 and Ser20 using (Phospho-p53 Antibody Sampler Kit, Cell Signaling Technology) in MCF7 cells lines **(A)**, and **(B)** MCF10A cell lines. In all cases,  $\beta$ -Actin was used as the loading control. Densitometry was performed with ImageJ software (NIH) and relative p53 or p53 Ser15 or p53 Ser392 or p53 Ser20 or p53 Ser37 band intensity was normalized to  $\beta$ -actin. These blots represent a minimum of two replicates.

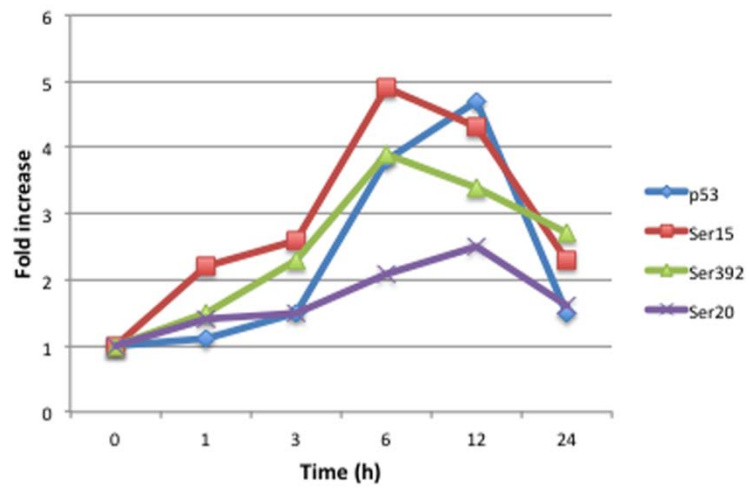
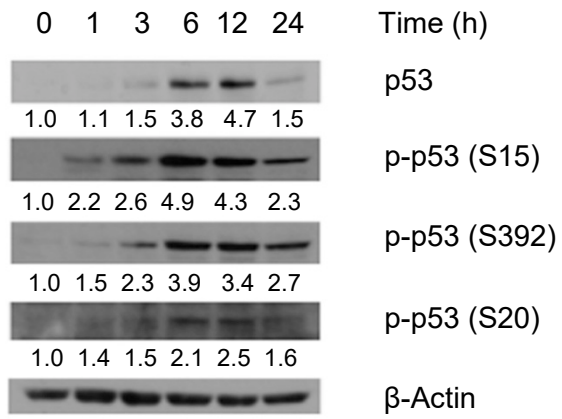
An initial screening for the potential engagement of phosphorylation sites, including Ser6, Ser9, Ser15, Ser20, Ser37, Ser46, Ser392, and Thr18, occurred in LCL cells. Only three residues, Ser15, Ser20 and Ser392, were detected in the EBV-transformed LCL cells (Figure 14 A-C).

Upon exposure to 6 Gy, similar phosphorylation patterns of p53 occurred at Ser15 and Ser392 residues in wild type cells (Figure 14A) and two ATM-mutant (Figure 14 B,C) LCL cells. In both types of cells, the levels of the phosphorylated p53 at Ser15 and Ser392 gradually started to increase at 1 h and declined after 12 h. Likewise, when exposed to 2 Gy (Figure 14 D-F), both normal and mutant LCL cells exhibited the same pattern of phosphorylation.

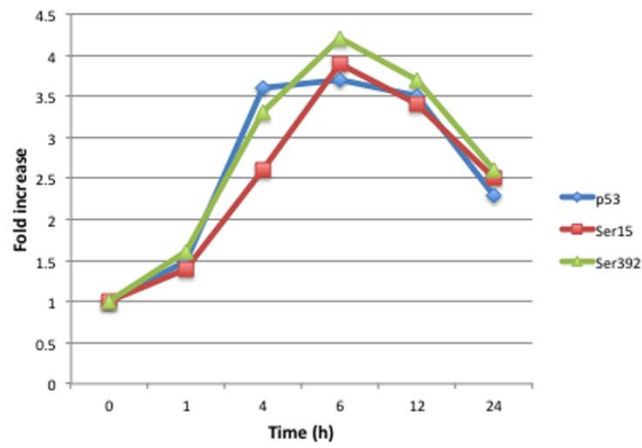
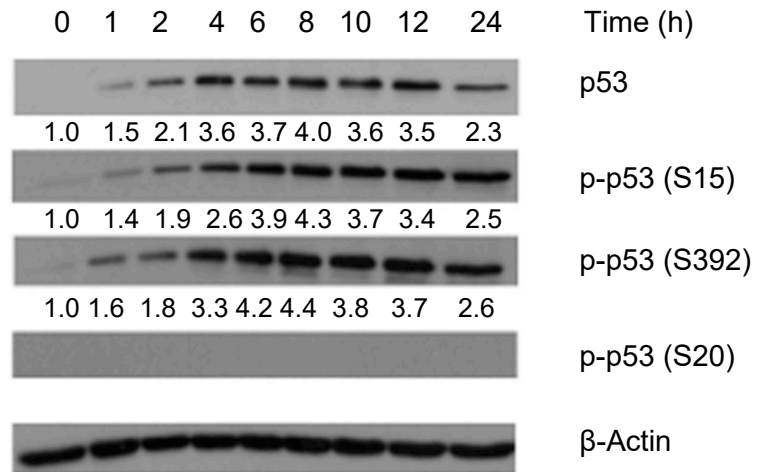
Collectively, these observations indicate that p53 phosphorylation occurs at Ser15 and Ser392 residues in these cells. Hence, p53 activation is not exclusively ATM-dependent. Although most studies associate the efficient phosphorylation of p53 at Ser392 with UV-induced DNA damage [171,172], the findings in this study, which use IR, demonstrate consistency with the data released by other reports linking modified p53 at Ser392 with other stressors [173].

In addition, p53 phosphorylation in LCL cells may exhibit a dose-independent relationship. The results revealed that following exposure to 6 Gy, p53 phosphorylation at the Ser20 residue occurs exclusively in wild type cells (Figure 14A). However, exposure to 2 Gy resulted in the induction of Ser20 in both wild-type and mutant LCL cells (14 D-F), indicating that Ser20 phosphorylation might be ATM-dependent in a dose-dependent manner. This finding demonstrates consistency with previous studies, which failed to induce Ser20 in several AT cells at early stages of post-irradiation [174].

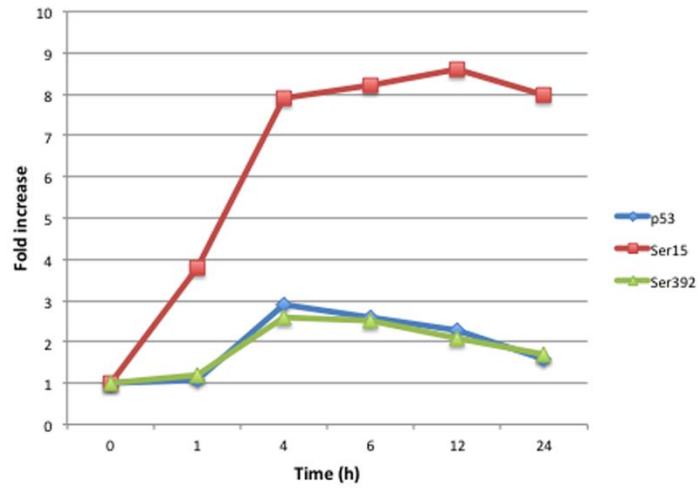
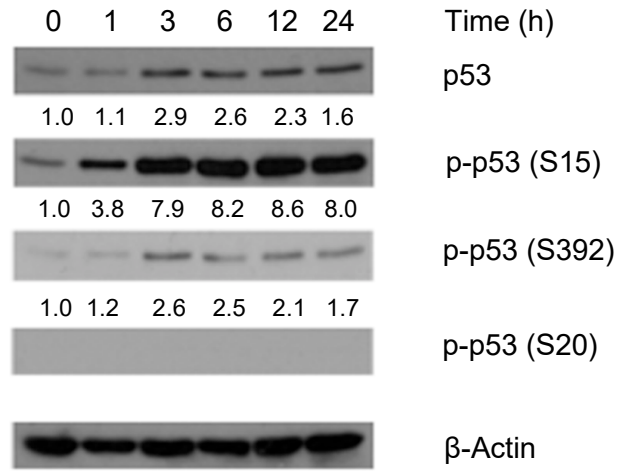
A



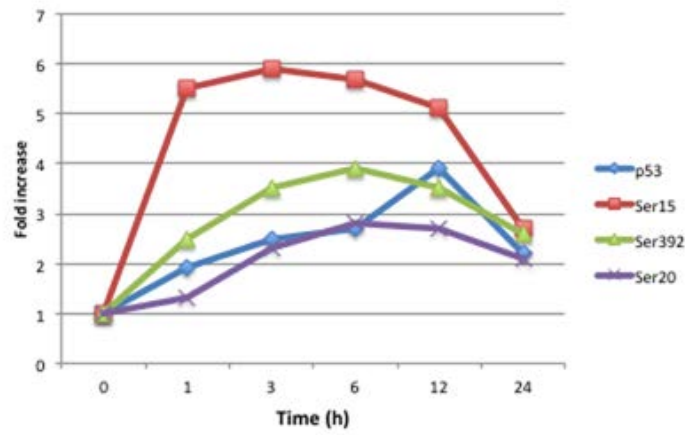
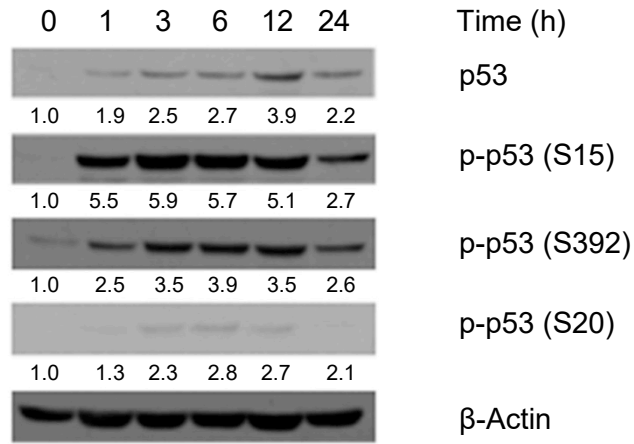
B



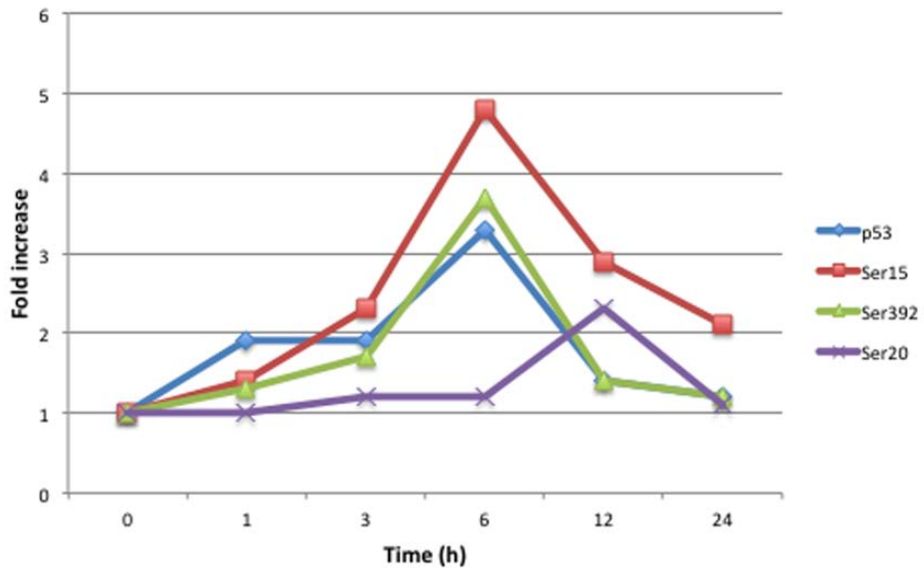
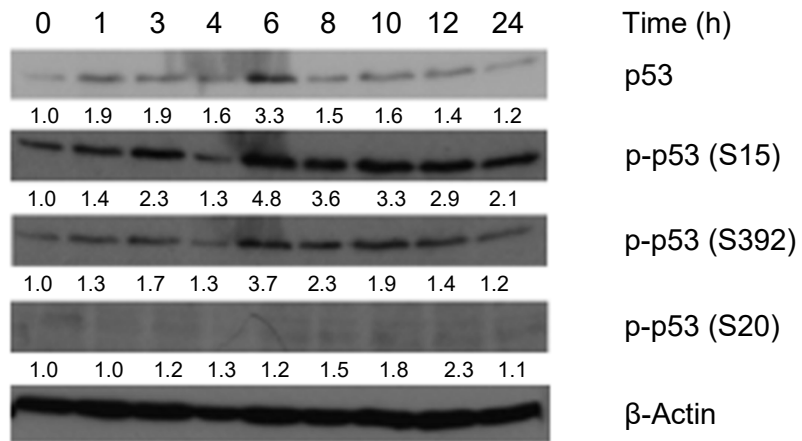
C



D



E



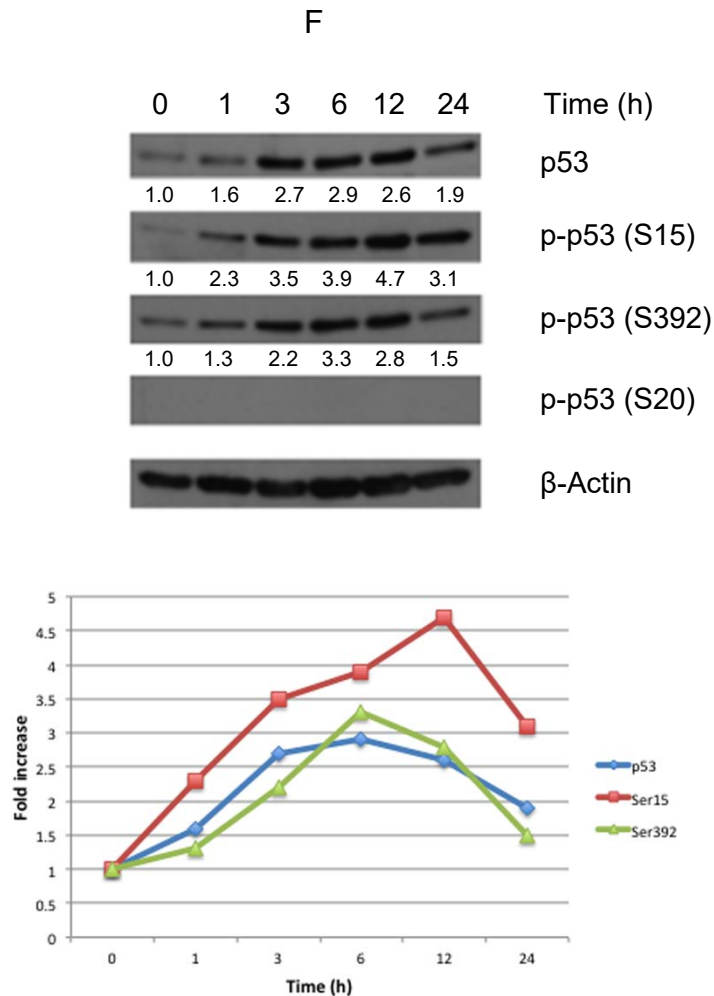


**Figure 14. p53 phosphorylation in LCL cells (6 Gy, 2 Gy)**

Following treatment with 6 Gy of IR, cells were collected at designated time points and western blot analysis was performed to detect p53 phosphorylated sites at Ser15, Ser392 and Ser20 in (A) wild-type (GM03714), (B) AT (GM0719B) and (C) AT (VKE) LCL cells. Similarly, following treatment with 2 Gy of IR, cells were collected at designated time points and western blot analysis was performed to detect p53 phosphorylated sites at Ser15, Ser392 and Ser20 in (D) wild-type (GM03714), (E) AT (GM0719B) and (F) AT (VKE) LCL cells. In all cases,  $\beta$ -Actin was used as the loading control. Densitometry was performed with ImageJ software (NIH) and relative p53 or p53 Ser15 or p53 Ser392 or p53 Ser20 band intensity was normalized to  $\beta$ -actin. Corresponding graphs demonstrate the densitometry analysis of the western blots, which represent a minimum of two replicates.

Further analysis of ATM and ATR in LCL cell models revealed that following exposure to 6 Gy, while ATM is absent as expected, ATR seems to experience upregulation in both types of mutant AT cells post-irradiation (Figure 15 B,C).

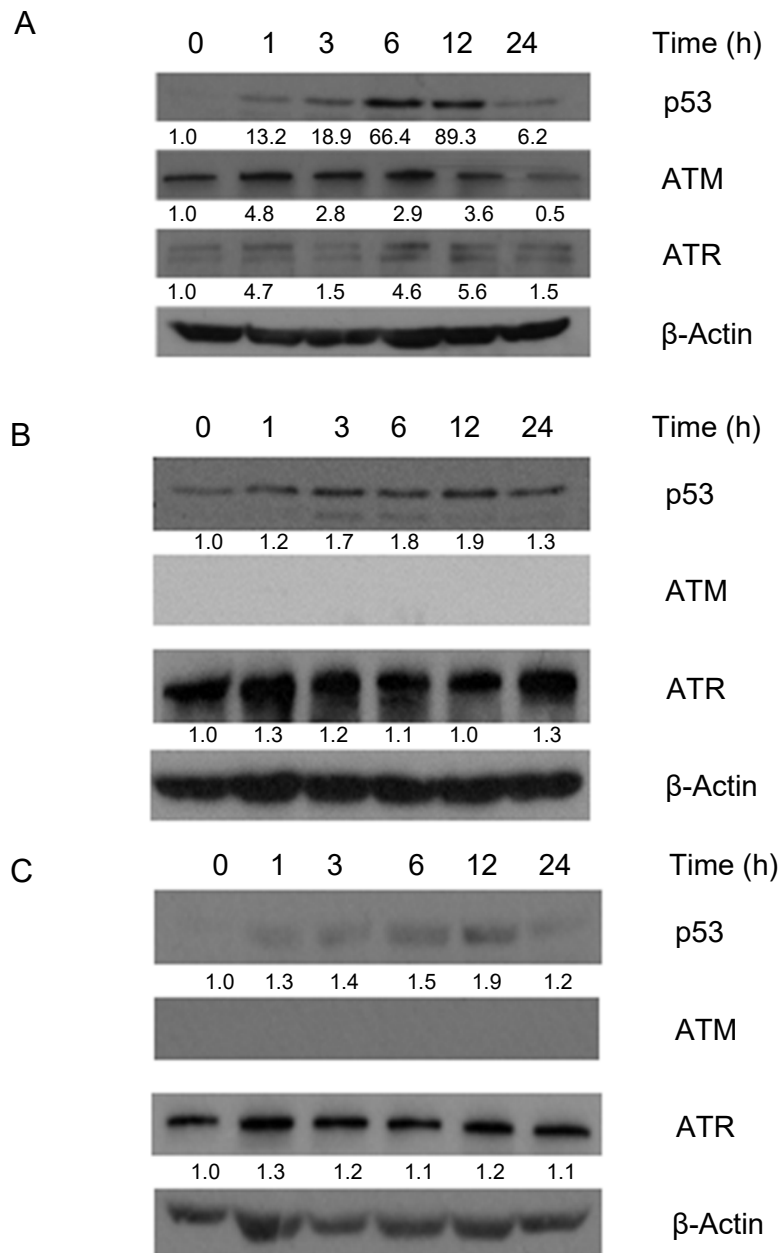


**Figure 15 A-C. Induction of ATM and ATR post-irradiation (6 Gy) in LCLs**

Following treatment with 6 Gy of IR, cells were collected at designated time points and western blot analysis was performed to detect ATM and ATR using ATM D2E2 Rabbit mAb specific antibody and ATR Rabbit specific antibody (Cell Signaling) in (A) wild-type (GM03714), (B) AT (GM0719B) and (C) AT (VKE) LCL cells. In all cases, β-Actin was used as the loading control. Densitometry was performed with ImageJ software (NIH) and relative p53 or ATM or ATR band intensity was normalized to β-actin. These blots represent a minimum of two replicates.

Similarly, after exposure to 2 Gy, the ATR was expressed in the mutant LCL cells; however, the ATR basal level failed to exhibit a remarkable change during the testing period (Figure 15 E,F). Altogether, these findings suggest that the ATR-signalling pathway might constitute the predominant pathway in AT cells.

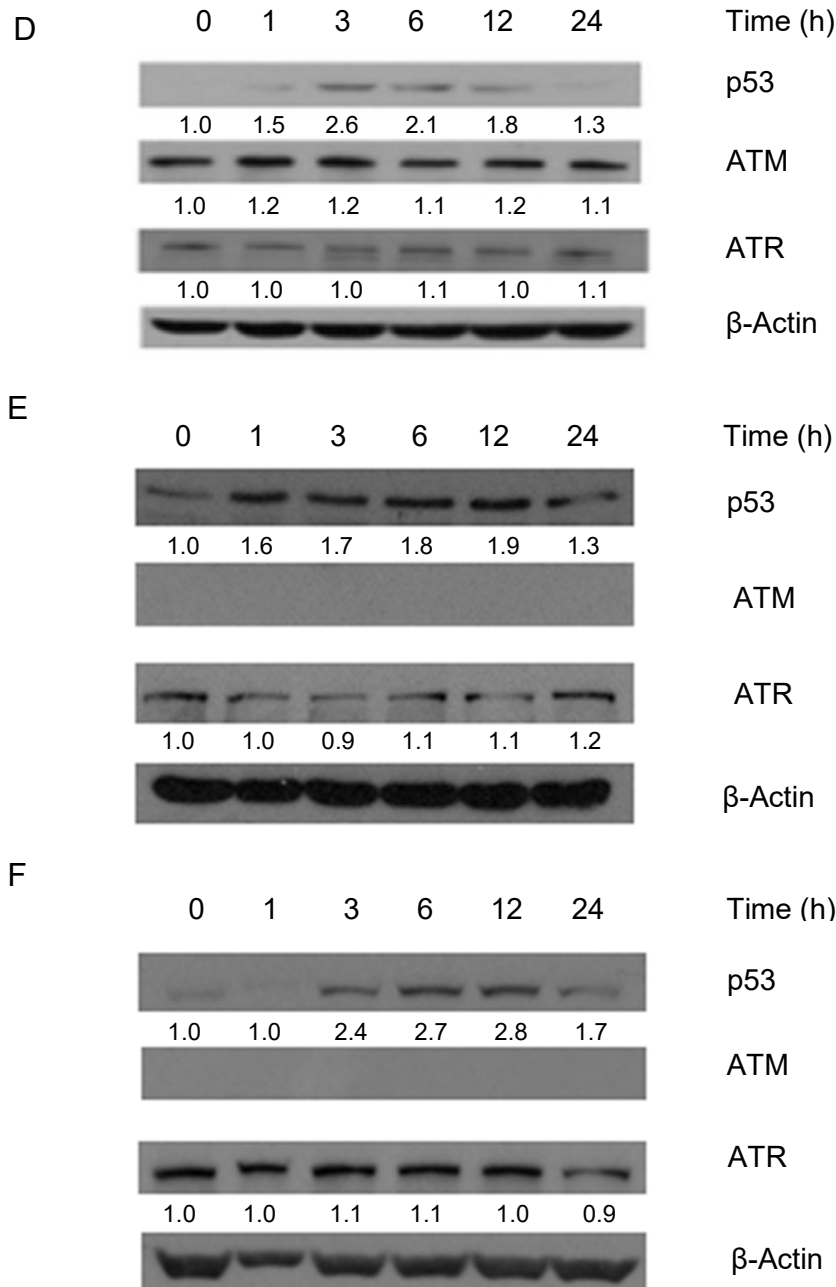


**Figure 15 D-F. Induction of ATM and ATR post irradiation (2 Gy) in LCLs**

Following treatment with 2 Gy of IR, cells were collected at designated time points and western blot analysis was performed to detect ATM and ATR using ATM D2E2 Rabbit mAb specific antibody and ATR Rabbit specific antibody (Cell Signaling) in **(D)** wild-type (GM03714), **(E)** AT (GM0719B) and **(F)** AT (VKE) LCL cells. β-Actin was used as the loading control. In all cases, β-Actin was used as the loading control. Densitometry was performed with ImageJ software (NIH) and relative p53 or ATM or ATR band intensity was normalized to β-actin. These blots represent a minimum of two replicates.

## **UBE4B induction in response to UV light and 5-FU drug is**

### **ATM-independent**

In addition, this study analyzed the behaviour of UBE4B and MDM2 E3 ligases in response to DNA damage with two additional agents: UV light and 5-Fluorouracil (5-FU) chemotherapeutic drug.

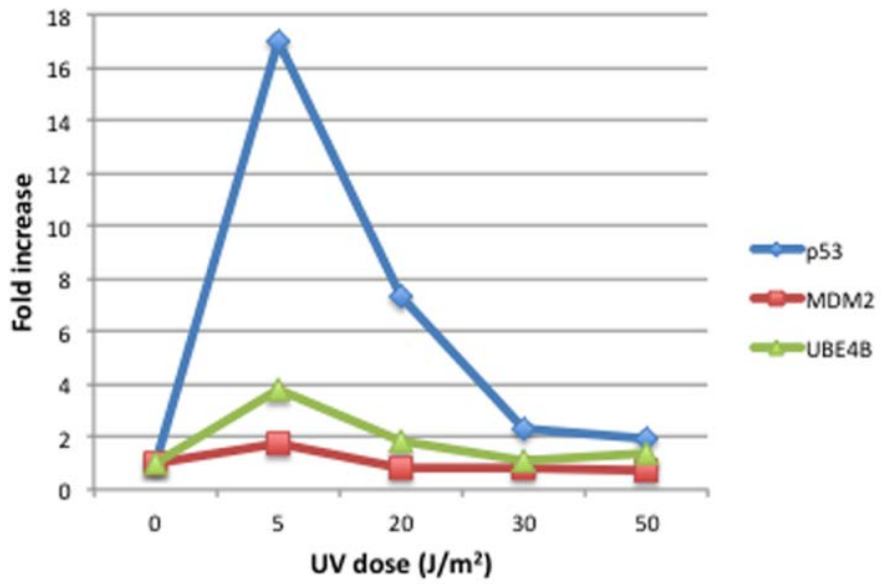
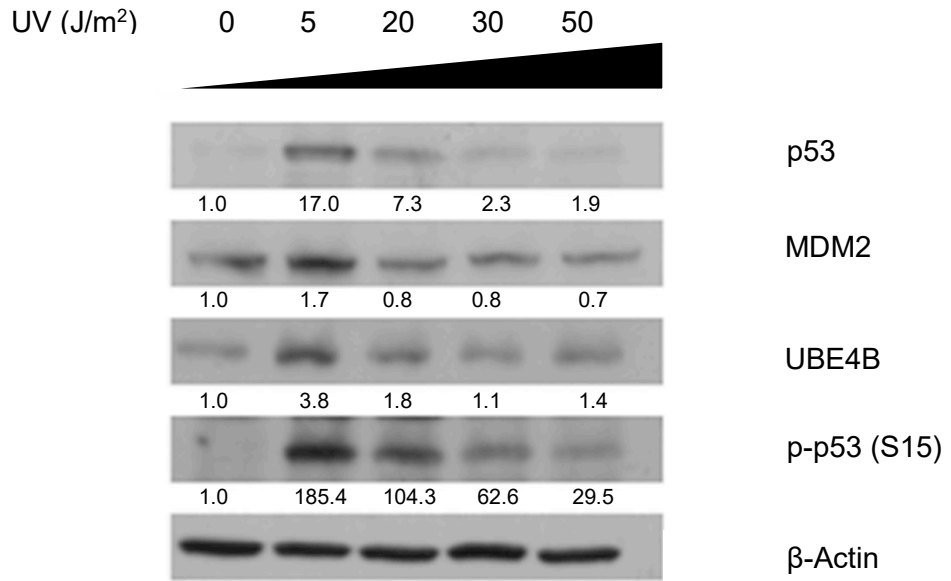
Following exposure to increasing doses of UV light, MCF7 showed a gradual decrease in the level of p53, MDM2, UBE4B, and phosphorylated p53 at Ser15. However, MCF7 demonstrated a major drop at a higher dose (50 J/m<sup>2</sup>), shown in Figure 16A. Likewise, in wild-type (GM03714) LCL cells, an increase in the dose of UV light resulted in a gradual decline in the level of all proteins despite the slight fluctuation in the level of MDM2 (Figure 16B). The same pattern occurred in mutant (GM0719B) LCL cells (Figure 16C). At higher doses, the lower induction of p53 may indicate excessive cell death. Clearly, UBE4B underwent equal induction in all cells, including wild type and mutant cells. Altogether, these observations indicate that UBE4B induction in response to UV light damage occurs independently of ATM.

Both LCL cells were exposed to 20 J/m<sup>2</sup> of UV light and protein levels were examined over 24 h. The findings demonstrated that in wild type cells, the level of p53, Ser15, MDM2, and UBE4B started to increase at 1 h and reached the highest peak at 24 h (Figure 16E). In mutant cells, all protein levels started to rise at 1 h and obtained a maximum level at 24 h. At 3 h and 6 h, p53 and its phosphorylated Ser15 form showed a steadily gradual increase while MDM2 and UBE4B demonstrated fluctuation (Figure 16F). Overall, these findings suggest that unlike ionizing radiation, UV light leads to an increase in the induction of p53 and its ligases MDM2 and UBE4B in relatively later

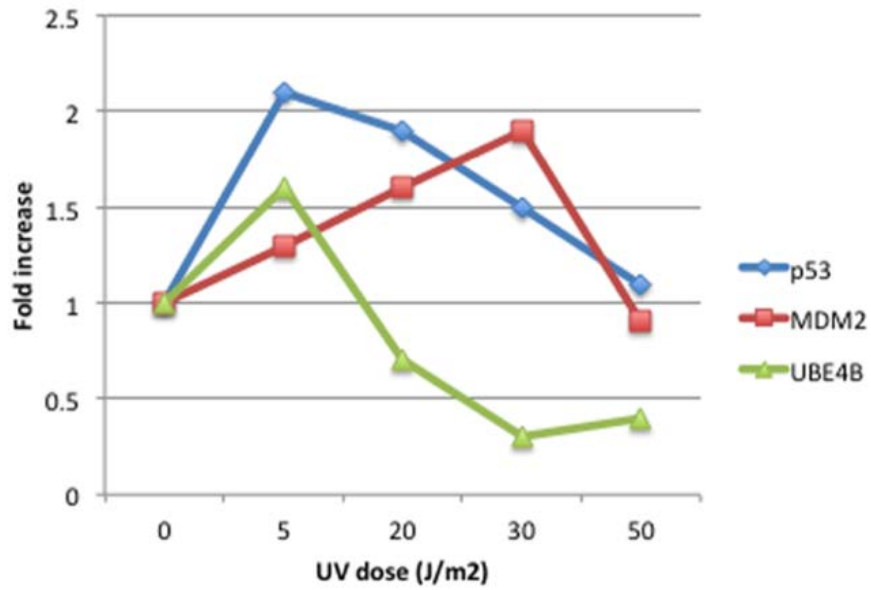
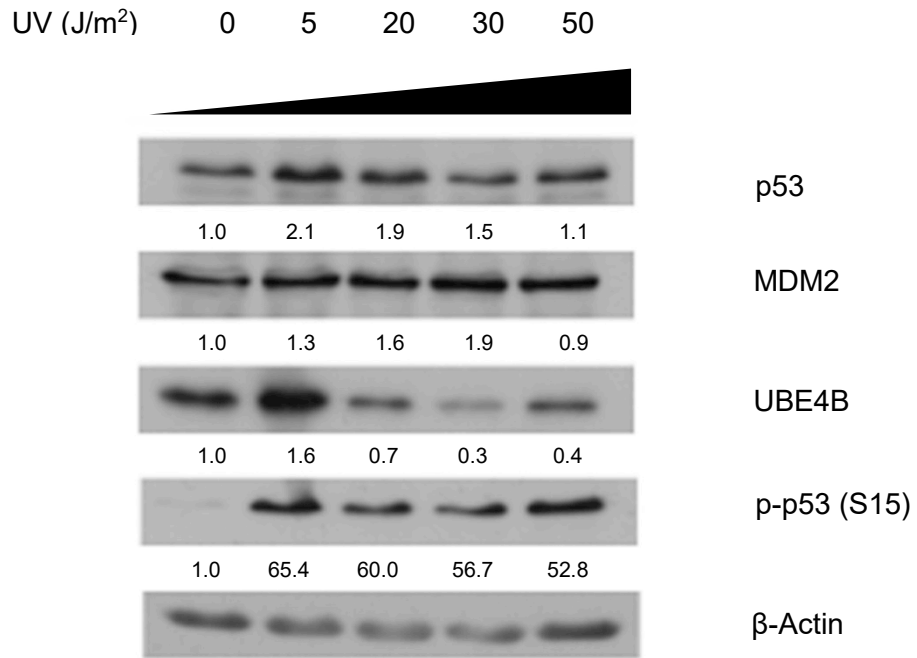
times (24 h) for the same cells. Moreover, in wild type cells, densitometry analysis shows that at 24 h, the fold increase in p53 levels, at 24, is higher than that in mutant cells, at 2. These results may indicate that for wild type LCL cells, p53 induction in response to UV might be ATM dependent. On the other hand, the fold increases in MDM2 and UBE4B exhibit similarity in both cells, indicating that their upregulation at later stages in response to UV is ATM-independent.

Upon exposure to increasing doses of 5-FU in wild type LCL cells, p53 and p-p53Ser15 followed the same pattern; specifically, they started to rise at 10  $\mu\text{g}/\text{mL}$ , continued to increase at 20  $\mu\text{g}/\text{mL}$ , experienced a major drop at 30  $\mu\text{g}/\text{mL}$ , and increased again at 50  $\mu\text{g}/\text{mL}$ . UBE4B and MDM2, on the other hand, showed the same pattern; they started to increase at 20  $\mu\text{g}/\text{mL}$  followed by decreases at 30 and 50  $\mu\text{g}/\text{mL}$  (Figure 17A). In mutant LCL cells, all proteins followed the same pattern, showing an increase at 10  $\mu\text{g}/\text{mL}$  followed by a major drop at 30  $\mu\text{g}/\text{mL}$  and a final rise at 50  $\mu\text{g}/\text{mL}$  (Figure 17B). Following exposure of LCL cells to 20  $\mu\text{g}/\text{mL}$ , all proteins exhibited peaks at 1 h and 24 h as well as fluctuations at 3 h and 6 h in wild type LCL cells (Figure 17C). On the other hand, in mutant cells, all proteins began to rise at 1 h and reached their peaks at 3 h before dropping at 6 h. At 24 h, UBE4B and MDM2 increased, p53 decreased, and p-p53Ser15 remained constant (Figure 17D). Altogether, as in the case of UV light exposure, these data show that the induction of UBE4B in response to the treatment by 5-FU chemotherapeutic drug is ATM independent.

A

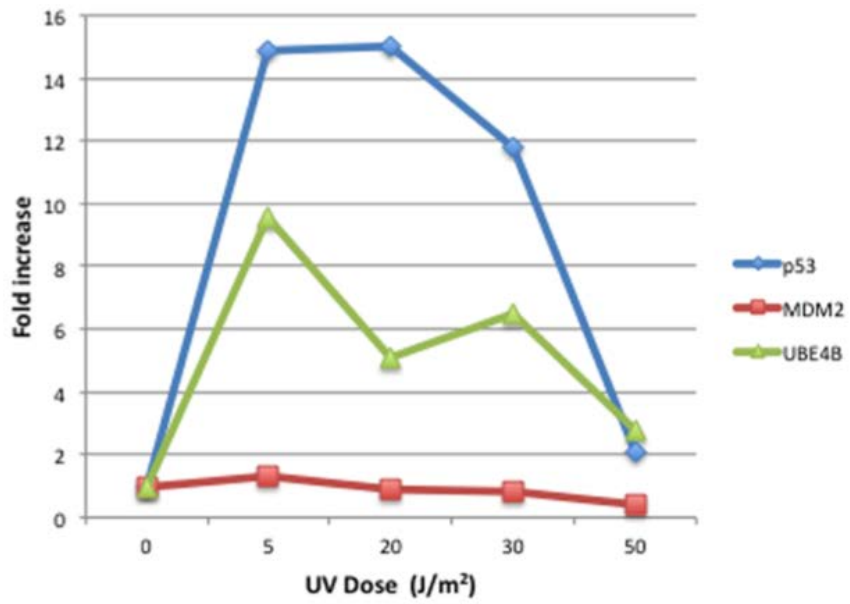
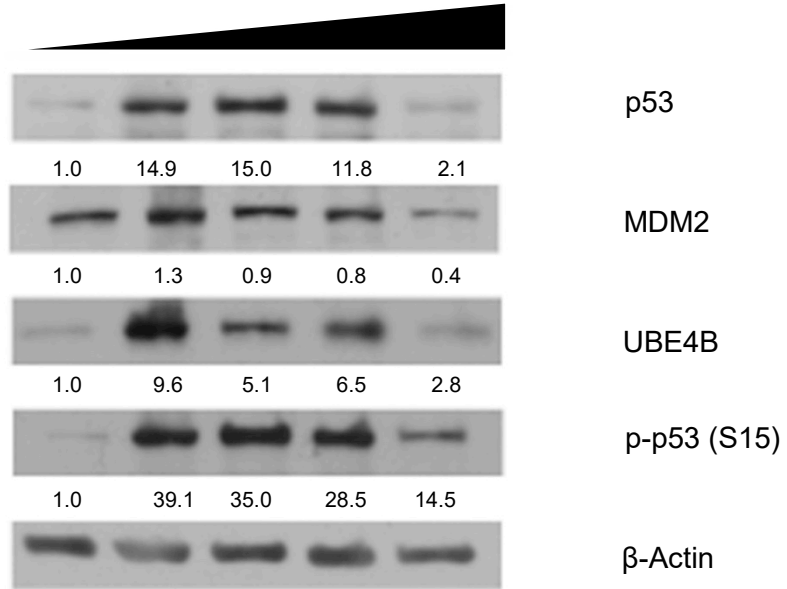


B

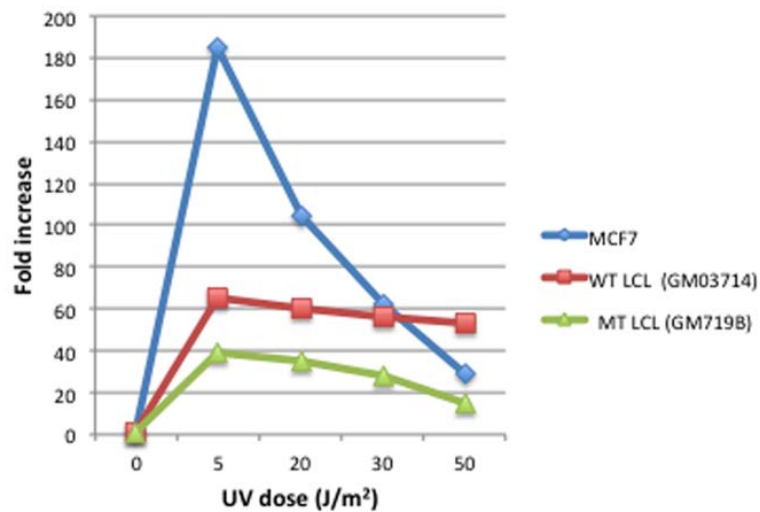


C

UV (J/m<sup>2</sup>)    0    5    20    30    50



D

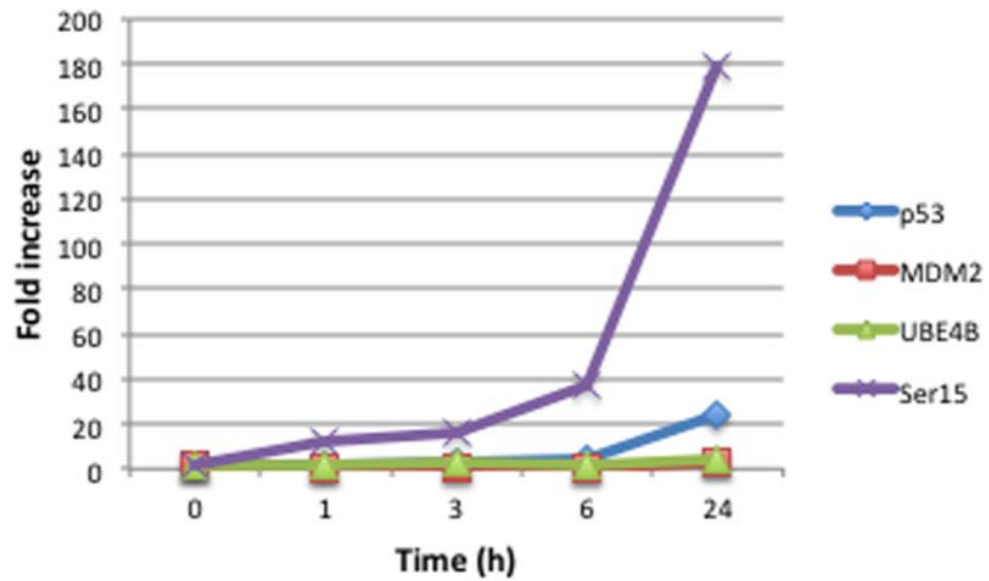
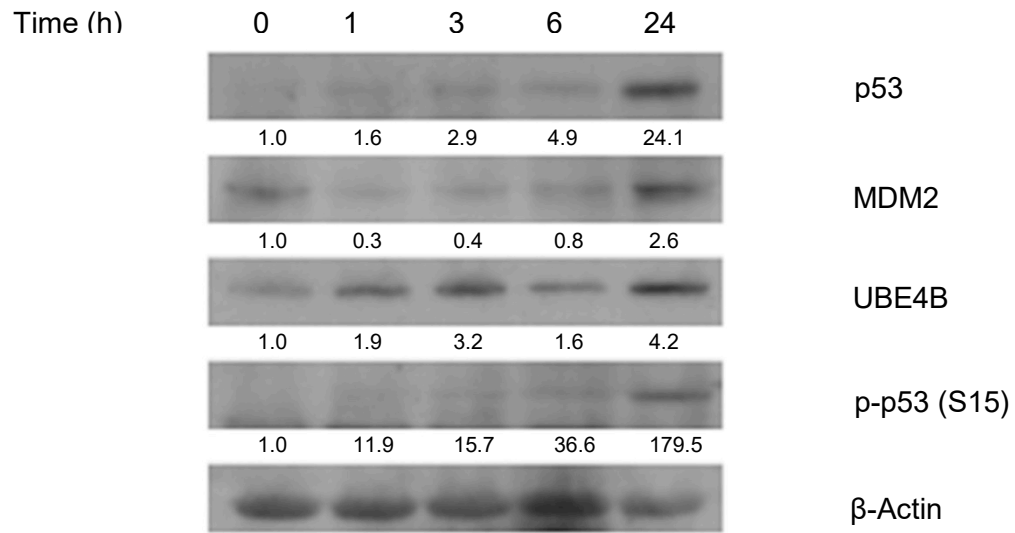


**Phosphorylation status in various cell lines in response to different doses of UV light**

**Figure 16 A-D UV dose-dependent inductions of ubiquitin ligases (MDM2, UBE4B) and Ser15 in LCLs**

Following treatment with various doses of UV light (5, 20, 30, 50 J/m<sup>2</sup>) or leaving without treatment, cells were collected at 3 h and protein level of induced ubiquitin ligases (MDM2 and UBE4B) and Ser15 were detected by western blotting in (A) MCF7, (B) wild-type (GM03714) and (C) AT (GM0719B). The induction of Ser15 in MCF7, Wild-type and mutant LCL cells is represented in (D). In all cases,  $\beta$ -Actin was used as the loading control. Densitometry was performed with ImageJ software (NIH) and relative p53 or p53 Ser15 or MDM2 or UBE4B band intensity was normalized to  $\beta$ -actin. Corresponding graphs demonstrate the densitometry analysis of the western blots, which represent a minimum of two replicates.

E



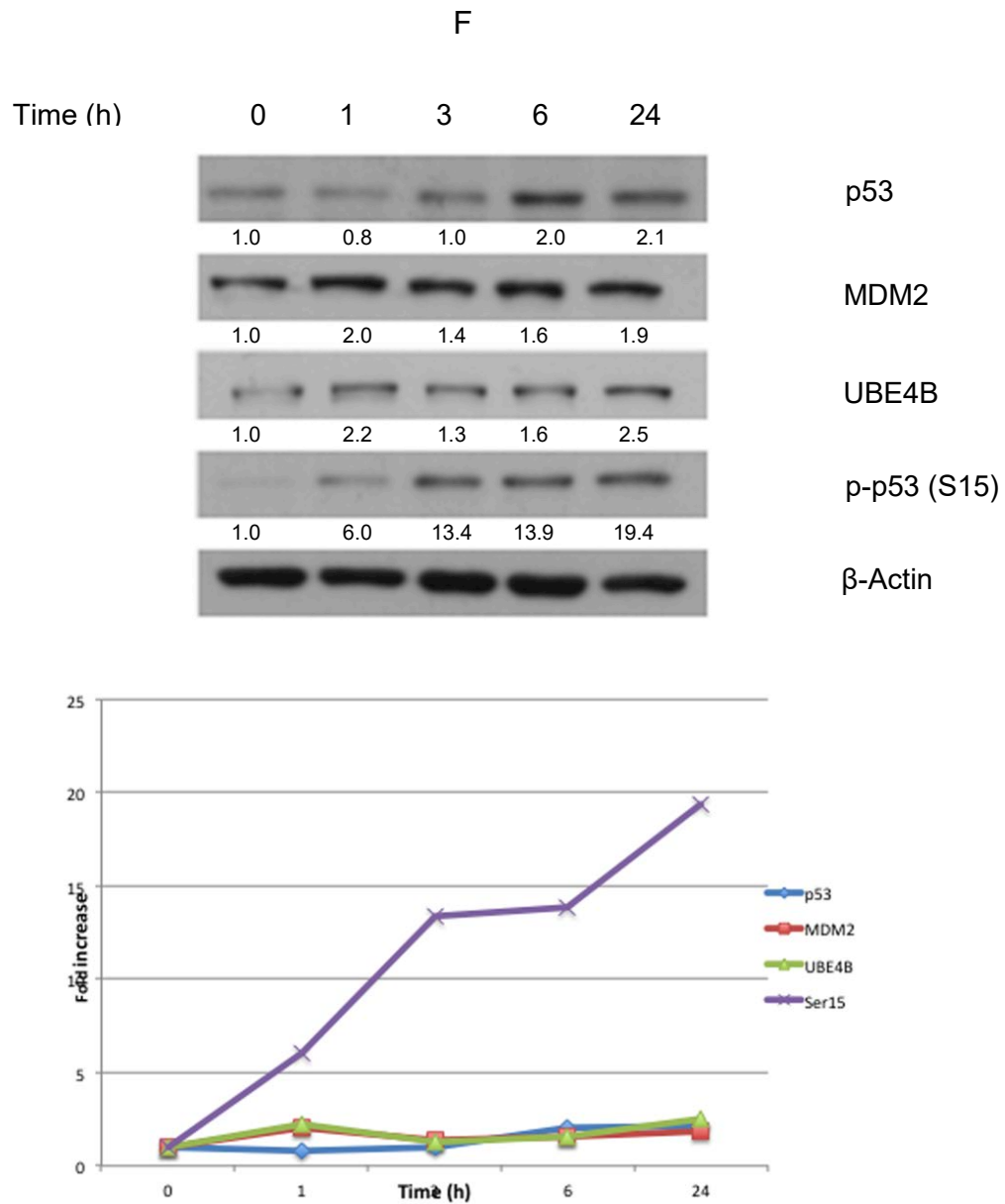


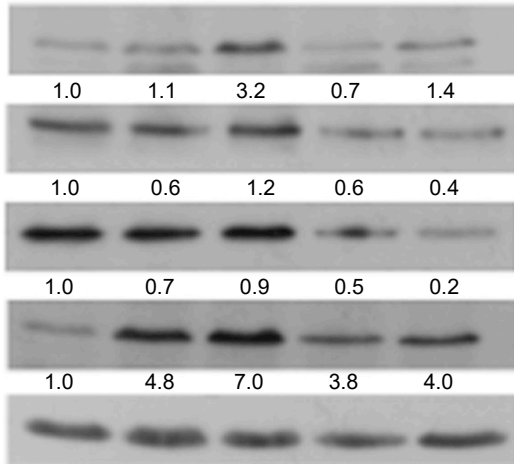
**Figure 16 E,F. Time-course assay for induction of ubiquitin ligases (MDM2,UBE4B) and Ser15 post-exposure to UV light**

Following treatment with 20 J/m<sup>2</sup> of UV light or leaving without treatment, cells were collected and protein level of induced ubiquitin ligases (MDM2 and UBE4B) and Ser15 were detected by western blotting in (E) wild-type (GM03714) and (F) AT (GM0719B) LCLs. In all cases,  $\beta$ -Actin was used as the loading control. Densitometry was performed with ImageJ software (NIH) and relative p53 or p53 Ser15 or MDM2 or UBE4B band intensity was normalized to  $\beta$ -actin. Corresponding graphs demonstrate the densitometry analysis of the western blots, which represent a minimum of two replicates.

A

5-FU ( $\mu\text{g/mL}$ )

0 10 20 30 50



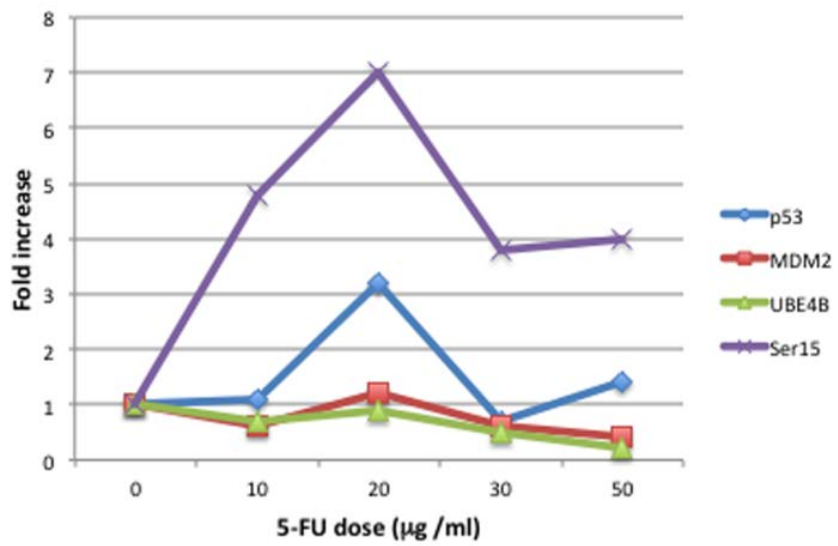
p53

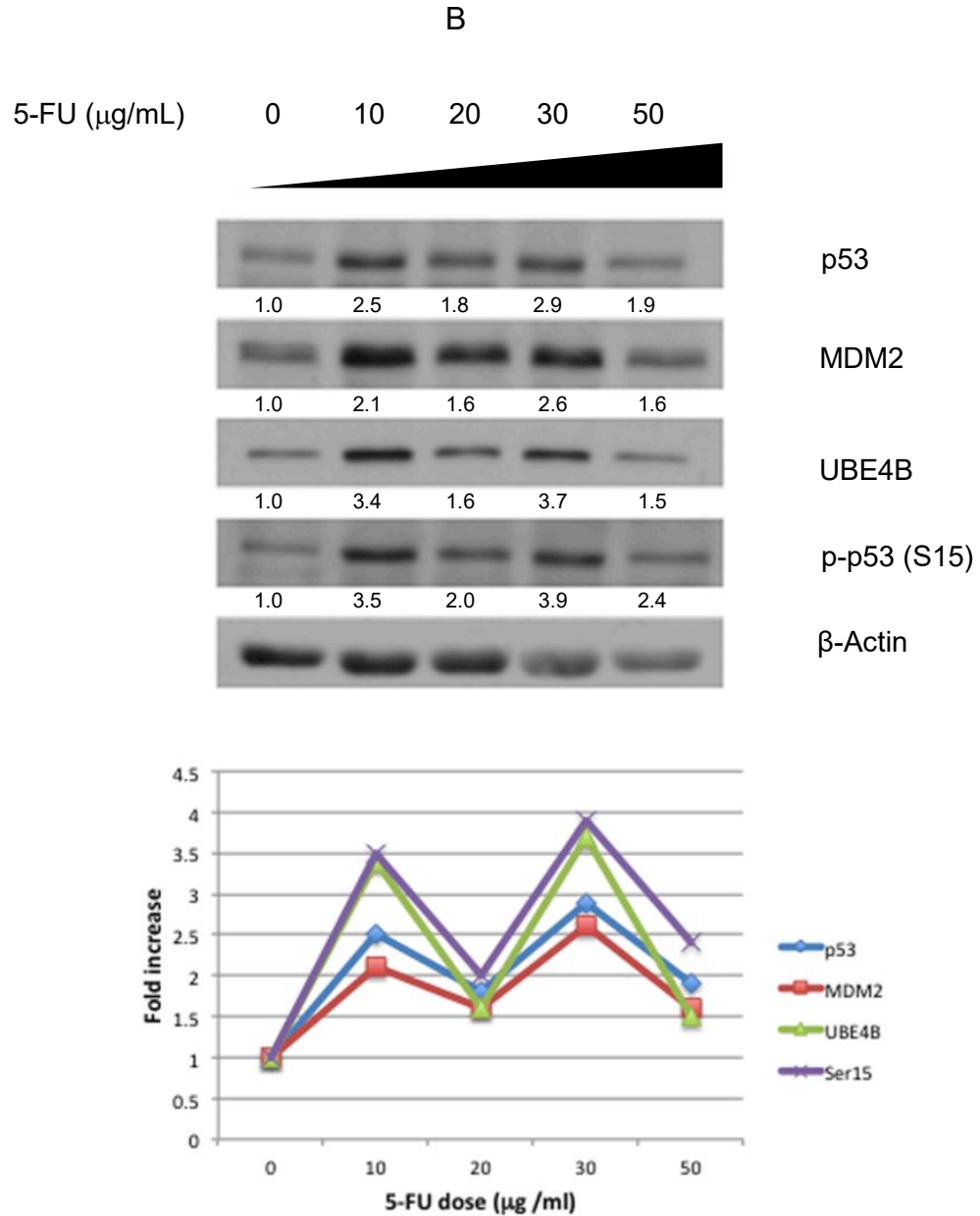
MDM2

UBE4B

p-p53 (S15)

β-Actin

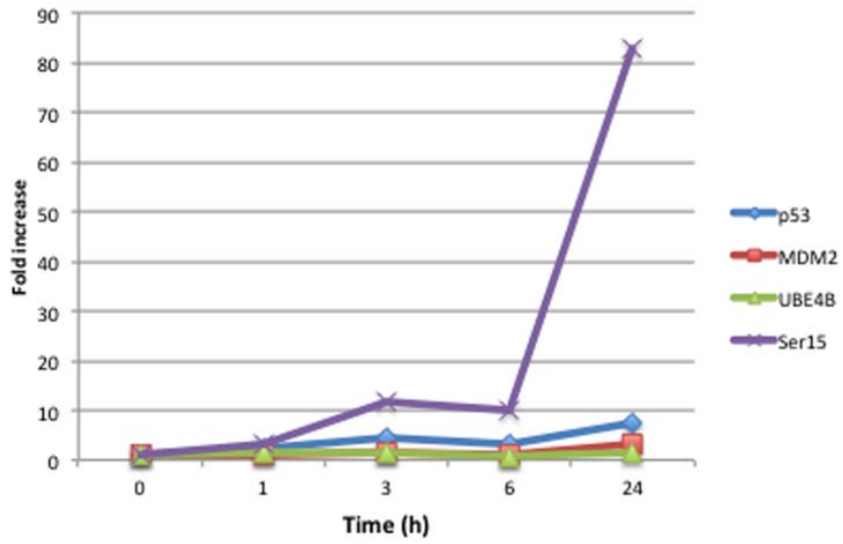
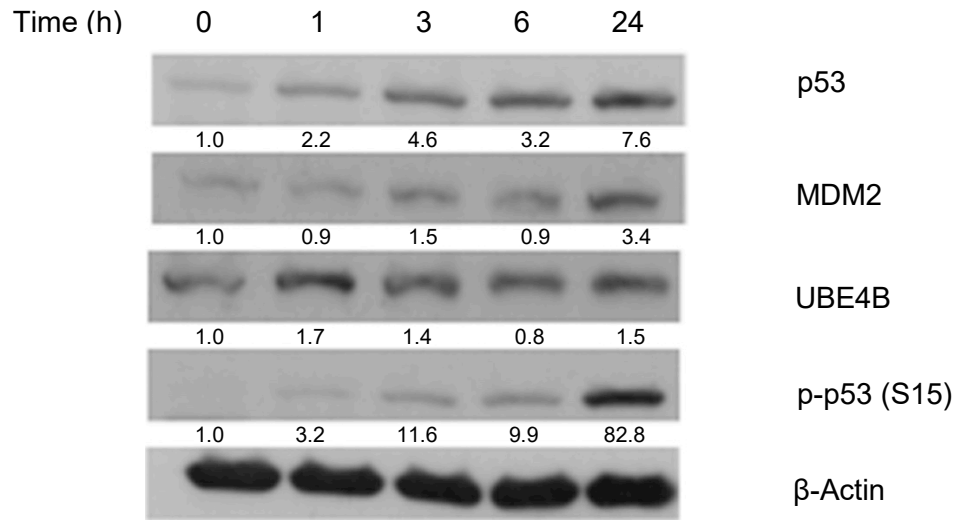




**Figure 17 A,B. Induction of ubiquitin ligases (MDM2, UBE4B) and Ser15 post-exposure to various doses of 5-FU drug**

Following treatment with various doses of 5-FU drug (10, 20, 30, 50  $\mu\text{g}/\text{mL}$ ) or leaving without treatment, cells were collected at 3 h and protein level of induced ubiquitin ligases (MDM2 and UBE4B) and Ser15 were detected by western blotting in (A) wild-type (GM03714) and (B) AT (GM0719B) LCLs. In all cases,  $\beta$ -Actin was used as the loading control. Densitometry was performed with ImageJ software (NIH) and relative p53 or p53 Ser15 or MDM2 or UBE4B band intensity was normalized to  $\beta$ -actin. Corresponding graphs demonstrate the densitometry analysis of the western blots, which represent a minimum of two replicates.

C



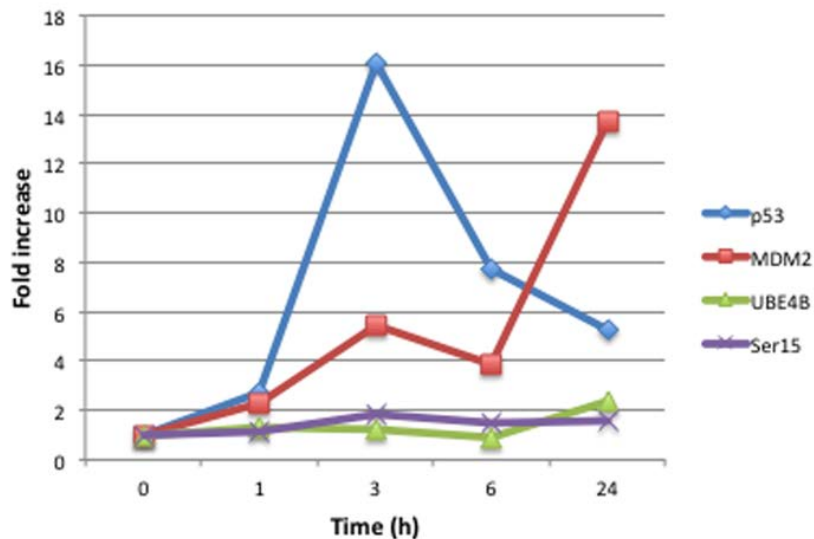
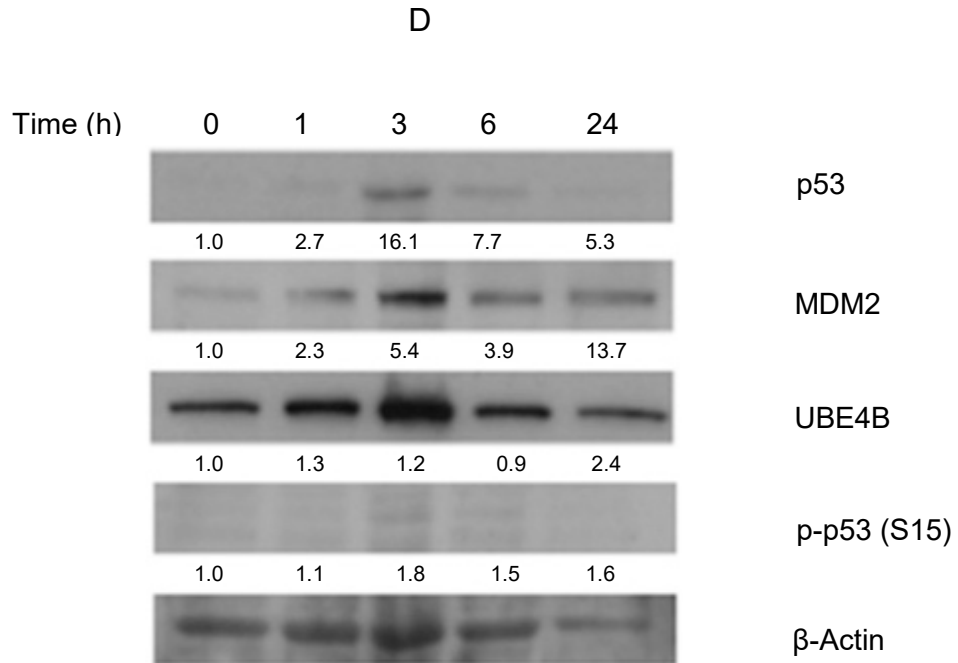


**Figure 17 C,D. Induction of ubiquitin ligases (MDM2,UBE4B) and Ser15 post-exposure to 5-FU**

Following treatment with 20  $\mu$ g/mL of 5-FU or leaving without treatment, cells were collected and protein level of induced ubiquitin ligases (MDM2 and UBE4B) and Ser15 were detected by western blotting in (C) wild-type (GM03714) and (D) AT (GM0719B) LCLs. In all cases,  $\beta$ -Actin was used as the loading control. Densitometry was performed with ImageJ software (NIH) and relative p53 or p53 Ser15 or MDM2 or UBE4B band intensity was normalized to  $\beta$ -actin. Corresponding graphs demonstrate the densitometry analysis of the western blots, which represent a minimum of two replicates.

## **p53 interacts with MDM2 and UBE4B and its affinity with MDM2 and UBE4B is augmented post-irradiation in ATM deficient-lymphoblastoid cells**

Since detecting the protein levels of different ubiquitin ligases might fail to indicate their association with p53, investigating the binding affinity between p53 and ligases ensures their potential function in p53 downregulation. One of the proposed mechanisms for p53 stability following DNA damage is mainly conducted through phosphorylation, which dissociates p53 from E3 ligases such as MDM2 [58]. Thus, investigations need to determine whether endogenous p53 interacts with MDM2 and UBE4B in stressed and unstressed conditions. Prior to performing this test, cells were cultured with 80%-90% confluence, exposed to 6 Gy of IR, and harvested. Subsequently, cell lysates were used to perform a co-immunoprecipitation study followed by western blot analysis. Unexpectedly, as shown in Figures 18 A and B, when p53 was immunoprecipitated in the wild type LCL cells at 3 h and 24 h, the affinity binding of MDM2 with p53 increased post-irradiation. Similarly, Figures 18 C and D revealed that at either 3 h or 24 h, the binding affinity of MDM2 with p53 also clearly increased in mutant stressed GM0719B AT cells as compared to unstressed cells. In contrast, while the binding affinity of UBE4B with p53 in the stressed wild type LCL cells remained constant (Figures 18 A and B), stressed mutant GM0719B at 3 h and 24 h (Figures 18 C and D) as well as VKE AT cells at 3 h (Figure 18E) displayed elevated binding affinity in comparison with unstressed cells. By and large, according to the tested model in the hypothesis, the identical phenotype of p53 interactions with MDM2 in both wild-type and mutant LCL

cells may suggest that MDM2 interactions with p53 might be dispensable for p53 stability post-irradiation in both normal and mutant LCL cells.

In addition, the observed unexpected increased binding affinity of MDM2 with p53 in LCL cells, which contradicts with the current literature and understanding might be explained in many ways. Firstly, The phenotype of MDM2-p53 interactions could be cell specific, rather than a general phenomenon. Secondly, the apparently observed rise in MDM2 affinity with p53 may not necessarily reflects a physical binding between these proteins. Instead, it could be attributed to variations in p53 levels between unstressed and stressed cells. Comparison of the densitometry outcomes of IP with the normal western blots for both p53 and MDM2 reveals similar patterns. Consequently, the observed increase in p53 binding with MDM2 most likely reflects a change in basal level of p53 and MDM2 rather than a change in affinity bindings. Finally, the phenotype of MDM2-p53 interactions in MCF7 cells was consistent with the literature, which confirms the validity of our findings in LCL cells, as this could be used as a positive control.

Most importantly, UBE4B-p53 interactions in LCL cells in response to IR are ATM-independent.

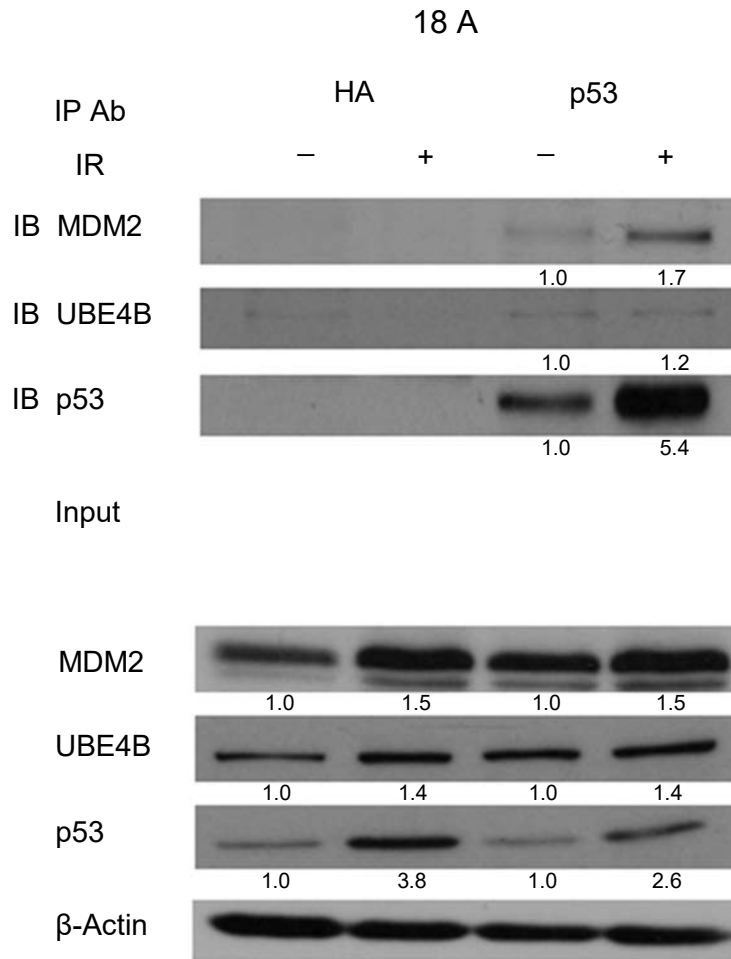


**Figure 18A. MDM2 and UBE4B interact with p53 in wild-type LCL cells at 3 h post-irradiation**

Following treatment with 6 Gy of IR, wild-type (GM03714) LCL cells were harvested after 3 h, 800 µg of total proteins were used to immunoprecipitate total p53 protein using Pab1801 specific antibodies and hemagglutinin (HA)-tag antibodies (as negative controls). 10%-15% of the total whole cell lysate was used for the IP as input. Western blot analysis was performed using specific antibodies (Pab1801 for p53, SMP 14 for MDM2, UFD2 for UBE4B). β-Actin was used as the loading control. Densitometry was performed with ImageJ software (NIH) and relative UBE4B or MDM2 or p53 band and intensity normalized to IgG heavy chain for Co-IP or β-actin for Input. These blots represent a minimum of two replicates.

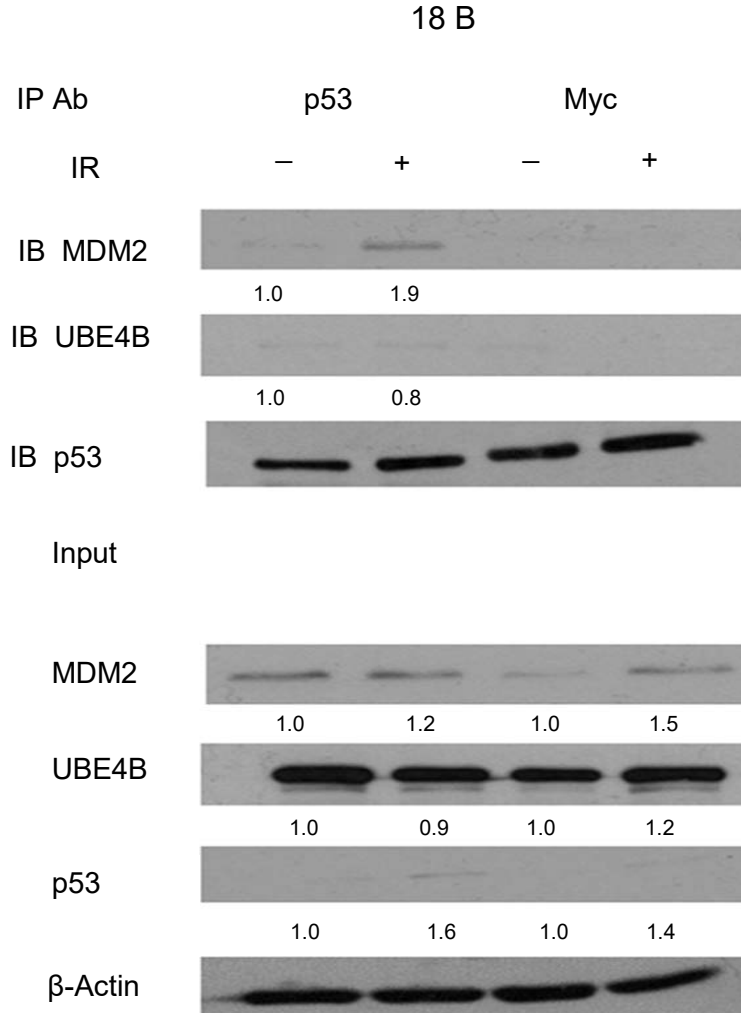


**Figure 18B. MDM2 and UBE4B interact with p53 in wild-type LCL cells at 24 h post-irradiation**

Following treatment with 6 Gy of IR, wild-type LCL cells (GM03714) were harvested after 24 h, 700-1000  $\mu$ g of total proteins were used to immuno-precipitate total p53 protein using Pab 1801 specific antibodies and Myc-tag antibodies (as negative controls). 10%-15% of the total whole cell lysate was used for the IP as input. Western blot analysis was performed using specific antibodies (Pab 1801 for p53, SMP 14 for MDM2, UFD2 for UBE4B).  $\beta$ -Actin was used as the loading control. Densitometry was performed with ImageJ software (NIH) and relative UBE4B or MDM2 or p53 band and intensity normalized to IgG heavy chain for Co-IP or  $\beta$ -actin for Input. These blots represent a minimum of two replicates.

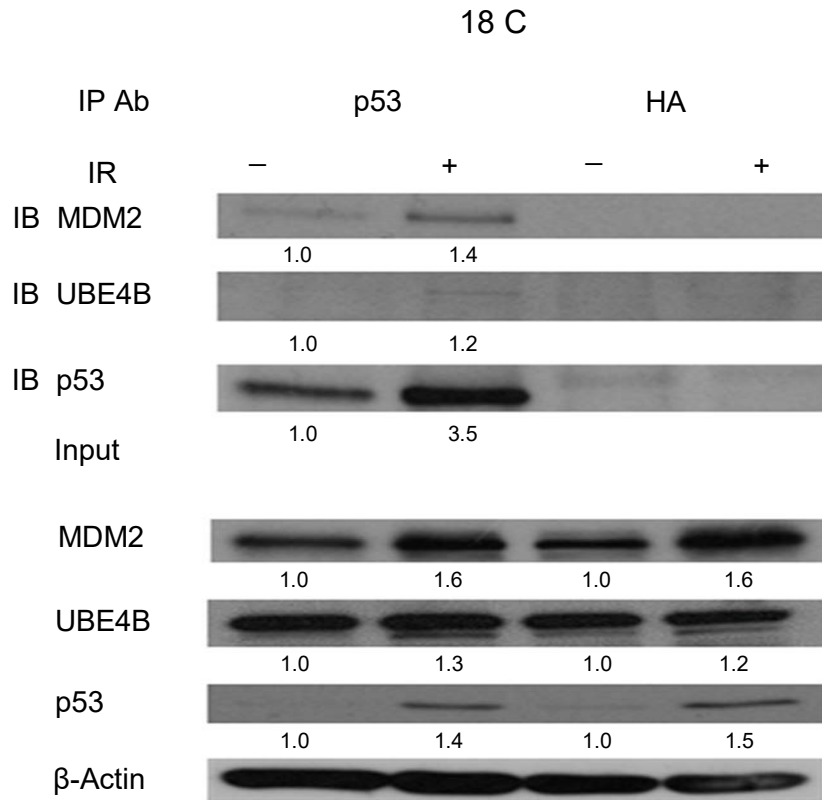


**Figure 18C. MDM2 and UBE4B interact with p53 in mutant AT LCL cells at 3 h post-irradiation**

Following treatment with 6 Gy of IR, AT (GM0719B) LCL cells were harvested after 3 h, 700-1000  $\mu$ g of total proteins were used to immunoprecipitate total p53 protein using Pab 1801 specific antibodies and HA-tag antibodies (as negative controls). 10%-15% of the total whole cell lysate was used for the IP as input. Western blot analysis was performed using specific antibodies (Pab 1801 for p53, SMP 14 for MDM2, UFD2 for UBE4B).  $\beta$ -Actin was used as the loading control. Densitometry was performed with ImageJ software (NIH) and relative UBE4B or MDM2 or p53 band and intensity normalized to IgG heavy chain for Co-IP or  $\beta$ -actin for Input. These blots represent a minimum of two replicates.

18 D

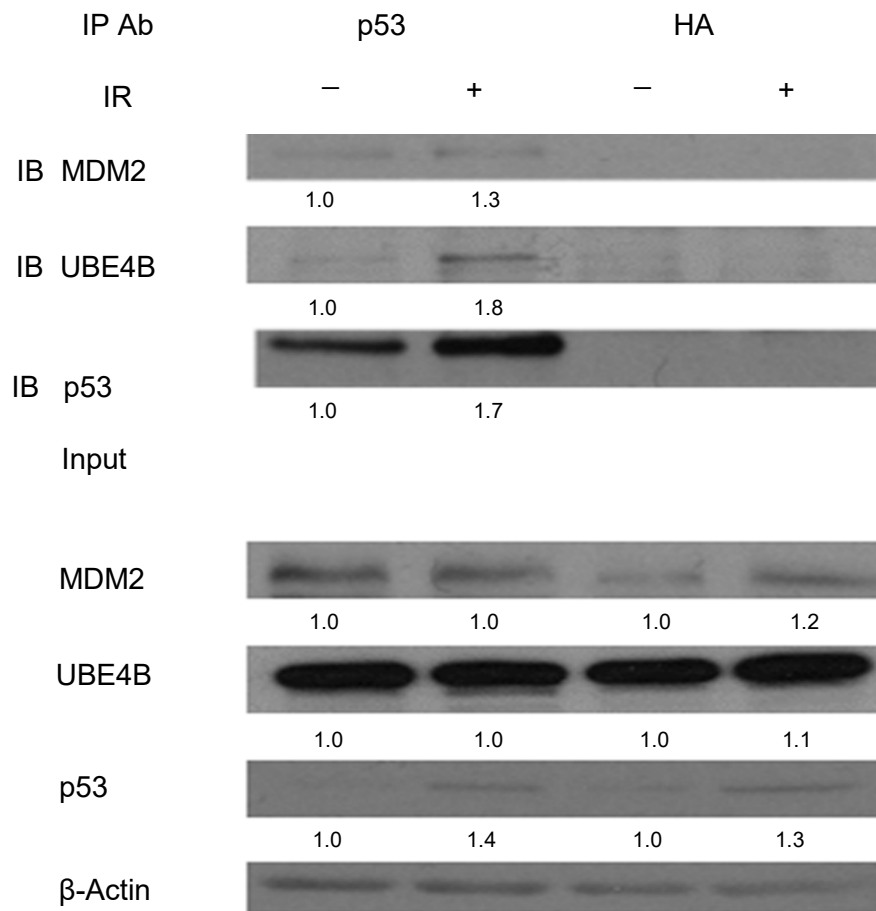


**Figure 18D. MDM2 and UBE4B interact with p53 in mutant cells at 24 h post-irradiation**

Following treatment with 6 Gy of IR, AT (GM0719B) LCL cells were harvested after 24 h, 700-1000 µg of total proteins were used to immuno-precipitate total p53 protein using Pab 1801 specific antibodies and HA-tag antibodies (as negative controls). 10%-15% of the total whole cell lysate was used for the IP as input. Western blot analysis was performed using specific antibodies (Pab1801 for p53, SMP 14 for MDM2, UFD2 for UBE4B). β-Actin was used as the loading control. Densitometry was performed with ImageJ software (NIH) and relative UBE4B or MDM2 or p53 band and intensity normalized to IgG heavy chain for Co-IP or β-actin for Input. These blots represent a minimum of two replicates.

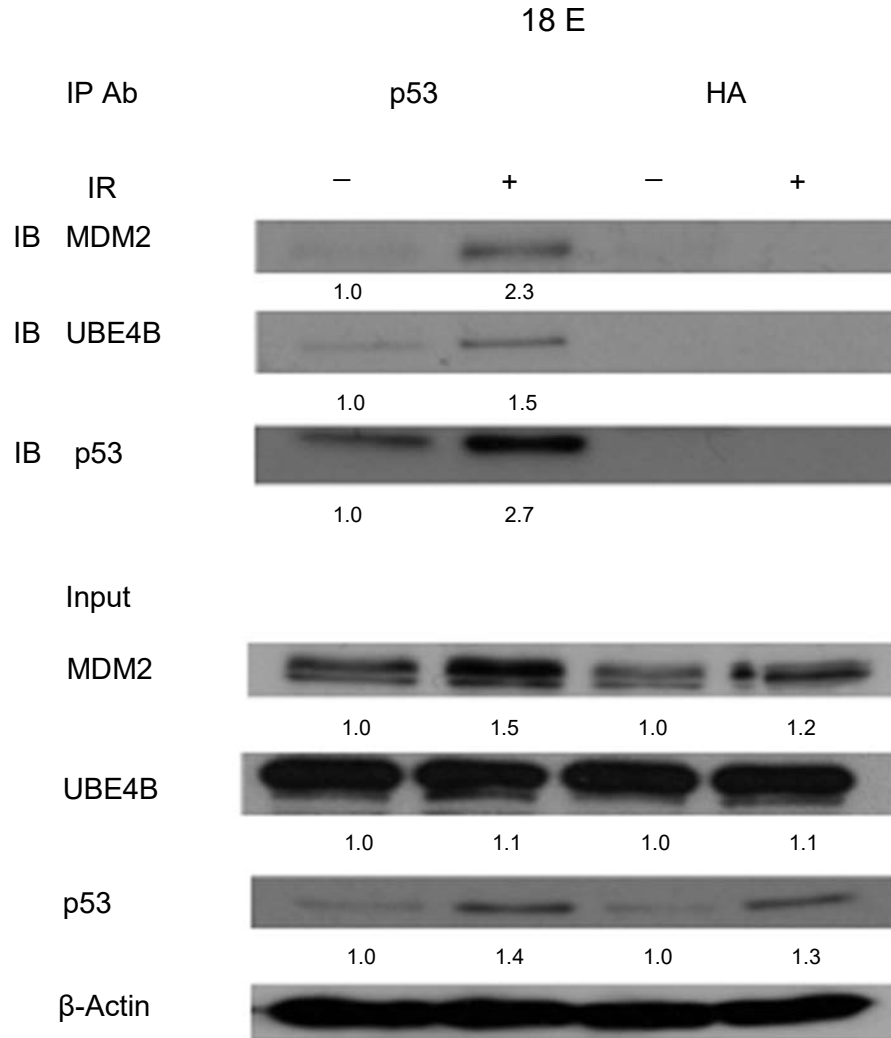


**Figure 18E. MDM2 and UBE4B interact with p53 in mutant VKE AT LCL cells at 3 h post-irradiation**

Following treatment with 6 Gy of IR, AT (VKE) LCL cells were harvested after 3 h, 700-1000  $\mu$ g of total proteins were used to immuno-precipitate total p53 protein using Pab 1801 specific antibodies and HA-tag antibodies (as negative controls). 10%-15% of the total whole cell lysate was used for the IP as input. Western blot analysis was performed using specific antibodies (Pab 1801 for p53, SMP 14 for MDM2, UFD2 for UBE4B).  $\beta$ -Actin was used as the loading control. Densitometry was performed with ImageJ software (NIH) and relative MDM2 or UBE4B or p53 band and intensity normalized to IgG heavy chain for Co-IP or  $\beta$ -actin for Input. These blots represent a minimum of two replicates.

## **MCF7 Cells: UBE4B bound p53 at Ser15 and Ser392 phosphorylated residues and interactions between UBE4B and MDM2 was diminished in response to DNA damage**

In the MCF7 human breast cancer cell line, immunoprecipitation assays (Co-IPs) were conducted to test the potential interactions of E3 ligases with p53 under stressed and unstressed conditions. After treatment with 6 Gy and coimmunoprecipitation with a p53 specific-antibody (DO-1), cell extracts were examined with western blot analysis by employing antibodies against UBE4B, MDM2, and phosphorylated p53 at Ser15 and Ser392. The data consistently revealed that while the binding of p53 with MDM2 was decreased, the binding of p53 with UBE4B was obviously strengthened (Figure 19A). Moreover, to further explore whether E3 ligases bind with phosphorylated p53 (Ser15, Ser392), a reciprocal confirmatory Co-IP was conducted in which MDM2 and UBE4B were immunoprecipitated. The results showed that UBE4B interacts with phosphorylated p53 at 3 h post-irradiation, whereas MDM2 seemingly fails to demonstrate any interaction with p53 (Figure 19B). However, when UBE4B and MDM2 are immunoprecipitated, indirect protein interactions between these substances and phosphorylated p53 are only implied, while phosphorylated p53 at Ser15 or Ser392 may primarily have a direct *in vivo* interaction with other proteins that directly bind with MDM2 or UBE4B. Hence, the western blot data of Co-IP studies fails to necessarily reflect a direct protein interaction, thus requiring *in vitro* Co-IP examinations to further confirm the *in vivo* Co-IP results. To investigate the ability of UBE4B to bind with MDM2 in response to DNA damage, reciprocal immunoprecipitation was performed in

MCF10A cells in response to ionizing radiation using specific UBE4B or MDM2 antibodies. In comparison to the untreated control cells, cells treated with IR demonstrated a significant decline in the binding affinity between UBE4B and MDM2 (Figure 19C), suggesting the initial activation of UBE4B by DNA damage through the inhibition of the interaction between MDM2 and UBE4B. In addition, these observations indicated that UBE4B might act on p53 independently of MDM2 [175] .

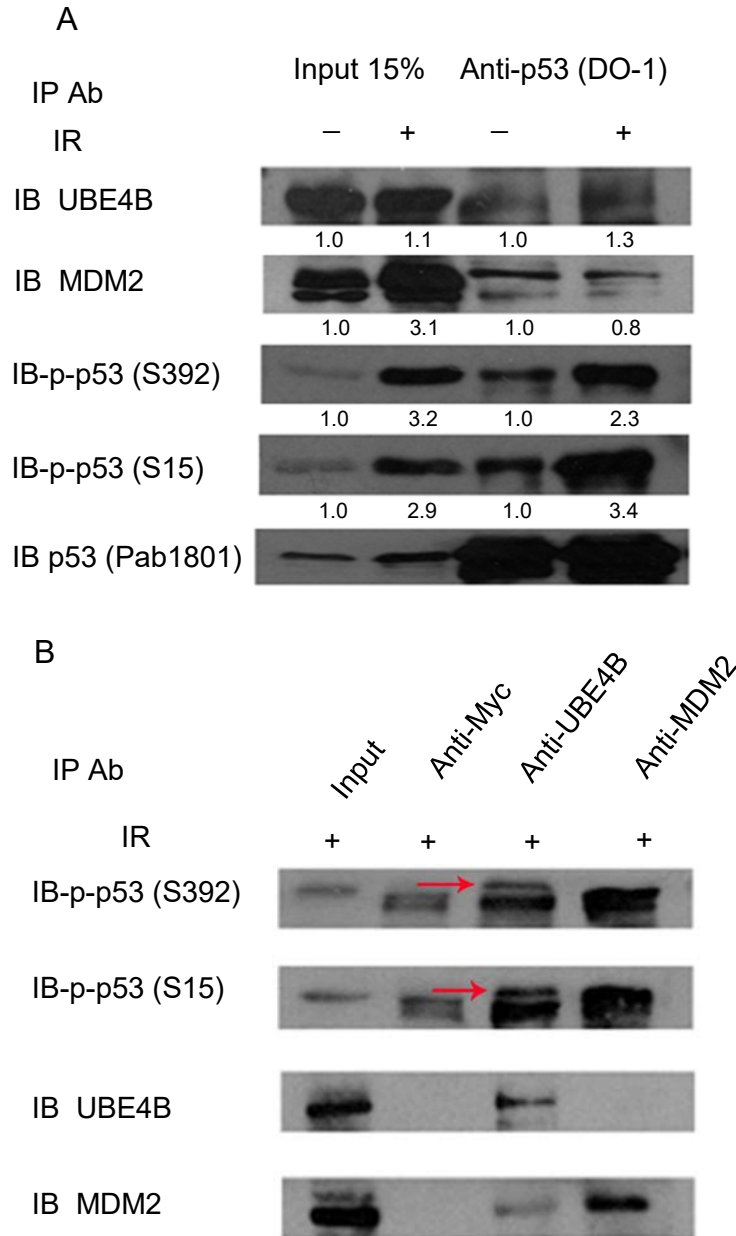


**Figure 19 A,B. UBE4B binds phosphorylated residues of p53 at Ser15 and Ser392 post-irradiation**

Following treatment with 6 Gy of IR, MCF7 cells were harvested after 3 h, 600 µg of total proteins were used to immuno-precipitate total p53 protein using p53 specific antibody (DO-1). 15% of the total whole cell lysate was used for the IP as input. Western blot analysis was performed using specific antibodies (Pab 1801 for p53, SMP 14 for MDM2, UFD2 for UBE4B, anti-p53Ser15 and anti-p53Ser392). Densitometry was performed with ImageJ software (NIH) and relative UBE4B or MDM2 or p53 Ser15 or p53 Ser392 or total p53 band and intensity normalized to IgG heavy chain for Co-IP. **B** Following treatment with 6 Gy of IR, MCF7 cells were harvested after 3 h. Cell lysates were immunoprecipitated with Anti-UBE4B and Anti-MDM2 and Myc followed by western blot analysis using the same specified antibodies in A. Red arrows indicate corresponding bands. Blots represent a minimum of two replicates.

C

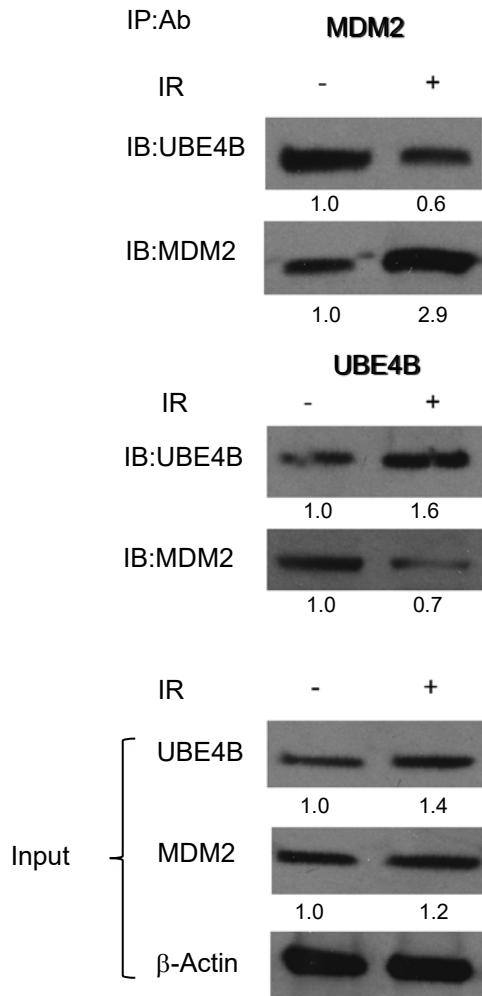
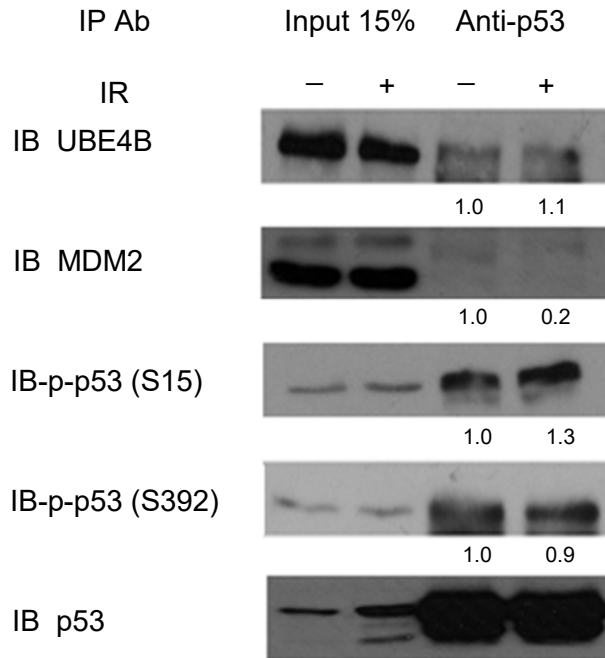


**Figure 19C. UBE4B dissociates from MDM2 post-irradiation**

Following treatment with 6 Gy of IR, MCF10A cells were harvested after 3 h. Cell lysates were immuno-precipitated with Anti-MDM2 (2A10) or Anti-UBE4B followed by western blot analysis using specific Anti-UBE4B and Anti-MDM2 antibodies. 15% of extract used as input and directly analyzed by western blot as shown in the lower panel.  $\beta$ -Actin was used as a loading control. Densitometry was performed with ImageJ software (NIH) and relative UBE4B or MDM2 band and intensity normalized to IgG heavy chain for Co-IP or  $\beta$ -actin for input. Blots represent a minimum of two replicates.

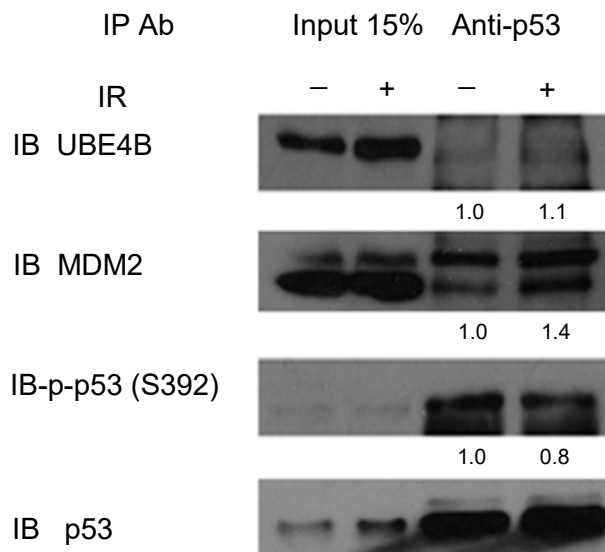
To further confirm that UBE4B binds to phosphorylated p53 post-irradiation, Co-IP analysis included wild type and other two mutant constructed H1299 cells that lack wild type Ser15 (H1299 S15A) or wild type Ser392 (H1299 S392A). Consistent with the data observed in MCF7 cells (Figure 19A), findings showed that the transfected wild type p53 associated with UBE4B after IR in the Co-IP experiments; however, the wild type p53 failed to bind with MDM2 in p53-negative H1299 cells (Figure 20A). Subsequently, H1299 cells were transfected with p53 S15A and p53 S392A expression plasmids. In addition, the cell lysates were coimmunoprecipitated with anti-p53 specific antibody (DO-1), and analyzed by western blotting. The observations revealed that UBE4B also bound to the p53 S15A or p53 S392A *in vivo*, confirming that UBE4B associates with both phosphorylated p53 at Ser15 and Ser392 after exposure to IR. The results additionally suggested that this association might not require the simultaneous co-existence of both intact residues; specifically, the UBE4B interaction with Ser15 does not need an intact Ser392 residue and vice versa (Figure 20 B and C).

A



H1299 cells  
(transfected with the wild-type p53 expression plasmid)

B



H1299 cells  
(transfected with the p53 S15A expression plasmid)

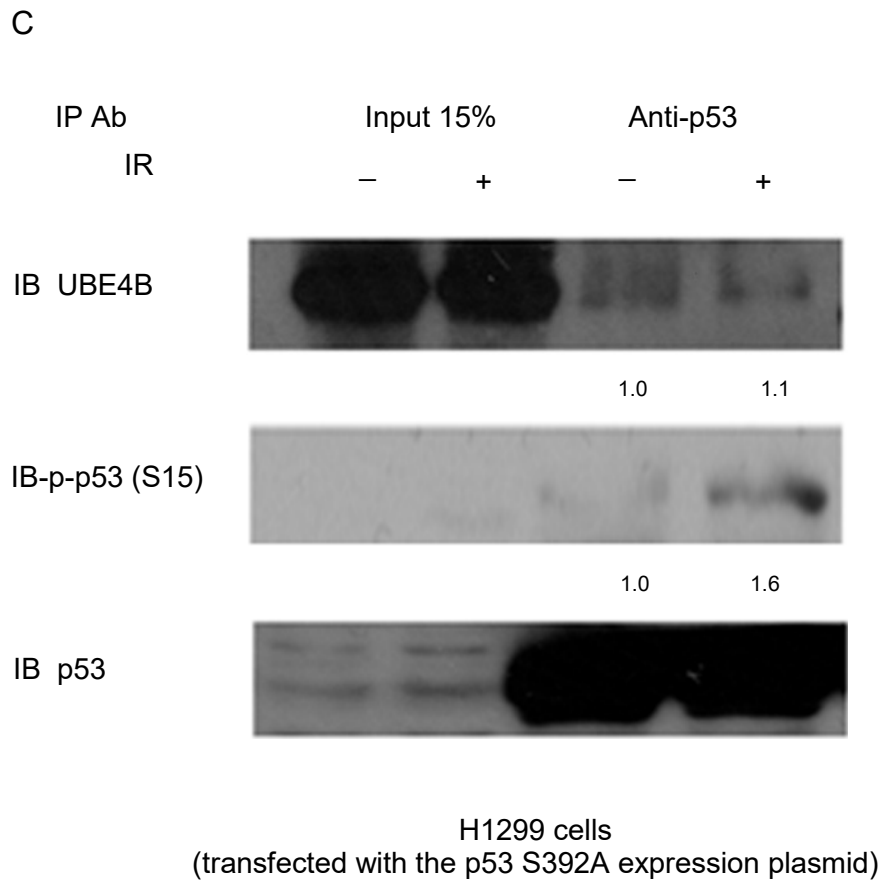


**Figure 20. UBE4B binds phosphorylated residues of p53 at Ser15 and Ser392 post-irradiation**

**A.** H1299 cells were transfected with the wild-type p53 expression plasmid. Following treatment with 6 Gy of IR, H1229 cells were harvested after 3 h, 600  $\mu$ g of total proteins were used to immune-precipitate total p53 protein using p53 specific antibody (DO-1). 15% of the total whole cell lysate was used for the IP as input. Western blot analysis was performed using specific antibodies (Pab1801 for p53, SMP 14 for MDM2, UFD2 for UBE4B, anti-p53Ser15 and anti-p53Ser392). **B.** Similar to the **A**, except that H1299 cells were transfected with p53 S15A expression plasmid. **C.** Similar to the **A**, except that H1299 cells were transfected with p53 S392A expression plasmid. Densitometry was performed with ImageJ software (NIH) and relative UBE4B or MDM2 or p53 S15 or p53 S392 band and intensity normalized to IgG heavy chain for Co-IP. Blots represent a minimum of two replicates.

## **UBE4B enhances the degradation of phospho-p53 (Serine 15) and phospho-p53 (Serine 392)**

The fact that UBE4B binds with phosphorylated p53 Ser15 and Ser392 [175] , raised questions about the ability of UBE4B to assist in the proteasomal degradation of phosphorylated p53. To address this question, H1299 cells were transfected with p53 expression plasmid as well as an empty vector pcDNA3, UBE4B, or MDM2. After 30 h of transfection, the cells were treated with 6 Gy of IR, harvested, and analyzed by western blotting. As shown in Figure 21, the overexpression of UBE4B decreased the levels of total p53, p53 Ser15, and p53 Ser392. Surprisingly, the overexpression of MDM2 also resulted in a decline in the levels of p53 Ser15 and p53 Ser392 (Figure 21). However, mechanisms governing the way in which the ectopic expression of MDM2 decreased p53 Ser15 or p53 S392 require further investigation.

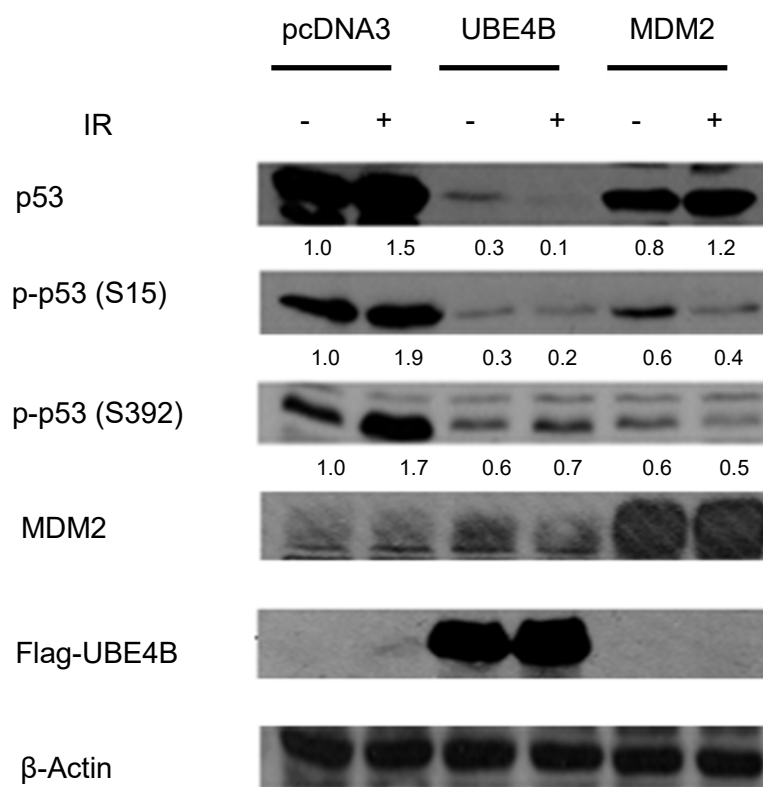


**Figure 21. Phosphorylated residues of p53 at Ser15 and Ser392 are targets for UBE4B-mediated p53 degradation**

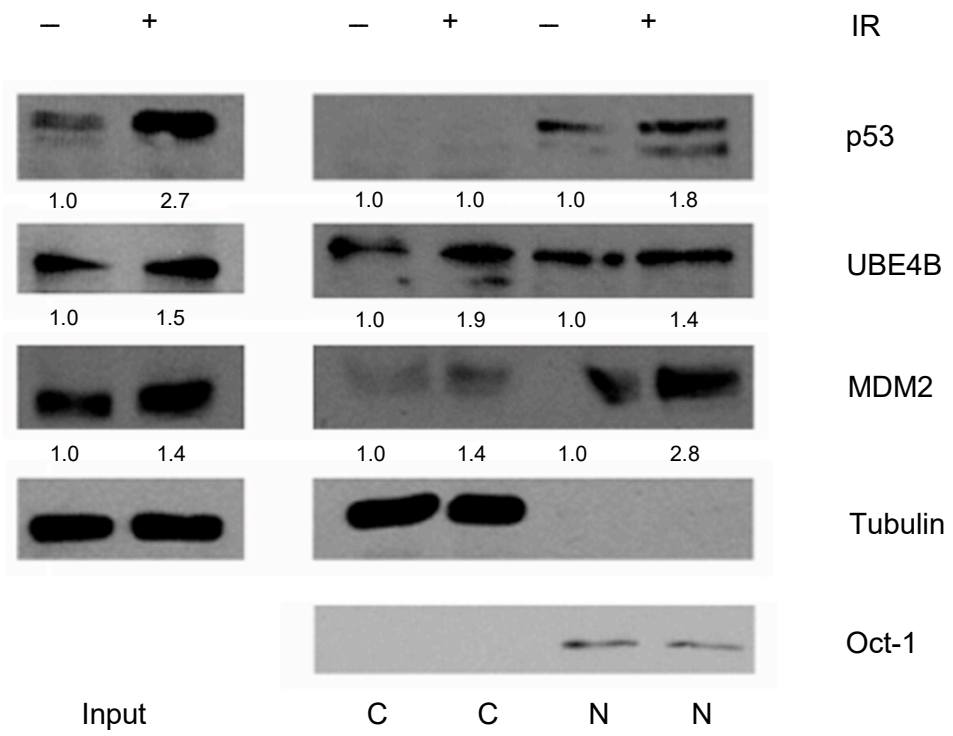
H1299 cells were transfected with p53 expression plasmid, in combination with empty vector (pcDNA3), or UBE4B, or MDM2 as indicated. After 30 h transfection, the transfected cells were treated with 6 Gy of IR, and analyzed by western blots. The anti-p53 (DO-1) for p53, anti-p-p53Ser15 for p53Ser15, anti-p-p53Ser392 for p53Ser392, SMP 14 antibody for MDM2, anti-Flag (M2) for UBE4B and anti-actin for loading control ( $\beta$ -Actin) antibodies. Densitometry was performed with ImageJ software (NIH) and relative total p53, or p53 Ser15, or p53 Ser392 band and intensity normalized to  $\beta$ -actin. Blots represent a minimum of two replicates.

## **Subcellular localization: UBE4B is mainly localized in cytoplasm post-exposure to DNA damage**

The subcellular localization of p53, MDM2, and UBE4B were investigated through the use of fractionation analysis using human epithelial breast cancer cell lines (MCF7). Following exposure to 6 Gy of gamma irradiation, nuclear and cytoplasmic fractions were extracted and then evaluated via western blot analysis utilizing the nucleus (N)-specific marker Oct-1 antibody or the cytoplasm (C)-specific marker tubulin antibody [176] . Subsequently, cell fractionation analysis was extended to study the effect of UV light on the trafficking of ubiquitin ligases.

For UBE4B in MCF7 breast cancer cells, the data showed that at 1.5 h post-irradiation, only the cytoplasmic level of the UBE4B protein was elevated while no change was observed in its nuclear level (Figure 22A). Furthermore, the level of UBE4B was notably elevated in the cytoplasm, whereas the level of MDM2 in the nucleus was significantly increased following IR. In fact, the cytoplasmic UBE4B and nuclear MDM2 underwent the same rate of elevation. These findings demonstrate consistency with previous reports, which showed that at later time periods, such as three hours, the nuclear level of UBE4B demonstrated a remarkable decrease, indicating a trafficking of UBE4B from the nucleus to the cytoplasm following exposure to IR [175] . However, this data requires further experiments at more time points, such as 3 h and 24 h, as discussed in subsequent sections. Additionally, following the treatment of MCF7 cells with UV light, the level of nuclear UBE4B decreased while the level of nuclear MDM2 increased. Both cytoplasmic MDM2 and UBE4B proteins clearly increased (Figure 22B).

A



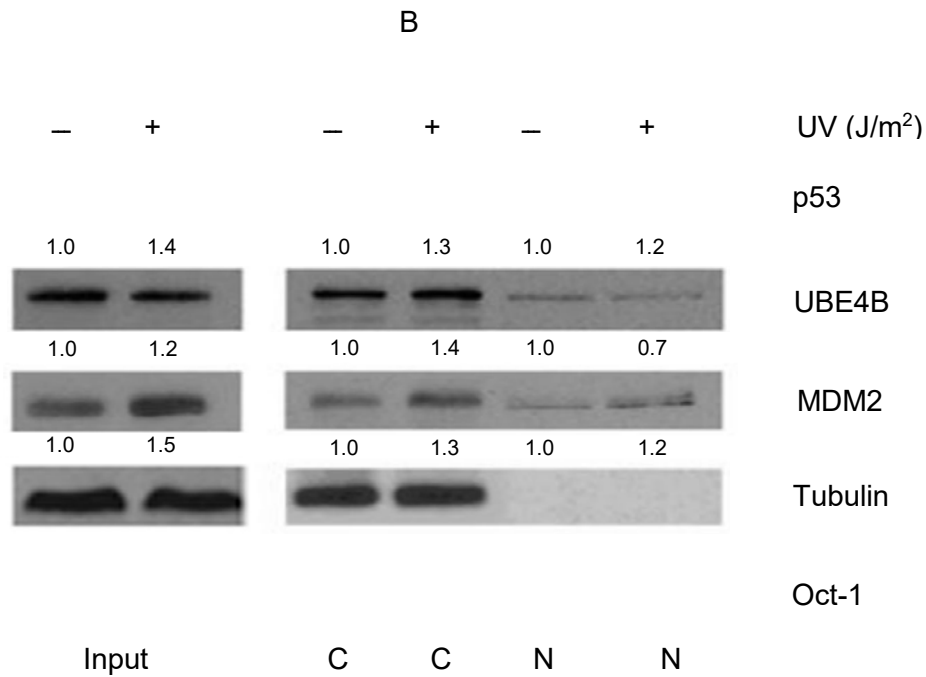


**Figure 22. Subcellular localization of ubiquitin ligases in response to DNA damage**

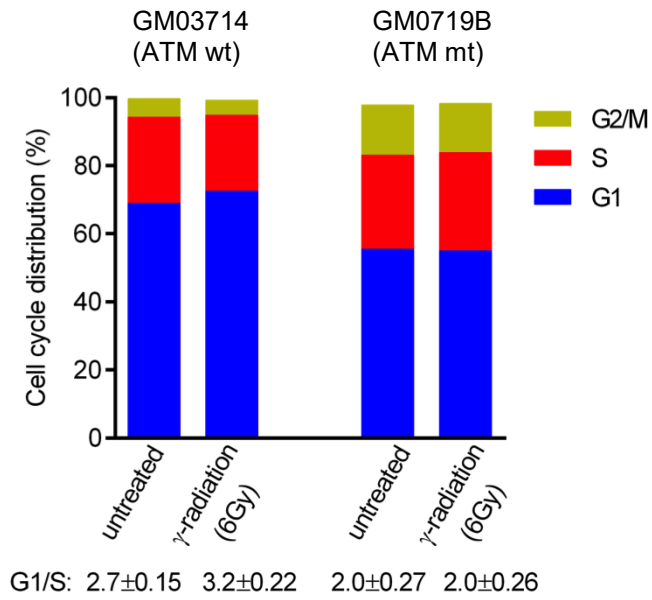
**A.** MCF7 cells were subjected to 6 Gy of IR followed by extraction of cytoplasmic and nuclear fractions from the whole cell (input) 1.5 h after irradiation. Extracts were analyzed by western blotting using Anti-p53 (Pab1801), anti-UBE4B, anti-MDM2 (2A10) specific antibodies. Cytoplasmic fractions (C) were detected by Tubulin marker, and nuclear fractions (N) were detected by Oct-1 marker. **B.** MCF7 cells were subjected to 10 J/m<sup>2</sup> UV light followed by extraction of cytoplasmic and nuclear fractions from the whole cell (Input) 1.5 h after irradiation (Fermentas, USA). Extracts were analyzed by western blotting using Anti-p53 (Pab 1801), anti-UBE4B (BD), anti-MDM2 (2A10) specific antibodies. Densitometry was performed with ImageJ software (NIH) and relative UBE4B or MDM2 or p53 band and intensity normalized to Tubulin (C) or Oct-1 (N). Blots represent a minimum of two replicates.

## Cell cycle analysis in wild-type and mutant LCL cells

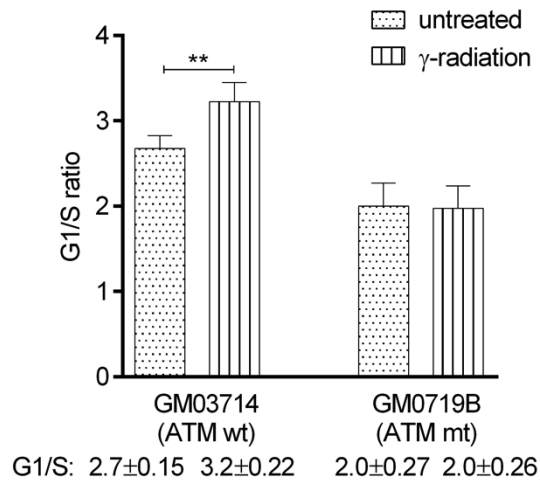
As previously established, UBE4B becomes induced in response to various DNA damaging stressors while UBE4B binds and targets phosphorylated p53 in response to IR. Consequently, an examination of the cell fate in the tested cell models would provide some clues that assist in correlating p53-UBE4B interactions with any type of DNA damage response at early stages, such as cell cycle arrest or apoptosis.

Thus, flow cytometric evaluation of DNA content was conducted in both ATM wild type and ATM mutant LCL cells. As shown in Figures 23 A and B, the G1/S ratio in stressed wild type cells statistically exceed that of its counterpart in unstressed cells (Figure 23A). However, G1/S ratio in both stressed and unstressed mutant cells was comparable (Figure 23B), which suggest that wild type LCL cells may undergo some type of transient cell cycle arrest at the G1-S checkpoint; conversely, mutant LCL cells lack the same response at the comparable time point. This finding demonstrates consistency with the literature [177] and exhibits predictability based on the absence of ATM in mutant cells, thus resulting in the delayed activation of p53 and its downstream target p21, which supposedly activates the cell cycle checkpoint at G1/S. Additionally, the fraction of sub-G1, presumably apoptotic, cells in both cases was extremely negligible, indicating the absence of any potential apoptotic response (Figures 23 C and D).

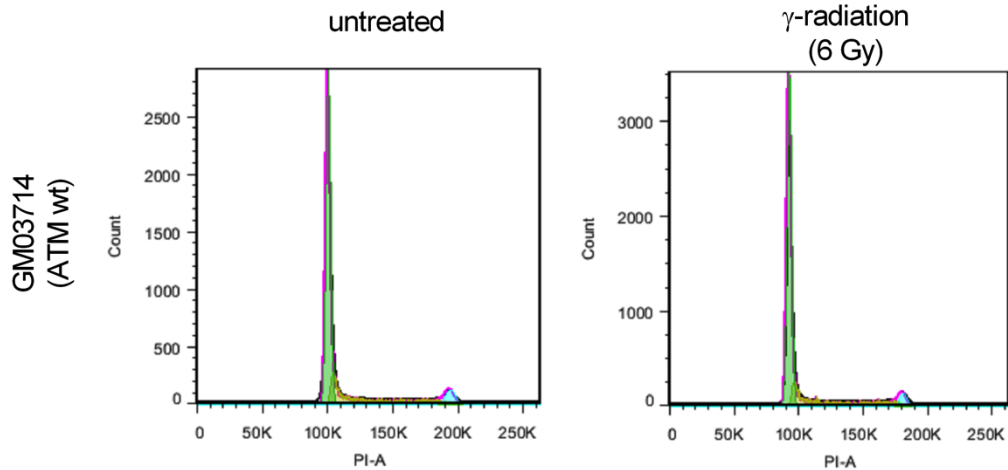
A



B



C



D

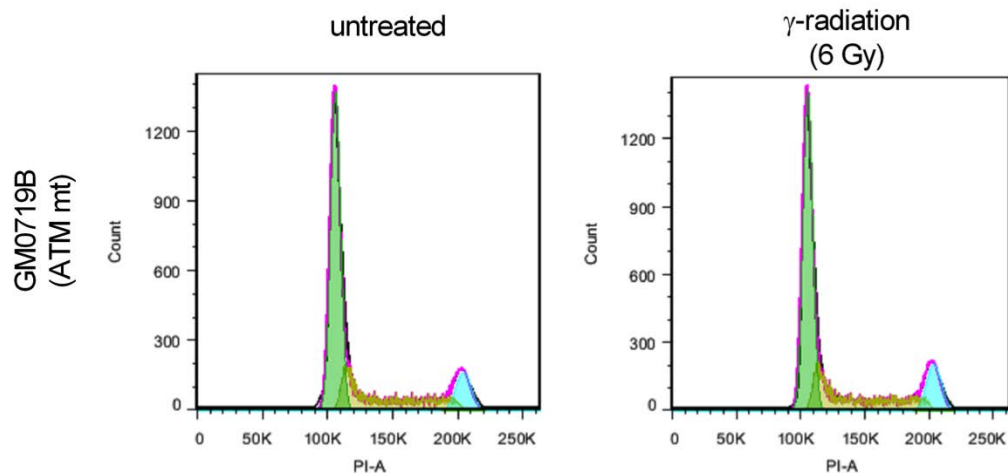


**Figure 23. Cell cycle analysis in response to ionizing radiation in wild-type Vs. mutant LCLs**

After treatment with 6 Gy of IR (3 h) or leaving without treatment, flow cytometric analysis was performed using PI staining, to measure the DNA content and analyze cell cycle distributions in wild-type GM03714 and mutant GM0719B LCLs (A). Coloured bars indicate subpopulations of cells in G1, S and G2/M phases. G1/S ratio demonstrates the extent of G1 arrest in each cell. Individual G1/S ratios were shown and compared in (B),  $P < 0.01$  (two-tailed t-test). Histograms of fixed PI stained wild-type (GM03714) (C) and mutant (GM0719B) LCL cells (D) are shown. Blots represent a minimum of two replicates.

*Chapter 4*

*Discussion*

## Discussion

In recent years, the research group conducting this study found that MDM2 ubiquitination activity might lack the ability to independently cause an efficient proteasomal degradation of p53. Rather, UBE4B ubiquitin ligase reportedly enhances MDM2-mediated p53 degradation both *in vivo* and *in vitro* [178,179]. Accordingly, this present study also questioned whether UBE4B might contribute to p53 regulation in response to DNA damage. This research hypothesized that ATM or ATR phosphorylates p53, which affects its level and leads to the disruption of UBE4B-p53 interactions in response to DNA damage. Furthermore, this study conjectured that UBE4B comprises a critical p53 negative regulator in an ATM- or ATR-dependent pathway. To test this hypothesis, both ATM-proficient and ATM-deficient lymphoblastoid cell lines were initially employed.

Consistent with previous studies in AT LCL cells, the findings revealed that p53 induction and activation in these cells is ATM-independent and that ATR-signalling might represent the predominant pathway in AT cells. In addition, the investigations demonstrated that MDM2 and UBE4B are induced independently of ATM in response to DNA damage in LCL cells. Interestingly, the results demonstrated that ATM is dispensable for the interactions of p53 with both MDM2 and UBE4B in response to IR in LCL cells, hence indicating that the stability of p53 may not be influenced by ATM activity.

Subsequently, the investigations further analyzed the potential role of UBE4B in response to ionizing radiation by utilizing breast normal and cancer cell lines. The results revealed that in MCF7, which constitutes ATM-proficient cells, UBE4B binds to p53

independently of MDM2 and may enhance the degradation of phosphorylated p53 at Ser15 and Ser392 post-irradiation. These findings demonstrate consistency with previous studies [175]. Interestingly, localization studies showed that UBE4B is mainly localized in the cytoplasm in response to DNA damage, thus supporting the previous finding that UBE4B may promote the degradation of cytoplasmic phosphorylated p53 forms. Finally, cell cycle analysis of LCL cells showed that these cells may not undergo DNA damage-induced apoptosis at early stages.

## **p53 dynamics in lymphoblastoid cells**

As discussed in the introduction, recent p53 dynamic studies reported that in MCF7 cells, radiation induces a characteristic dynamic behaviour, which researchers consider as universal [88,91] . After irradiation, p53 levels increased until 2 h, decreased until 4 h, and increased until ~8 h; this fluctuating response continued for a significant period of time post-irradiation. In the current study, however, the analysis of both wild type ATM and mutant lymphoblastoid cell lines detected p53 induction at different time points following exposure to ionizing radiation. The results found that the patterns of p53 induction detected in these cells lacked consistency with the predictable patterns that occur in other cell types, such as MCF7; thus, radiation-induced p53 dynamics seem to demonstrate cell-type-specific behaviour. The extent to which this inconsistency results from the effect of EBV-transformation requires further investigation.

## **ATR signalling might be the predominant pathway in ATM-deficient cells**

The p53 protein is activated via various protein kinases in response to DNA damage [180] . Two main upstream activators of p53 include ATM and ATR [55,56] . While ATM was associated with p53 activation in response to ionizing radiation, ATR was connected with p53 activation in response to ultraviolet light [181] . Despite these general tendencies, the potential for overlap exists concerning the roles of these kinases for inducing the same response in different contexts, which are influenced by various factors such as time and types of modification [180] . Since the ATM-deficient

lymphoblastoid cells lack the normally-expressed ATM protein, this study anticipated that these cells would display reduced p53 activation as well as an alternate upstream p53 activator to compensate for ATM. Unexpectedly, the findings showed that, as in the case of wild-type lymphoblastoid cells (Figure 11 A,D), p53 underwent normal activation in mutant lymphoblastoid cells (Figure 11 B,C,E,F), suggesting that p53 regulation in ATM-deficient lymphoblastoid cells is not exclusively ATM-dependent.

Previous studies that have addressed p53 activation post-irradiation in AT cells reported contradictory results concerning the levels and time period of this activation. Consistent with the findings in this study, some groups reported that a number of skin fibroblast strains from different AT patients displayed a normal induction of p53 after exposure to ionizing radiation [156] . However, other researchers reported a reduction, delay, or absence of p53 induction in different cells, such as skin fibroblast strains and lymphoblastoid cell lines, from different patients [157-160] . A recent study using immunofluorescence microscopy revealed that AT fibroblasts demonstrate p53 upregulation only during a relatively late period, such as 4 days, after irradiation [160] . However, the researchers neglected to confirm whether this inconsistency results from cell-specificity, variable cellular genetic backgrounds, or unidentified experimental conditions.

Furthermore, as shown in Figures 15 B, C, E, and F, when lymphoblastoid cells were exposed to 6 Gy and 2 Gy of IR, the findings demonstrated that the ATR protein was upregulated in both ATM-deficient cells. This result suggests that ATR may undergo substitution for ATM in AT cells and that ATR-signalling might constitute the predominant pathway that stabilizes and activates p53 in AT cells. These data are

consistent with previous reports, which indicated that the ATR-Chk1 pathway supersedes ATM-Chk2 in AT cells [182]. Further confirmation of these findings through an in-depth examination of the ATR-Chk1 pathway may uncover the potential role of ATR, which therefore may determine whether ATR can be utilized in targeted cancer therapy. An examination of the ATR-Chk1 pathway may involve an initial assessment concerning the role of ATR by screening for ATR-downstream targets such as Chk1. Next, researchers can obtain additional clues by detecting ATR phosphorylated forms, which provide reliable markers for its activity. Several studies have reported that ATR undergoes phosphorylation at Ser 435 and Thr1989 [183], [184] following DNA damage. Moreover, investigations can further confirm the role of ATR using ATR inhibitors such as VE-821 [185] to modulate its level in wild-type cells, thus enabling researchers to study the effect of its inhibition on p53 regulation. Finally, the use of Chk1 and Chk2 knockout cell models to compare the phosphorylation status of these cells with the previously-studied cells will provide further confirmation concerning the role of ATR.

These preceding approaches will enable researchers to explain the way in which p53 regulation in AT cells is ATM-independent. If studies confirm that ATR, rather than ATM, influences p53 regulation, this result would constitute a novel finding requiring further confirmation in other types of AT cells, such as AT fibroblasts, to determine the extent of cell specificity. If investigations find that ATR fulfills an insignificant role, this result will provide impetus for further studies to identify other protein kinases that are essential for p53 regulation in AT cells.

However, the exposure of lymphoblastoid cells to a lesser dose of radiation, such as 2 Gy (Figures 15 D-F) causes only a slight change in the ATR basal level during the tested time period. This finding indicates that ATR signaling in lymphoblastoid cells might be dose-dependent and suggest that in mutant EBV-transformed AT lymphoblastoid cells, variable doses of gamma irradiation likely induces different p53 upstream activators.

While ATR induction post-irradiation seems to be dose-dependent in lymphoblastoid cells, the present phosphorylation studies demonstrated that the expression of phosphorylated forms at Ser15 and Ser392 in these cells might be dose-independent, as shown in Figures 14 A-F. In lymphoblastoid cells, the exposure to 6 Gy of ionizing radiation induced phosphorylated p53 at Ser15 and Ser392 (Figures 14 A-C). Similarly, the exposure to 2 Gy of ionizing radiation resulted in the induction of the same phosphorylated p53 forms (Figures 14 D-F). Hence, no matter what type of kinase is employed, phosphorylation in LCL cells is carried out in a dose-independent manner.

Overall, it should be critically noted that the notion of ATM-independency in the context of the findings of this study does not necessarily reflect the absolute state in all cases. Our data can only suggest that UBE4B acts independently of ATM when the cells lack ATM, as is the case with AT cells. However, our data do not rule out the possibility that UBE4B is regulated by ATM in cells expressing functional ATM.

## **ATM is not essential for p53 interactions with MDM2 and UBE4B ubiquitin ligases in lymphoblastoid cells**

The ATM-p53-MDM2 model constitutes one of the most widely proposed early paradigms that accounts for p53 stabilization. The literature concurs that the phosphorylation of p53 in its binding sites with MDM2 is crucial for disrupting MDM2-p53 interactions and hence contributes to the stability and activation of p53 [58,60-63]. Researchers have suggested that several p53 residues lying in the MDM2-p53 interaction N-terminal region, including Ser15, Thr18, and Ser20, represent essential targets for p53 phosphorylation [53,54,186]. The data in this study showed that in LCLs, ionizing radiation resulted in the induction of phosphorylated p53 at Ser15 and Ser392 independently of ATM (Figures 14 A-F). Simultaneously, MDM2 and UBE4B were upregulated independently of ATM following exposure to ionizing radiation in these cells (Figure 11 A-F). Research has established that MDM2 and UBE4B incur transcriptional induction by p53 in a negative feedback loop [187], which explains their upregulation.

Moreover, further investigations involving additional DNA damaging agents, such as UV-light and 5-FU chemotherapeutic drug, confirmed these previous findings (Figures 16 B-E and Figures 17 A-D). Hence, regardless of the type of DNA damage, UBE4B is induced independently of ATM in LCL cells despite differences in the patterns of p53 upregulations. Unlike other ubiquitin ligases, such as COP1, which reportedly stabilizes p53 in ATM-dependent fashion [47], UBE4B seems to act on p53 independently of ATM.

Since the induced level of different ubiquitin ligases may fail to reflect their association with p53, studies must investigate the binding affinity between p53 and

ligases to ensure their potential function in p53 downregulation. Therefore, this study sought to determine whether endogenous p53 interacts with MDM2 and UBE4B in response to IR. According to the previously-mentioned model, this study anticipated that affinity binding of p53 with both MDM2 and UBE4B would decrease post-irradiation in lymphoblastoid cells. Surprisingly, p53 interactions with MDM2 and UBE4B in LCL cells in response to ionizing radiation consistently revealed an increase in the binding affinity of MDM2 with p53 in both wild type and mutant lymphoblastoid cells. However, the binding affinity of UBE4B with p53 showed an increase in mutant cells without any obvious change in wild type cells. These findings, along with the ATM-MDM2-p53 tested model, indicate that the interactions of p53 with MDM2 or UBE4B are ATM-independent, and thus, the effect of UBE4B on p53 stability, if any, is ATM-independent in either normal or mutant EBV-transformed lymphoblastoid cells. These implications suggest that other p53 upstream kinases may fulfill a role in these cells.

Considering the complexity of p53 regulation by post-translational modifications, the phenotype of the association of p53 with MDM2 and UBE4B most likely becomes affected by cell type [186]. Since the process of EBV transformation does not seem to influence p53 stability and function (159,160), further investigations should exclude EBV transformation effects. In addition, the question of whether other mechanisms influence the stability of p53 in response to DNA damage in LCLs requires additional studies. For instance, one investigation has proposed that MDM2 phosphorylation at Ser 395 may prevent MDM2-mediated p53 transport from the nucleus to cytoplasm and thus inhibit p53 degradation [61]. Also, researchers have suggested that the rapid MDM2 degradation by the SCF<sup>β-TRCR</sup> ubiquitin ligase following MDM2 phosphorylation at

several residues contributes to p53 stabilization [188]. Recently, investigations found that interaction of p53 mRNA with MDM2, mediated by ATM, transforms MDM2 from a negative to a positive p53 regulator [189].

In addition, recent studies have revealed that protein-protein interactions between MDM2 and p53 are dispensable for p53 stability [190]. In those investigations, researchers employed a genetically engineered Mdm2 knock-in mouse, which lost the capability of ubiquitinating p53 but maintained the ability to bind p53 and suppress its transcriptional activation [190]. Remarkably, the studies found that, as in the case of the phenotype of Mdm2 null mice, embryonic lethality in these mice was p53-dependent [27]. Moreover, these mice had the capacity to ubiquitinate and degrade Mdm2. Collectively, these studies propose that during the early development stage, MDM2-p53 protein interactions may fail to independently prevent programmed cell death (apoptosis) mediated by p53, thus suggesting that other MDM2-independent ubiquitination mechanisms may control the stabilization of both p53 and MDM2 proteins [26].

## **UBE4B, a potential role in regulating p53 at Ser15 and Ser392 in response to DNA damage**

In this attempt to explore the potential role of UBE4B in response to DNA damage, this investigation was extended to include the human breast cell lines MCF7 and MCF10A. Obtained data showed that both UBE4B and phosphorylated p53 at Ser15 and Ser392 were upregulated post-irradiation. The results verified the *in vivo* interaction of UBE4B with phosphorylated p53 at Ser15 and Ser392 in stressed cells via co-immuno-

precipitation. Furthermore, using H1299 cell lines, the data further demonstrated that UBE4B might enhance the degradation of phosphorylated p53 at Ser15 and Ser392 post-irradiation.

Additionally, consistent with previously reported data, the results of this investigation found a decrease in UBE4B-MDM2 interactions in response to IR (Figure 19C), which might suggest that UBE4B-directed degradation in breast cells could occur independently of MDM2. These findings concur with previous studies in mice, which revealed that the overexpression of UBE4B negatively affected the level of p53 in Mdm2-null MEFs, indicating that Mdm2 may not always be necessary for degrading p53 and that UBE4B may degrade p53 independently of Mdm2 [86]. Also, as noted previously, Co-IP studies in ATM-deficient LCL cells consistently showed high affinity binding between UBE4B and p53 in response to ionizing irradiation. However, these studies failed to investigate if this increased association results in the ubiquitination and degradation of p53 at Ser15, Ser392, or Ser20 in those cells. Such a finding in lymphoblastoid cells would confirm that UBE4B might act as a negative regulator of phosphorylated p53 forms in response to DNA damage. Prior studies indicated the significant role of UBE4B in p53 regulation [86]. Wu et al. found that compared to parental murine wild-type MEFs, mouse UBE4B-null MEFs display a significantly elevated basal level of endogenous p53 protein, thus suggesting the essential role of UBE4B for regulating the p53 basal level under normal conditions [86].

In addition, the findings of this current study support recent reports verifying that UBE4B promotes the degradation of phosphorylated p53 [175]. Interestingly, UBE4B is overexpressed in several types of cancer, such as breast cancer [191] and hepatocellular

carcinoma [192] . Furthermore, the detected overexpression of UBE4B in such tumours was associated with a decline in p53 expression level [191,192] . The findings in this study display consistency with previous reports and thus highlight the significance of UBE4B as a negative regulator for phosphorylated p53. Similarly, previous research reported that other ligases such as Caspase 8/10-associated RING proteins (CARPs), including CARP1 and CARP2, ubiquitinate and promote the degradation of phosphorylated p53 at the Ser20 residue in an Mdm2-independent manner [193] . One study proposed the CARP2-mediated degradation of phosphorylated p53 at Ser15; however, this finding has not yet been confirmed [193] . Moreover, some adaptor proteins of E3 ligases, such as BZLF1, associated with the ECS ligases complex, contribute to the degradation of virally-induced p53 phosphorylated forms [194] .

The finding that UBE4B targets phosphorylated p53 for degradation represents an intriguing discovery and thus adds to the well-known complex and diverse roles of various ligases that regulate p53. This study found that p53 is commonly phosphorylated at Ser15 and Ser392 in response to DNA damage. These phosphorylation sites reside in the N-terminus and C-terminus respectively. Specifically, the N-terminus contains MDM2 binding sites and is associated with the transcriptional activation property of p53. The C-terminus, which contains the Ser392 residue, constitutes the tetramerization domain. Thus, these phosphorylation sites might be essential for p53 stabilization and activation.

Accordingly, Ser15 is phosphorylated by ATM, ATR and DNA-PK protein kinases in response to DNA damage [58,195,196] as well as by AMPK following exposure to other stressors, such as metabolic stress [197] . The role of Ser15 in p53 stabilization

occurs through its biochemical ability to recruit histone/lysine acetyltransferase (HAT) proteins [198,199] , which enhance the acetylation of several sites within the DNA-binding and C-terminus regions of p53. These acetylations prevent ubiquitination and hence stabilize p53 [200,201] . Moreover, the phosphorylation of Ser15 initiates a cascade of subsequent phosphorylations at several residues, such as Ser9, Ser20, Ser46, and Thr81, which foster p53 stability and activity [73,201-204] . In addition, recent reports confirmed the involvement of Ser15 phosphorylation in promoting p53 transcriptional activity [205] .

Furthermore, the phosphorylation of p53 at Ser392 was implicated in p53 stabilization and activation. Initially, researchers believed that phosphorylated p53 at Ser392 is exclusively induced by UV light [171] ; however, other groups, in agreement with the results of the present study, reported that this modification occurred in response to other stimuli, including other-DNA damaging agents [206] . Several upstream activators, such as CK2 [200] , p38 MAPK [73,172] , and CDK9 [207] induced p53 phosphorylation at Ser392 *in vitro*.

Earlier research indicated that the phosphorylated Ser392 site, which equates to Ser389 in mice, shows a high degree of homology among organisms [208] and performs different p53-related functions. For example, studies reported that Ser392 activated DNA binding capabilities by CK2 *in vitro* [209] , most likely because it enhances the formation of stable tetramers [210] . Also, Ser392 promotes p53-mediated growth suppression *in vitro* [211] . Additionally, Ser389 mutant mice demonstrated a higher susceptibility to skin cancer when exposed to UV light [212] and bladder cancer when exposed to chemotherapeutic agents [213] . Moreover, multiple investigations observed

the modified expression of p53-target genes in Ser389 mutant mice cells when compared to wild type cells [214,215] , thus suggesting a potential role for the phosphorylated residue at Ser392 in p53 tumour suppressive effects.

Despite the indicated significance of individual phosphorylation modifications, studies conducted with S392A mutations were associated with relatively mild physiological changes, which may result from the redundant nature of *in vivo* phosphorylation. In fact, many activators phosphorylate the same residues and many residues are phosphorylated by the same activator, thus decreasing the likelihood that one individual phosphorylation event functions to switch p53 from a latent to a stable and transcriptionally-active entity. Alternatively, each individual phosphorylation event likely assists in fine-tuning and regulating p53 function in a “tissue and promoter specific manner” [216] .

Based on the aforementioned role of phosphorylated p53 forms in maintaining the stabilization and activation of wild-type p53, the reported targeted degradation of these forms via UBE4B ubiquitin ligase, in this study and other research, presumably halts the tumour-suppressive effect of p53 and thus could physiologically constitute an oncogenic step, particularly in wild type p53 bearing tumours. Hence, further analysis and extended investigations of these findings, as discussed in the future direction section, may enable researchers to better understand the molecular pathways that control p53 regulation and appreciate the constantly increasing knowledge about the complexity of this field. Ultimately, this research would potentially assist in developing new effective targeted therapeutic approaches for treating cancer.

## **Subcellular localization of p53, MDM2 and UBE4B in response to DNA damage: Possible connection with UBE4B role and suggestive of a new insight on p53 trafficking regulation**

One essential level of p53 regulation involves considerations about the subcellular localizations of p53 [217] . The functional significance of p53 localization is shown by the fact that in response to various stressors, p53 needs to remain in the nucleus for the growth inhibition of tumour cells [217] . Furthermore, studies found that in wild type p53 bearing tumours, the loss of p53 functionality was associated with a lack of p53 nuclear retention due to either the cytoplasmic sequestration or the hyperactivity of nuclear export machinery, thus indicating that these kinds of tumours exhibit an impaired response to radiotherapy and chemotherapy. Additionally, p53 sequestration in cytoplasm represents a prognostic factor in malignancy [218-222] . The results of such investigations indicate that p53 activity depends on its location. For instance, nuclear p53 acts mainly as a transcriptional regulator of various target genes, while mitochondrial p53 directly stimulates apoptosis [223] .

The subcellular localization of p53 occurs as a result of many factors [224] . One major factor involves the association of p53 with its main negative regulators, ubiquitin ligases. Studies have established that p53 activation in response to DNA damage leads to its increased accumulation in the nucleus, thus resulting in the accumulation and activation of MDM2 [224] . However, in the absence of genotoxic stress, MDM2 interacts with p53 to restore normal p53 levels, resulting in the translocation of p53 from the nucleus to cytoplasm. To pinpoint the mechanism of MDM2-mediated p53 nuclear

export, researchers proposed two models. In the first and earlier model, studies postulated that the binding of MDM2 with p53 leads to the translocation of both proteins into the cytoplasm through the nuclear pores, thus causing p53 to undergo degradation in the cytoplasm [225-227]. The second widely accepted model focused on the role of the RING domain of MDM2 as a determinant factor in p53 transport. This model proposed that the MDM2-mediated monoubiquitination of p53 in the nucleus exposes p53 NES, which results in the nuclear export of p53 and its subsequent cytoplasmic proteasomal degradation [228]. Considerable experimental evidence supports the second model. Studies found that the MDM2 RING domain mutation prevents the nuclear export of p53, indicating the necessity of MDM2 ubiquitin ligase activity to translocate p53 [229,230]. In addition, research demonstrated that an intact NES of p53, rather than MDM2, is required to perform MDM2-mediated p53 translocation [231,232]. These results suggest the non-simultaneous shuttling of MDM2 and p53 from the nucleus; in addition, such findings indicate that the presence of MDM2 in the cytoplasm is not mandatory for the complete proteasomal degradation of p53 [217].

Consistent with a recent reported study [175] investigating the subcellular localization of ubiquitin ligases in MCF7 cells, the results of this report showed that the nuclear UBE4B level was notably reduced, while the level of MDM2 in the nucleus was significantly elevated post-irradiation (Figure 22A). Also, the p53 level was increased in both nucleus and cytoplasm post-irradiation. The observed disruption of MDM2-UBE4B interactions in response to IR may indirectly suggest that UBE4B assists in degrading phosphorylated p53 independently of MDM2. Although the results showed that UBE4B tended to bind and promote the degradation of phosphorylated p53 following exposure to

ionizing irradiation, the nuclear level of UBE4B was diminished post-irradiation. Thus, consistent with other studies [175], this investigation concludes that after p53 activation, UBE4B partially contributes to the degradation of nuclear phosphorylated p53 while mostly enhancing the degradation of cytoplasmic phosphorylated p53. The cytoplasmic localization of UBE4B poses several questions. Firstly, since the UBE4B-MDM2 affinity binding diminished in response to IR, and UBE4B, similar to MDM2, undergoes transcriptional regulation, future studies need to investigate the extent to which nuclear MDM2 or UBE4B monoubiquitinates p53 while cytoplasmic UBE4B polyubiquitinates p53 and thus targets it for degradation. Secondly, this study found that UBE4B promotes the degradation of phosphorylated p53 using an ectopic expression approach in H1299 cells, while other reports found similar results in other cells, such as MCF7, HCT116 human colon cancer cells, and HEK293 embryonic kidney cells [175]. However, future studies need to determine whether UBE4B promotes the degradation of endogenous phosphorylated p53 in the same cells and subsequently link these results to localization findings. Finally, investigations should seek to identify whether the phenotype of UBE4B localization is cell-type specific or DNA damage specific.

Using UV light, this study observed that the levels of p53, MDM2, and UBE4B in the cytoplasm increased (Fig 22B), which may imply the potential involvement of UBE4B in MDM2-mediated ubiquitination of p53. Future research can confirm this post-UV light observation by further affinity binding testing of MDM2-UBE4B interactions and verify their interactions in the cytoplasm after exposure to UV light. Accordingly, such studies can conclude that the trafficking behaviours of ligases following exposure to

UV light differ from those following ionizing irradiation, hence confirming the specificity of DNA-damaging agents in p53 regulation.

Subcellular localization of various proteins was investigated using cell fractionation analysis. Principally, various kits were employed to extract both intact non-denatured cytoplasmic component and nuclei from the tested cells in a stepwise manner. Cellular fractionation commences with harvesting and lysing the cells using non-ionic detergents. Then, cytoplasmic proteins are separated from nuclei through serial centrifugations. Finally, nuclear fraction is purified, lysed and used for analysis. Proteins from both nuclear and cytoplasmic fractions are separated by electrophoresis and then analyzed by western blot using specific known nuclear and cytoplasmic markers to assess the purity and yield of the fractionated parts. This method is rapid, easy to use and cost-effective. However, commercial used buffers may interfere with the functions of tested proteins [233], although this limitation does not pertain to the main purpose of using this approach in this study.

Despite its advantages, fractionation analysis is subjected to contaminants and thus may produce false positive outcomes. Quantitative mass spectrometry (Q-MS), which combine the cellular fractionation with MS is considered to detect low level of contaminations and thus improve the overall reproducibility and specificity [234]

Alternative approaches to study subcellular localization of proteins may involve the use of mass spectrometry (MS) and the employment of imaging techniques, such as immunofluorescence microscopy, confocal microscopy and gold-coated antibody electron microscopy. The main advantage of all microscopic imaging-based techniques is the provision of localization data from single cells [235]. However, fluorescence

microscopy is limited by its low resolution while confocal microscopy has a relatively higher resolution and electron microscopy has exceedingly the highest resolution and has the additional advantage of disclosing organelles, membranes and macromolecules, which assist to better comprehend the complex organization of the cell and the relation of a particular protein location to other cellular compartments [236] . In addition, compared to florescence microscopy, confocal microscopy enables the detection of multi-coloure differences and thus assists to detect the co-localized proteins in a live manner [237]

## **UBE4B role in DNA damage and a suggested model**

Overall, this study revealed two major findings. Firstly, as depicted in Figure 9, the hypothesis of this project surmised that in response to DNA damage, ATM phosphorylates p53, which affects its level and leads to the disruption of UBE4B-p53 interactions. In addition, another hypothesis maintained that UBE4B is a critical p53 negative regulator in ATM or ATR-dependent pathways. Interestingly, the overall findings of this current study suggest a new model, shown in Figure 24, which does not entail the presence of ATM for UBE4B stabilization and its interactions with p53 in response to DNA damage. Secondly, consistent with other studies, these current investigations demonstrated that UBE4B binds with and may degrade phosphorylated p53 in response to DNA damage.

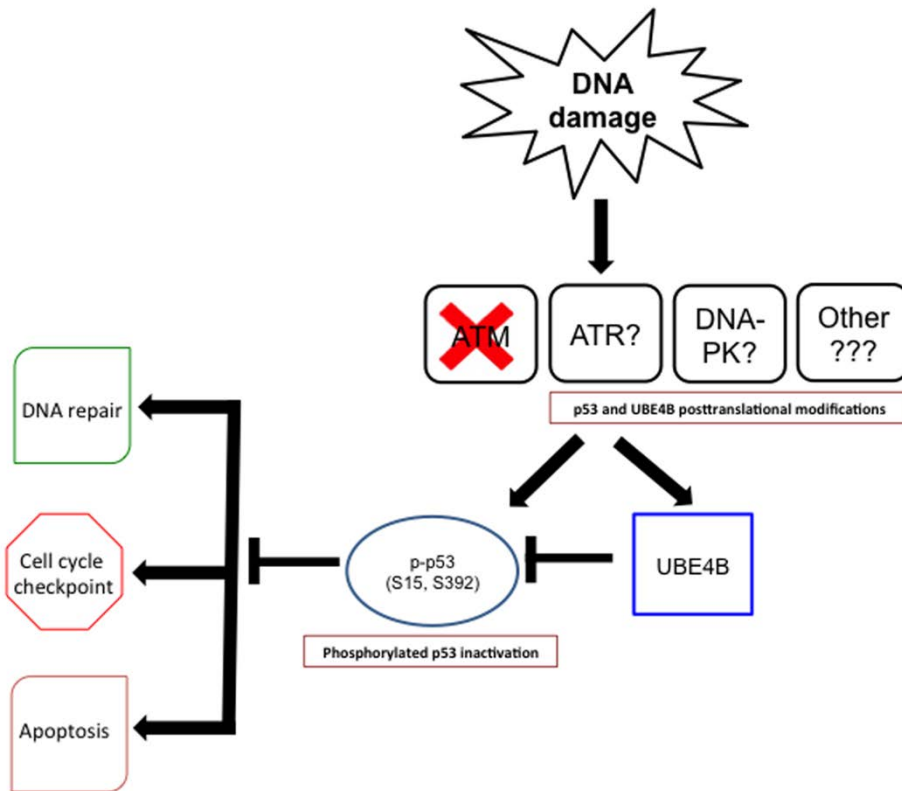


**Figure 24. Role of UBE4B in regulation of wild-type p53 protein; a proposed model**

Model showing that in response to DNA damage, UBE4B binds and may contribute to proteasomal degradation of phosphorylated p53 at Ser15 and Ser392. UBE4B induction and its interaction with p53 is carried out in an ATM-independent manner and may suppress the p53-mediated DNA damage responses.

This new model presents intriguing possibilities for future studies to investigate the plausible importance of UBE4B in p53 regulation in response to DNA damage. Firstly, research has established that ATM activates p53 and MDM2 in response to DNA damage; however, the findings of this study revealed the potentially non-essential nature of ATM for inducing and activating UBE4B. The involvement of other alternative upstream protein kinases remains unknown. This study observed that ATR was induced in ATM-deficient cell lines; however, the investigation did not indicate whether ATR induces UBE4B. Hence, new research identifying the UBE4B upstream activator will provide insights into the complex pathways contributing to p53 regulation. Once this unknown activator has been identified, its interaction with UBE4B and their combined significance for p53 stability in response to DNA damage constitutes another tenable inquiry. In addition, this study discovered the involvement of UBE4B in targeting phosphorylated p53, which is essential for initiating various p53-mediated tumour suppressive effects. Hence, research uncovering the potential negative regulators of UBE4B would assist in counteracting UBE4B oncogenic activity in this context. In this regard, the question of whether WIP1 interacts with, dephosphorylates, and inactivates UBE4B, as it does on a wide array of targets in response to DNA damage, requires further exploration.

Answers to the previous questions would unveil another complex level of p53 regulation. Other UBE4B upstream activators may stimulate UBE4B and WIP1 in the same manner as ATM activates MDM2 and engages in the ATM-p53-WIP1-MDM2 model. These findings might suggest that both the reported UBE4B-mediated degradation and previously established WIP1-mediated de-phosphorylation of phosphorylated p53

simultaneously result in p53 down-regulation and inactivation after the resolution of a DNA damage response in normal conditions. Finally, these findings would highlight the importance of the interactions and coordination between various p53 regulatory pathways, which, at first glance, appear to be separated and operate independently in regulating the phosphorylated forms of p53.

In conclusion, this study is among other investigations that attempted to uncover the potential role of UBE4B ubiquitin ligase as an emerging candidate in p53 regulation in response to DNA damage. The data from this study represents the first investigation to reveal ATM's effect on UBE4B level and interactions with p53 in response to DNA damage in AT LCL cells. Also, consistent with previous reports, this study demonstrates that UBE4B may negatively regulate phosphorylated p53 in response to ionizing radiation. The extent to which these new findings may constitute a definitive p53 inactivation mechanism by which wild-type harbouring tumours can evade therapeutic applications, such as radiotherapy and chemotherapy, remains undetermined. Thus, further future investigations are needed to uncover the contribution of UBE4B in p53 regulation in response to DNA damage or other stressors. Ultimately, this accumulated knowledge can assist in better understanding the complex molecular pathways that control p53 regulation, thus leading to the discovery of new effective p53-based targeted therapeutic approaches of wild-type p53 bearing cancers.

***Chapter 5***  
***Future Direction***

## Future Directions

The findings in this study enable several potential routes for future study. These directions constitute both short-term and long-term investigations. The short-term directions can compensate for the major shortcomings and limitations of this study, including the lack of confirmatory approaches to support the findings for most objectives. The long-term avenues can expand on the final proposed model. Together, the suggested explorations would provide a more comprehensive vision of the role of UBE4B in p53 regulation in response to DNA damage, eventually paving the way to a better understanding of the ever-expanding complex field of p53 regulation.

### Short-term directions

Short-term approaches may include chromatin immunoprecipitation (ChIP) analysis in LCLs to confirm the binding of UBE4B gene with phosphorylated p53 by revealing the protein-DNA binding between p53 transcription factor and its targeted binding regions to the *MDM2* and *UBE4B* genes before and after ionizing irradiation. Also, subcellular localization/co-localization of various ligases and phosphorylated p53 can undergo further investigation using fluorescent microscopy, confocal microscopy and electron microscopy. An extension of the localization study to include extra time points at 3 h and 24 h is essential for confirming the current findings. In addition, *in vivo* and *in vitro* ubiquitination assays, along with or without Co-IPs, are mandatory to further uncover and verify the role of UBE4B in either MDM2-dependent or independent mediated degradation of phosphorylated p53. In this regard, previous reported ubiquitination studies confirmed UBE4B-mediated ubiquitination effect on ectopically

expressed p53 or phosphomutants in H1299 cells in response to IR [175]. However, the extent to which UBE4B exerts its potential ubiquitination activity endogenously in AT cells and other cancer cells and tissues should be elucidated. Most importantly, a major possible limitation of the employed cell model, lymphoblastoid cells, involves EBV-transformation. New research should determine the extent to which EBV-mediated immortalization interferes with the data and interpretation in AT cells. Accordingly, the findings of this study in other AT non-transformed derived cells, such as fibroblasts, should undergo exploration. Finally, to verify the role of UBE4B in proteasomal degradation of phosphorylated p53, experiments can employ half-life assessment, combined with usage of genetic knockdown and proteasome inhibition.

## **Long-term directions**

Long-term directions may include examining the extent to which any upstream activator other than ATM, such as ATR, influences UBE4B's induction and interactions with p53. The identification of UBE4B-p53 upstream activators will aid in providing a better understanding of the molecular pathways that control UBE4B and therefore facilitate the prospective invention of novel-targeted therapies for cancer. Furthermore, research can investigate the possible relationship between UBE4B and WIP1 in regulating phosphorylated forms of p53. The rationale behind this suggestion relies on two facts; firstly, WIP1 constitutes an essential component of the well-studied ATM-p53-MDM2 pathway as previously discussed in the introduction. Secondly, the potential role of UBE4B in the negative regulation of phosphorylated p53 via ubiquitination activity along with WIP1 as a major p53 phosphatase justifies further exploration of a possible

relationship between these two negative regulators of p53. In addition, investigations that study the correlation between UBE4B and p53 expression on both genetic and protein levels in additional malignant tissues would assure the potential oncogenic effect of UBE4B and add to the validity of its clinical significance. Finally, the findings in this study showed no sub-G1 population upon cell cycle analysis (Figure 11), indicating that AT LCL cells do not undergo apoptosis in response to DNA damage in early stage. Since p53 constitutes a key regulator of DSB repair and SIPS, these findings require additional investigation to uncover the way in which UBE4B regulation of phosphorylated p53 influences the physiological outcome in response to DNA damage.

# References

- [1] Matlashewski G, Lamb P, Pim D, Peacock J, Crawford L, Benchimol S. Isolation and characterization of a human p53 cDNA clone: expression of the human p53 gene. *EMBO J* 1984;3(13):3257-3262.
- [2] Isobe M, Emanuel BS, Givol D, Oren M, Croce CM. Localization of gene for human p53 tumour antigen to band 17p13. *Nature* 1986;320(6057):84-85.
- [3] May P, May E. Twenty years of p53 research: Structural and functional aspects of the p53 protein. *Oncogene* 1999;18(53):7621-7636.
- [4] Viadiu H. Molecular architecture of tumor suppressor p53. *Curr Top Med Chem* 2008;8(15):1327-1334.
- [5] Olivier M, Eeles R, Hollstein M, Khan MA, Harris CC, Hainaut P. The IARC TP53 database: New online mutation analysis and recommendations to users. *Hum Mutat* 2002;19(6):607-614.
- [6] Cho Y, Gorina S, Jeffrey PD, Pavletich NP. Crystal structure of a p53 tumor suppressor-DNA complex: Understanding tumorigenic mutations. *Science* 1994;265(5170):346-355.
- [7] Strachan, T Read, Andrew P. *Human molecular genetics 2 / Tom Strachan and Andrew P. Read. . 2nd ed ed.: New York : Wiley-Liss; 1999.*
- [8] Bieganski KT, Mello SS, Attardi LD. Unravelling mechanisms of p53-mediated tumour suppression. *Nat Rev Cancer* 2014;14(5):359-370.
- [9] Farrell PJ, Allan GJ, Shanahan F, Vousden KH, Crook T. P53 is frequently mutated in Burkitt's lymphoma cell lines. *EMBO J* 1991;10(10):2879-2888.
- [10] Levine AJ. p53, the cellular gatekeeper for growth and division. *Cell* 1997;88(3):323-331.
- [11] Vogelstein B, Lane D, Levine AJ. Surfing the p53 network. *Nature* 2000;408(6810):307-310.
- [12] Michael D, Oren M. The p53-Mdm2 module and the ubiquitin system. *Semin Cancer Biol* 2003;13(1):49-58.
- [13] Ljungman M. Dial 9-1-1 for p53: Mechanisms of p53 activation by cellular stress. *Neoplasia* 2000;2(3):208-225.
- [14] Meek DW. The p53 response to DNA damage. *DNA Repair* 2004;3(8-9):1049-1056.
- [15] Melchior F, Hengst L. SUMO-1 and p53. *Cell Cycle* 2002;1(4):245-249.

- [16] Maclaine NJ, Hupp TR. The regulation of p53 by phosphorylation: a model for how distinct signals integrate into the p53 pathway. *Aging (Albany NY)* 2009;1(5):490-502.
- [17] Goldstein G., Scheid M., Hammerling U., Schlesinger D.H., Niall H.D., Boyse E.A. Isolation of a polypeptide that has lymphocyte differentiating properties and is probably represented universally in living cells. *Proc Natl Acad Sci U S A* 1975;72(1):11-15.
- [18] Pickart CM. Mechanisms underlying ubiquitination. *Annu Rev Biochem* 2001;70:503-533.
- [19] Hershko A., Heller H., Elias S., Ciechanover A. Components of ubiquitin-protein ligase system. Resolution, affinity purification, and role in protein breakdown. *J Biol Chem* 1983;258(13):8206-8214.
- [20] Hicke L, Schubert HL, Hill CP. Ubiquitin-binding domains. *Nat Rev Mol Cell Biol* 2005;6(8):610-621.
- [21] Grabbe C, Dikic I. Functional roles of ubiquitin-like domain (ULD) and ubiquitin-binding domain (UBD) containing proteins. *Chem Rev* 2009;109(4):1481-1494.
- [22] Hatakeyama S, Yada M, Matsumoto M, Ishida N, Nakayama K-. U Box Proteins as a New Family of Ubiquitin-Protein Ligases. *J Biol Chem* 2001;276(35):33111-33120.
- [23] Koegl M, Hoppe T, Schlenker S, Ulrich HD, Mayer TU, Jentsch S. A novel ubiquitination factor, E4, is involved in multiubiquitin chain assembly. *Cell* 1999;96(5):635-644.
- [24] Berndsen CE, Wolberger C. New insights into ubiquitin E3 ligase mechanism. *Nat Struct Mol Biol* 2014;21(4):301-307.
- [25] Dikic I, Robertson M. Ubiquitin ligases and beyond. *BMC Biol* 2012;10.
- [26] Wenzel DM, Klevit RE. Following Ariadne's thread: A new perspective on RBR ubiquitin ligases. *BMC Biol* 2012;10.
- [27] Jain A.K., Barton M.C. Making sense of ubiquitin ligases that regulate p53. *Cancer Biol Ther* 2010;10(7):665-672.
- [28] Lee J.T., Gu W. The multiple levels of regulation by p53 ubiquitination. *Cell Death Differ* 2010;17(1):86-92.
- [29] Lane DP. p53 from pathway to therapy. *Carcinogenesis* 2004;25(7):1077-1081.
- [30] Tang J, Qu L-, Zhang J, Wang W, Michaelson JS, Degenhardt YY, et al. Critical role for Daxx in regulating Mdm2. *Nature Cell Biol* 2006;8(8):855-862.
- [31] Zhang Y, Xiong Y. Mutations in human ARF exon 2 disrupt its nucleolar localization and impair its ability to block nuclear export of MDM2 and p53. *Mol Cell* 1999;3(5):579-591.
- [32] Weber JD, Taylor LJ, Roussel MF, Sherr CJ, Bar-Sagi D. Nucleolar Arf sequesters Mdm2 and activates p53. *Nature Cell Biol* 1999;1(1):20-26.

- [33] De Oca Luna RM, Wagner DS, Lozano G. Rescue of early embryonic lethality in mdm2-deficient mice by deletion of p53. *Nature* 1995;378(6553):203-206.
- [34] Jones SN, Roe AE, Donehower LA, Bradley A. Rescue of embryonic lethality in Mdm2-deficient mice by absence of p53. *Nature* 1995;378(6553):206-208.
- [35] Haupt Y, Maya R, Kazaz A, Oren M. Mdm2 promotes the rapid degradation of p53. *Nature* 1997;387(6630):296-299.
- [36] Kubbutat MHG, Jones SN, Vousden KH. Regulation of p53 stability by Mdm2. *Nature* 1997;387(6630):299-303.
- [37] Thrower JS, Hoffman L, Rechsteiner M, Pickart CM. Recognition of the polyubiquitin proteolytic signal. *EMBO J* 2000;19(1):94-102.
- [38] Lai Z, Ferry KV, Diamond MA, Wee KE, Kim YB, Ma J, et al. Human mdm2 Mediates Multiple Mono-ubiquitination of p53 by a Mechanism Requiring Enzyme Isomerization. *J Biol Chem* 2001;276(33):31357-31367.
- [39] Li M, Brooks CL, Wu-Baer F, Chen D, Baer R, Gu W. Mono- Versus Polyubiquitination: Differential Control of p53 Fate by Mdm2. *Science* 2003;302(5652):1972-1975.
- [40] Grossman SR, Deato ME, Brignone C, Chan HM, Kung AL, Tagami H, et al. Polyubiquitination of p53 by a ubiquitin ligase activity of p300. *Science* 2003;300(5617):342-344.
- [41] Sui G, Affar EB, Shi Y, Brignone C, Wall NR, Yin P, et al. Yin Yang 1 is a negative regulator of p53. *Cell* 2004;117(7):859-872.
- [42] Higashitsuji H, Higashitsuji H, Itoh K, Sakurai T, Nagao T, Sumitomo H, et al. The oncoprotein gankyrin binds to MDM2/HDM2, enhancing ubiquitylation and degradation of p53. *Cancer Cell* 2005;8(1):75-87.
- [43] Wang C, Ivanov A, Chen L, Fredericks WJ, Seto E, Rauscher III FJ, et al. MDM2 interaction with nuclear corepressor KAP1 contributes to p53 inactivation. *EMBO J* 2005;24(18):3279-3290.
- [44] Du W, Jiang P, Li N, Mei Y, Wang X, Wen L, et al. Suppression of p53 activity by Siva1. *Cell Death Differ* 2009;16(11):1493-1504.
- [45] Nie L, Sasaki M, Maki CG. Regulation of p53 nuclear export through sequential changes in conformation and ubiquitination. *J Biol Chem* 2007;282(19):14616-14625.
- [46] Leng RP, Lin Y, Ma W, Wu H, Lemmers B, Chung S, et al. Pirh2, a p53-Induced Ubiquitin-Protein Ligase, Promotes p53 Degradation. *Cell* 2003 3/21;112(6):779-791.
- [47] Dornan D., Wertz I., Shimizu H., Arnott D., Frantz G.D., Dowd P., et al. The ubiquitin ligase COP1 is a critical negative regulator of p53. *Nature* 2004;429(6987):86-92.

- [48] Leng P, Brown DR, Shivakumar CV, Deb S, Deb SP. N-terminal 130 amino acids of MDM2 are sufficient to inhibit p53-mediated transcriptional activation. *Oncogene* 1995;10(7):1275-1282.
- [49] Oliner JD, Pietenpol JA, Thiagalingam S, Gyuris J, Kinzler KW, Vogelstein B. Oncoprotein MDM2 conceals the activation domain of tumour suppressor p53. *Nature* 1993;362(6423):857-860.
- [50] Momand J, Zambetti GP, Olson DC, George D, Levine AJ. The mdm-2 oncogene product forms a complex with the p53 protein and inhibits p53-mediated transactivation. *Cell* 1992;69(7):1237-1245.
- [51] Zhang Z, Wang H, Li M, Agrawal S, Chen X, Zhang R. MDM2 Is a Negative Regulator of p21WAF1/CIP1, Independent of p53. *J Biol Chem* 2004;279(16):16000-16006.
- [52] Bode AM, Dong Z. Post-translational modification of p53 in tumorigenesis. *Nat Rev Cancer* 2004;4(10):793-805.
- [53] Siliciano JD, Canman CE, Taya Y, Sakaguchi K, Appella E, Kastan MB. DNA damage induces phosphorylation of the amino terminus of p53. *Genes Dev* 1997 Dec 15;11(24):3471-3481.
- [54] Banin S, Moyal L, Shieh S-, Taya Y, Anderson CW, Chessa L, et al. Enhanced phosphorylation of p53 by ATM in response to DNA damage. *Science* 1998;281(5383):1674-1677.
- [55] Khanna KK, Keating KE, Kozlov S, Scott S, Gatei M, Hobson K, et al. ATM associates with and phosphorylates p53: Mapping the region of interaction. *Nat Genet* 1998;20(4):398-400.
- [56] Tibbetts RS, Brumbaugh KM, Williams JM, Sarkaria JN, Cliby WA, Shieh S-, et al. A role for ATR in the DNA damage-induced phosphorylation of p53. *Genes Dev* 1999;13(2):152-157.
- [57] Appella E, Anderson CW. Post-translational modifications and activation of p53 by genotoxic stresses. *Eur J Biochem* 2001;268(10):2764-2772.
- [58] Shieh S-, Ikeda M, Taya Y, Prives C. DNA damage-induced phosphorylation of p53 alleviates inhibition by MDM2. *Cell* 1997;91(3):325-334.
- [59] Shieh S-, Ahn J, Tamai K, Taya Y, Prives C. The human homologs of checkpoint kinases Chk1 and Cds1 (Chk2) phosphorylate, p53 at multiple DNA damage-inducible sites. *Genes Dev* 2000;14(3):289-300.
- [60] Paul Hasty, Barbara A. Christy. p53 as intervention target for cancer and aging. *Pathology of Aging and Age-related Diseases* 2013;3:22702.
- [61] Maya R, Balass M, Kim S-, Shkedy D, Martinez Leal J-, Shifman O, et al. ATM-dependent phosphorylation of Mdm2 on serine 395: Role in p53 activation by DNA damage. *Genes Dev* 2001;15(9):1067-1077.

- [62] Takekawa M, Adachi M, Nakahata A, Nakayama I, Itoh F, Tsukuda H, et al. p53-inducible Wip1 phosphatase mediates a negative feedback regulation of p38 MAPK-p53 signaling in response to UV radiation. *EMBO J* 2000;19(23):6517-6526.
- [63] Vogt Sionov R, Haupt Y. The cellular response to p53: The decision between life and death. *Oncogene* 1999;18(45):6145-6157.
- [64] Chao C, Hergenahn M, Kaeser MD, Wu Z, Saito S, Iggo R, et al. Cell Type- and Promoter-specific Roles of Ser18 Phosphorylation in Regulating p53 Responses. *J Biol Chem* 2003;278(42):41028-41033.
- [65] Sluss HK, Armata H, Gallant J, Jones SN. Phosphorylation of Serine 18 Regulates Distinct p53 Functions in Mice. *Mol Cell Biol* 2004;24(3):976-984.
- [66] MacPherson D, Kim J, Kim T, Rhee BK, Van Oostrom CTM, DiTullio Jr. RA, et al. Defective apoptosis and B-cell lymphomas in mice with p53 point mutation at Ser 23. *EMBO J* 2004;23(18):3689-3699.
- [67] Chao C, Herr D, Chun J, Xu Y. Ser18 and 23 phosphorylation is required for p53-dependent apoptosis and tumor suppression. *EMBO J* 2006;25(11):2615-2622.
- [68] Blattner C, Tobiasch E, Litfen M, Rahmsdorf HJ, Herrlich P. DNA damage induced p53 stabilization: No indication for an involvement of p53 phosphorylation. *Oncogene* 1999;18(9):1723-1732.
- [69] Ashcroft M, Kubbutat MHG, Vousden KH. Regulation of p53 function and stability by phosphorylation. *Mol Cell Biol* 1999;19(3):1751-1758.
- [70] Wu Z, Earle J, Saito S, Anderson CW, Appella E, Xu Y. Mutation of mouse p53 Ser23 and the response to DNA damage. *Mol Cell Biol* 2002;22(8):2441-2449.
- [71] Ashcroft M, Taya Y, Vousden KH. Stress signals utilize multiple pathways to stabilize p53. *Mol Cell Biol* 2000;20(9):3224-3233.
- [72] Dumaz N, Meek DW. Serine 15 phosphorylation stimulates p53 transactivation but does not directly influence interaction with HDM2. *EMBO J* 1999;18(24):7002-7010.
- [73] Saito S, Goodarzi AA, Higashimoto Y, Noda Y, Lees-Miller SP, Appella E, et al. ATM mediates phosphorylation at multiple p53 sites, including Ser(46), in response to ionizing radiation. *J Biol Chem* 2002 Apr 12;277(15):12491-12494.
- [74] Nag A, Germaniuk-Kurowska A, Dimri M, Sassack MA, Gurumurthy CB, Gao Q, et al. An essential role of human Ada3 in p53 acetylation. *J Biol Chem* 2007;282(12):8812-8820.
- [75] Li M, Luo J, Brooks CL, Gu W. Acetylation of p53 inhibits its ubiquitination by Mdm2. *J Biol Chem* 2002;277(52):50607-50611.
- [76] Hoppe T. Multiubiquitylation by E4 enzymes: 'One size' doesn't fit all. *Trends Biochem Sci* 2005;30(4):183-187.

- [77] Pukatzki S, Tordilla N, Franke J, Kessin RH. A novel component involved in ubiquitination is required for development of *Dictyostelium discoideum*. *J Biol Chem* 1998;273(37):24131-24138.
- [78] Wu H, Leng RP. UBE4B, a ubiquitin chain assembly factor, is required for MDM2-mediated p53 polyubiquitination and degradation. *Cell Cycle* 2011;10(12):1912-1915.
- [79] Matsumoto M, Yada M, Hatakeyama S, Ishimoto H, Tanimura T, Tsuji S, et al. Molecular clearance of ataxin-3 is regulated by a mammalian E4. *EMBO J* 2004;23(3):659-669.
- [80] Okumura F, Hatakeyama S, Matsumoto M, Kamura T, Nakayama KI. Functional regulation of FEZ1 by the U-box-type ubiquitin ligase E4B contributes to neuritogenesis. *J Biol Chem* 2004;279(51):53533-53543.
- [81] Hosoda M, Ozaki T, Miyazaki K, Hayashi S, Furuya K, Watanabe K-, et al. UFD2a mediates the proteasomal turnover of p73 without promoting p73 ubiquitination. *Oncogene* 2005;24(48):7156-7169.
- [82] Kaneko-Oshikawa C, Nakagawa T, Yamada M, Yoshikawa H, Matsumoto M, Yada M, et al. Mammalian E4 is required for cardiac development and maintenance of the nervous system. *Mol Cell Biol* 2005;25(24):10953-10964.
- [83] Avantaggiati ML, Ogryzko V, Gardner K, Giordano A, Levine AS, Kelly K. Recruitment of p300/CBP in p53-dependent signal pathways. *Cell* 1997;89(7):1175-1184.
- [84] Shi D, Pop MS, Kulikov R, Love IM, Kung A, Grossman SR. CBP and p300 are cytoplasmic E4 polyubiquitin ligases for p53. *Proc Natl Acad Sci U S A* 2009;106(38):16275-16280.
- [85] Esser C, Scheffner M, Höhfeld J. The chaperone-associated ubiquitin ligase CHIP is able to target p53 for proteasomal degradation. *J Biol Chem* 2005;280(29):27443-27448.
- [86] Wu H, Pomeroy SL, Ferreira M, Teider N, Mariani J, Nakayama KI, et al. UBE4B promotes Hdm2-mediated degradation of the tumor suppressor p53. *Nat Med* 2011;17(3):347-355.
- [87] Zhang X-, Liu F, Wang W. Two-phase dynamics of p53 in the DNA damage response. *Proc Natl Acad Sci U S A* 2011;108(22):8990-8995.
- [88] Lahav G, Rosenfeld N, Sigal A, Geva-Zatorsky N, Levine AJ, Elowitz MB, et al. Dynamics of the p53-Mdm2 feedback loop in individual cells. *Nat Genet* 2004;36(2):147-150.
- [89] Batchelor E, Mock CS, Bhan I, Loewer A, Lahav G. Recurrent Initiation: A Mechanism for Triggering p53 Pulses in Response to DNA Damage. *Mol Cell* 2008;30(3):277-289.
- [90] Purvis JE, Karhohs KW, Mock C, Batchelor E, Loewer A, Lahav G. p53 dynamics control cell fate. *Science* 2012;336(6087):1440-1444.
- [91] Geva-Zatorsky N, Rosenfeld N, Itzkovitz S, Milo R, Sigal A, Dekel E, et al. Oscillations and variability in the p53 system. *Mol Syst Biol* 2006;2.

- [92] Adams KE, Medhurst AL, Dart DA, Lakin ND. Recruitment of ATR to sites of ionising radiation-induced DNA damage requires ATM and components of the MRN protein complex. *Oncogene* 2006;25(28):3894-3904.
- [93] Lowe J, Cha H, Lee M-, Mazur SJ, Appella E, Fornace AJ. Regulation of the wip1 phosphatase and its effects on the stress response. *Front Biosci* 2012;17(4):1480-1498.
- [94] Fiscella M, Zhang H, Fan S, Sakaguchi K, Shen S, Mercer WE, et al. Wip1, a novel human protein phosphatase that is induced in response to ionizing radiation in a p53-dependent manner. *Proc Natl Acad Sci U S A* 1997;94(12):6048-6053.
- [95] Lowe J, Cha H, Lee M-, Mazur SJ, Appella E, Fornace AJ. Regulation of the wip1 phosphatase and its effects on the stress response. *Front Biosci* 2012;17(4):1480-1498.
- [96] Rossi M, Demidov ON, Anderson CW, Appella E, Mazur SJ. Induction of PPM1D following DNA-damaging treatments through a conserved p53 response element coincides with a shift in the use of transcription initiation sites. *Nucleic Acids Res* 2008;36(22):7168-7180.
- [97] Song J-, Han H-, Sabapathy K, Lee B-, Yu E, Choi J. Expression of a homeostatic regulator, Wip1 (wild-type p53-induced phosphatase), is temporally induced by c-Jun and p53 in response to UV irradiation. *J Biol Chem* 2010;285(12):9067-9076.
- [98] Hershko T, Korotayev K, Polager S, Ginsberg D. E2F1 modulates p38 MAPK phosphorylation via transcriptional regulation of ASK1 and Wip1. *J Biol Chem* 2006;281(42):31309-31316.
- [99] Lu X, Nannenga B, Donehower LA. PPM1D dephosphorylates Chk1 and p53 and abrogates cell cycle checkpoints. *Genes Dev* 2005;19(10):1162-1174.
- [100] Takekawa M, Adachi M, Nakahata A, Nakayama I, Itoh F, Tsukuda H, et al. p53-inducible Wip1 phosphatase mediates a negative feedback regulation of p38 MAPK-p53 signaling in response to UV radiation. *EMBO J* 2000;19(23):6517-6526.
- [101] Fujimoto H, Onishi N, Kato N, Takekawa M, Xu XZ, Kosugi A, et al. Regulation of the antioncogenic Chk2 kinase by the oncogenic Wip1 phosphatase. *Cell Death Differ* 2006;13(7):1170-1180.
- [102] Shreeram S, Demidov ON, Hee WK, Yamaguchi H, Onishi N, Kek C, et al. Wip1 Phosphatase Modulates ATM-Dependent Signaling Pathways. *Mol Cell* 2006;23(5):757-764.
- [103] Lu X, Ma O, Nguyen T-, Jones SN, Oren M, Donehower LA. The Wip1 Phosphatase Acts as a Gatekeeper in the p53-Mdm2 Autoregulatory Loop. *Cancer Cell* 2007;12(4):342-354.
- [104] Wani MA, Wani G, Yao J, Zhu Q, Wani AA. Human cells deficient in p53 regulated p21waf1/cip1 expression exhibit normal nucleotide excision repair of UV-induced DNA damage. *Carcinogenesis* 2002;23(3):403-410.
- [105] Fang S, Jensen JP, Ludwig RL, Vousden KH, Weissman AM. Mdm2 is a RING finger-dependent ubiquitin protein ligase for itself and p53. *J Biol Chem* 2000;275(12):8945-8951.

- [106] Javelaud D, Besançon F. Inactivation of p21WAF1 sensitizes cells to apoptosis via an increase of both p14ARF and p53 levels and an alteration of the Bax/Bcl-2 ratio. *J Biol Chem* 2002;277(40):37949-37954.
- [107] Broude EV, Demidenko ZN, Vivo C, Swift ME, Davis BM, Blagosklonny MV, et al. p21 (CDKN1A) is a negative regulator of p53 stability. *Cell Cycle* 2007;6(12):1468-1471.
- [108] Levine AJ, Hu W, Feng Z. The P53 pathway: What questions remain to be explored? *Cell Death Differ* 2006;13(6):1027-1036.
- [109] Abbas T, Dutta A. P21 in cancer: Intricate networks and multiple activities. *Nat Rev Cancer* 2009;9(6):400-414.
- [110] Mirzayans R, Andrais B, Scott A, Murray D. New insights into p53 signaling and cancer cell response to DNA damage: Implications for cancer therapy. *J Biomed Biotechnol* 2012;2012.
- [111] Warfel NA, El-Deiry WS. P21WAF1 and tumorigenesis: 20 Years after. *Curr Opin Oncol* 2013;25(1):52-58.
- [112] Löhr K, Möritz C, Contente A, Dobbstein M. p21/CDKN1A mediates negative regulation of transcription by p53. *J Biol Chem* 2003;278(35):32507-32516.
- [113] Helton ES, Chen X. p53 modulation of the DNA damage response. *J Cell Biochem* 2007;100(4):883-896.
- [114] Sengupta S, Harris CC. p53: Traffic cop at the crossroads of DNA repair and recombination. *Nat Rev Mol Cell Biol* 2005;6(1):44-55.
- [115] Shiloh Y. ATM and related protein kinases: Safeguarding genome integrity. *Nat Rev Cancer* 2003;3(3):155-168.
- [116] Zhou B-S, Elledge SJ. The DNA damage response: Putting checkpoints in perspective. *Nature* 2000;408(6811):433-439.
- [117] Kastan MB, Onyekwere O, Sidransky D, Vogelstein B, Craig RW. Participation of p53 protein in the cellular response to DNA damage. *Cancer Res* 1991;51(23):6304-6311.
- [118] Kuerbitz SJ, Plunkett BS, Walsh WV, Kastan MB. Wild-type p53 is a cell cycle checkpoint determinant following irradiation. *Proc Natl Acad Sci U S A* 1992;89(16):7491-7495.
- [119] Slichenmyer WJ, Nelson WG, Slebos RJ, Kastan MB. Loss of a p53-associated G1 checkpoint does not decrease cell survival following DNA damage. *Cancer Res* 1993;53(18):4164-4168.
- [120] Enoch T, Norbury C. Cellular responses to DNA damage: Cell-cycle checkpoints, apoptosis and the roles of p53 and ATM. *Trends Biochem Sci* 1995;20(10):426-430.
- [121] Meyn MS. Ataxia-telangiectasia and cellular responses to DNA damage. *Cancer Res* 1995;55(24):5991-6001.

- [122] Yan H, McCane J, Toczylowski T, Chen C. Analysis of the Xenopus Werner syndrome protein in DNA double-strand break repair. *J Cell Biol* 2005;171(2):217-227.
- [123] Burma S, Chen DJ. Role of DNA-PK in the cellular response to DNA double-strand breaks. *DNA Repair* 2004;3(8-9):909-918.
- [124] Pang LY, Scott M, Hayward RL, Mohammed H, Whitelaw CBA, Smith GCM, et al. P21 WAF1 is component of a positive feedback loop that maintains the p53 transcriptional program. *Cell Cycle* 2011;10(6):932-950.
- [125] Crescenzi E, Palumbo G, De Boer J, Brady HJM. Ataxia telangiectasia mutated and p21CIP1 modulate cell survival of drug-induced senescent tumor cells: Implications for chemotherapy. *Clin Cancer Res* 2008;14(6):1877-1887.
- [126] Mirzayans R, Andrais B, Scott A, Wang YW, Murray D. Ionizing radiation-induced responses in human cells with differing TP53 status. *Int J Mol Sci* 2013;14(11):22409-22435.
- [127] Johnson ES, Ma PCM, Ota IM, Varshavsky A. A proteolytic pathway that recognizes ubiquitin as a degradation signal. *J Biol Chem* 1995;270(29):17442-17456.
- [128] Xinna Z, Lin L, Huarong G, Jianhua Y, Jones SN, Jochemsen A, et al. Phosphorylation and degradation of MdmX is inhibited by Wip1 phosphatase in the DNA damage response. *Cancer Res* 2009;69(20):7960-7968.
- [129] Lu X, Nguyen T-, Moon S-, Darlington Y, Sommer M, Donehower LA. The type 2C phosphatase Wip1: An oncogenic regulator of tumor suppressor and DNA damage response pathways. *Cancer Metastasis Rev* 2008;27(2):123-135.
- [130] Bulavin DV, Demidov ON, Saito S, Kauraniemi P, Phillips C, Amundson SA, et al. Amplification of PPM1D in human tumors abrogates p53 tumor-suppressor activity. *Nat Genet* 2002;31(2):210-215.
- [131] Li J, Yang Y, Peng Y, Austin RJ, Van Eyndhoven WG, Nguyen KCQ, et al. Oncogenic properties of PPM1D located within a breast cancer amplification epicenter at 17q23. *Nat Genet* 2002;31(2):133-134.
- [132] Saito-Ohara F, Imoto I, Inoue J, Hosoi H, Nakagawara A, Sugimoto T, et al. PPM1D is a potential target for 17q gain in neuroblastoma. *Cancer Res* 2003;63(8):1876-1883.
- [133] Suzuki HI, Yamagata K, Sugimoto K, Iwamoto T, Kato S, Miyazono K. Modulation of microRNA processing by p53. *Nature* 2009;460(7254):529-533.
- [134] Zhang X, Wan G, Mlotshwa S, Vance V, Berger FG, Chen H, et al. Oncogenic Wip1 phosphatase is inhibited by miR-16 in the DNA damage signaling pathway. *Cancer Res* 2010;70(18):7176-7186.
- [135] Shreeram S, Weng KH, Demidov ON, Kek C, Yamaguchi H, Fornace Jr. AJ, et al. Regulation of ATM/p53-dependent suppression of myc-induced lymphomas by Wip1 phosphatase. *J Exp Med* 2006;203(13):2793-2799.

- [136] Bulavin DV, Phillips C, Nannenga B, Timofeev O, Donehower LA, Anderson CW, et al. Inactivation of the Wip1 phosphatase inhibits mammary tumorigenesis through p38 MAPK-mediated activation of the p16Ink4a-p19 Arf pathway. *Nat Genet* 2004;36(4):343-350.
- [137] Demidov ON, Kek C, Shreeram S, Timofeev O, Fornace AJ, Appella E, et al. The role of the MKK6/p38 MAPK pathway in Wip1-dependent regulation of ErbB2-driven mammary gland tumorigenesis. *Oncogene* 2007;26(17):2502-2506.
- [138] Cittelly DM, Das PM, Salvo VA, Fonseca JP, Burow ME, Jones FE. Oncogenic HER2 $\Delta$ 16 suppresses miR-15a/16 and deregulates BCL-2 to promote endocrine resistance of breast tumors. *Carcinogenesis* 2010;31(12):2049-2057.
- [139] Gatt ME, Zhao JJ, Ebert MS, Zhang Y, Chu Z, Mani M, et al. MicroRNAs 15a/16-1 function as tumor suppressor genes in multiple myeloma (Blood DOI:10.1182/blood-2009-11-253294). *Blood* 2011;117(26):7186.
- [140] Roos WP, Kaina B. DNA damage-induced cell death by apoptosis. *Trends Mol Med* 2006;12(9):440-450.
- [141] Yoda A, Xiao ZX, Onishi N, Toyoshima K, Fujimoto H, Kato N, et al. Intrinsic kinase activity and SQ/TQ domain of Chk2 kinase as well as N-terminal domain of Wip1 phosphatase are required for regulation of Chk2 by Wip1. *J Biol Chem* 2006;281(34):24847-24862.
- [142] Kong W, Jiang X, Mercer WE. Downregulation of Wip-1 phosphatase expression in MCF-7 breast cancer cells enhances doxorubicin-induced apoptosis through p53-mediated transcriptional activation of Bax. *Cancer Biol Ther* 2009;8(6):555-563.
- [143] Pärssinen J, Alarmo E-, Karhu R, Kallioniemi A. PPM1D silencing by RNA interference inhibits proliferation and induces apoptosis in breast cancer cell lines with wild-type p53. *Cancer Genet Cytogenet* 2008;182(1):33-39.
- [144] Gartel A.L., Tyner A.L. The role of the cyclin-dependent kinase inhibitor p21 in apoptosis. *Mol Cancer Ther* 2002;1(8):639-649.
- [145] Weiss R.H. p21Waf1/Cip1 as a therapeutic target in breast and other cancers. *Cancer Cell* 2003;4(6):425-429.
- [146] Sohn D., Essmann F., Schulze-Osthoff K., Jänicke R.U. p21 blocks irradiation-induced apoptosis downstream of mitochondria by inhibition of cyclin-dependent kinase-mediated caspase-9 activation. *Cancer Res* 2006;66(23):11254-11262.
- [147] Roninson I.B. Oncogenic functions of tumour suppressor p21Waf1/Cip1/Sdi1: Association with cell senescence and tumour-promoting activities of stromal fibroblasts. *Cancer Lett* 2002;179(1):1-14.
- [148] Dotto G.P. p21(WAF1/Cip1): More than a break to the cell cycle? *Biochim Biophys Acta Rev Cancer* 2000;1471(1):M43-M56.

- [149] Sabin R.J., Anderson R.M. Cellular Senescence - its role in cancer and the response to ionizing radiation. *Genome Integrity* 2011;2.
- [150] Roninson I.B. Tumor cell senescence in cancer treatment. *Cancer Res* 2003;63(11):2705-2715.
- [151] Chang B.-D., Watanabe K., Broude E.V., Fang J., Poole J.C., Kalinichenko T.V., et al. Effects of p21(Waf1/Cip1/Sdi1) on cellular gene expression: Implications for carcinogenesis, senescence, and age-related diseases. *Proc Natl Acad Sci U S A* 2000;97(8):4291-4296.
- [152] Razmik Mirzayans, Bonnie Andrais, April Scott, Ying W. Wang, Robert H. Weiss and David Murray. Spontaneous  $\gamma$ H2AX Foci in Human Solid Tumor-Derived Cell Lines in Relation to p21WAF1 and WIP1 Expression. *Int J Mol Sci* 2015;16:11609-11628.
- [153] Lee C-, Wu S-, Hong C-, Yu H-, Wei Y-. Molecular mechanisms of UV-induced apoptosis and its effects on skin residential cells: The implication in UV-based phototherapy. *Int J Mol Sci* 2013;14(3):6414-6435.
- [154] Harms KL, Chen X. The functional domains in p53 family proteins exhibit both common and distinct properties. *Cell Death Differ* 2006;13(6):890-897.
- [155] Lavin MF. Ataxia-telangiectasia: from a rare disorder to a paradigm for cell signalling and cancer. *Nat Rev Mol Cell Biol* 2008 Oct;9(10):759-769.
- [156] Lu X, Lane DP. Differential induction of transcriptionally active p53 following UV or ionizing radiation: defects in chromosome instability syndromes?. *Cell* 1993 Nov 19;75(4):765-778.
- [157] Khanna KK, Lavin MF. Ionizing radiation and UV induction of p53 protein by different pathways in ataxia-telangiectasia cells. *Oncogene* 1993 Dec;8(12):3307-3312.
- [158] Enns L, Barley RDC, Paterson MC, Mirzayans R. Radiosensitivity in ataxia telangiectasia fibroblasts is not associated with deregulated apoptosis. *Radiat Res* 1998;150(1):11-16.
- [159] Mirzayans R, Famulski KS, Enns L, Fraser M, Paterson MC. Characterization of the signal transduction pathway mediating  $\gamma$  ray-induced inhibition of DNA synthesis in human cells: Indirect evidence for involvement of calmodulin but not protein kinase C nor p53. *Oncogene* 1995;11(8):1597-1605.
- [160] Mirzayans R, Andrais B, Scott A, Paterson MC, Murray D. Single-cell analysis of p16 INK4a and p21 WAF1 expression suggests distinct mechanisms of senescence in normal human and Li-Fraumeni syndrome fibroblasts. *J Cell Physiol* 2010;223(1):57-67.
- [161] Ali SH, DeCaprio JA. Cellular transformation by SV40 large T antigen: Interaction with host proteins. *Semin Cancer Biol* 2001;11(1):15-22.
- [162] O'Nions J, Turner A, Craig R, Allday MJ. Epstein-Barr virus selectively deregulates DNA damage responses in normal B cells but has no detectable effect on regulation of the tumor suppressor p53. *J Virol* 2006;80(24):12408-12413.

- [163] Allday MJ, Sinclair A, Parker G, Crawford DH, Farrell PJ. Epstein-Barr virus efficiently immortalizes human B cells without neutralizing the function of p53. *EMBO J* 1995;14(7):1382-1391.
- [164] Wu H, Leng RP. MDM2 mediates p73 ubiquitination: A new molecular mechanism for suppression of p73 function. *Oncotarget* 2015;6(25):21479-21492.
- [165] Gotoff SP, Amirmokri E, Liebner EJ. Ataxia telangiectasia: Neoplasia, untoward response to x-irradiation, and tuberous sclerosis. *Am J Dis Child* 1967;114(6):617-625.
- [166] Taylor AMR, Harnden DG, Arlett CF, Harcourt SA, Lehmann AR, Stevens S, et al. Ataxia telangiectasia: A human mutation with abnormal radiation sensitivity. *Nature* 1975;258(5534):427-429.
- [167] Chen PC, Lavin MF, Kidson C, Moss D. Identification of ataxia telangiectasia heterozygotes, a cancer prone population [20]. *Nature* 1978;274(5670):484-486.
- [168] Lavin MF, Gueven N, Bottle S, Gatti RA. Current and potential therapeutic strategies for the treatment of ataxia-telangiectasia. *Br Med Bull* 2007;81-82(1):129-147.
- [169] Duchaud E, Ridet A, Stoppa-Lyonnet D, Janin N, Moustacchi E, Rosselli F. Deregulated apoptosis in ataxia telangiectasia: Association with clinical stigmata and radiosensitivity. *CANCER RES* 1996;56(6):1400-1404.
- [170] Price BD, Park SJ. DNA damage increases the levels of MDM2 messenger RNA in wtp53 human cells. *Cancer Res* 1994;54(4):896-899.
- [171] Kapoor M, Lozano G. Functional activation of p53 via phosphorylation following DNA damage by UV but not  $\gamma$  radiation. *Proc Natl Acad Sci U S A* 1998;95(6):2834-2837.
- [172] Saito S, Yamaguchi H, Higashimoto Y, Chao C, Xu Y, Fornace Jr. AJ, et al. Phosphorylation site interdependence of human p53 post-translational modifications in response to stress. *J Biol Chem* 2003;278(39):37536-37544.
- [173] Saito S, Goodarzi AA, Higashimoto Y, Noda Y, Lees-Miller SP, Appella E, et al. ATM mediates phosphorylation at multiple p53 sites, including Ser46, in response to ionizing radiation. *J Biol Chem* 2002;277(15):12491-12494.
- [174] Boehme KA, Kulikov R, Blattner C. p53 stabilization in response to DNA damage requires Akt/PKB and DNA-PK. *Proc Natl Acad Sci U S A* 2008;105(22):7785-7790.
- [175] Du C, Wu H, Leng RP. UBE4B targets phosphorylated p53 at serines 15 and 392 for degradation. *Oncotarget* 2016;7(3):2823-2836.
- [176] Macaluso M, Montanari M, Marshall CM, Gambone AJ, Tosi GM, Giordano A, et al. Cytoplasmic and nuclear interaction between Rb family proteins and PAI-2: A physiological crosstalk in human corneal and conjunctival epithelial cells. *Cell Death Differ* 2006;13(9):1515-1522.

- [177] Kastan MB, Zhan Q, el-Deiry WS, Carrier F, Jacks T, Walsh WV, et al. A mammalian cell cycle checkpoint pathway utilizing p53 and GADD45 is defective in ataxia-telangiectasia. *Cell* 1992 Nov 13;71(4):587-597.
- [178] Wu H, Leng RP. UBE4B, a ubiquitin chain assembly factor, is required for MDM2-mediated p53 polyubiquitination and degradation. *Cell Cycle* 2011;10(12):1912-1915.
- [179] Wu H, Pomeroy SL, Ferreira M, Teider N, Mariani J, Nakayama KI, et al. UBE4B promotes Mdm2-mediated degradation of the tumor suppressor p53. *Nat Med* 2011;17(3):347-355.
- [180] Gu B, Zhu W-. Surf the Post-translational Modification Network of p53 Regulation. *Int J Biol Sci* 2012;8(5):672-684.
- [181] Lakin ND, Jackson SP. Regulation of p53 in response to DNA damage. *Oncogene* 1999;18(53):7644-7655.
- [182] Wang X, Khadpe J, Hu B, Iliakis G, Wang Y. An overactivated ATR/CHK1 pathway is responsible for the prolonged G2 accumulation in irradiated AT cells. *J Biol Chem* 2003;278(33):30869-30874.
- [183] Daub H, Olsen JV, Bairlein M, Gnad F, Oppermann FS, Körner R, et al. Kinase-Selective Enrichment Enables Quantitative Phosphoproteomics of the Kinome across the Cell Cycle. *Mol Cell* 2008;31(3):438-448.
- [184] Nam EA, Zhao R, Glick GG, Bansbach CE, Friedman DB, Cortez D. Thr-1989 phosphorylation is a marker of active ataxia telangiectasia- mutated and Rad3-related (ATR) kinase. *J Biol Chem* 2011;286(33):28707-28714.
- [185] Sellekom.com for ATR. Available at:  
<http://refworks.scholarsportal.info/refworks2/?groupcode=RWUAlberta>.
- [186] Bode AM, Dong Z. Post-translational modification of p53 in tumorigenesis. *Nat Rev Cancer* 2004;4(10):793-805.
- [187] Harris SL, Levine AJ. The p53 pathway: Positive and negative feedback loops. *Oncogene* 2005;24(17):2899-2908.
- [188] Inuzuka H, Tseng A, Gao D, Zhai B, Zhang Q, Shaik S, et al. Phosphorylation by Casein Kinase I promotes the turnover of the Mdm2 oncoprotein via the SCF $\beta$ -TRCP ubiquitin ligase. *Cancer Cell* 2010;18(2):147-159.
- [189] Gajjar M, Candeias MM, Malbert-Colas L, Mazars A, Fujita J, Olivares-Illana V, et al. The p53 mRNA-Mdm2 interaction controls mdm2 nuclear trafficking and is required for p53 activation following dna damage. *Cancer Cell* 2012;21(1):25-35.
- [190] Itahana K, Mao H, Jin A, Itahana Y, Clegg HV, Lindström MS, et al. Targeted Inactivation of Mdm2 RING Finger E3 Ubiquitin Ligase Activity in the Mouse Reveals Mechanistic Insights into p53 Regulation. *Cancer Cell* 2007;12(4):355-366.

- [191] Zhang Y, Lv Y, Zhang Y, Gao H. Regulation of p53 level by UBE4B in breast cancer. *PLoS ONE* 2014;9(2).
- [192] Zhang X-, Pan Q-, Pan K, Weng D-, Wang Q-, Zhao J-, et al. Expression and prognostic role of ubiquitination factor E4B in primary hepatocellular carcinoma. *Mol Carcinog* 2016;55(1):64-76.
- [193] Yang W, Rozan LM, McDonald ER. 3rd, Navaraj A, Liu JJ, Matthew EM, Wang W, Dicker DT, EL-Deiry WS. CARPs are ubiquitin ligases that promote MDM2 independent p53 and phospho-p53 Ser20 degradation. *J Biol Chem* 2007(282):3273-3281.
- [194] Sato Y, Kamura T, Shirata N, Murata T, Kudoh A, Iwahori S, et al. Degradation of phosphorylated p53 by viral protein-ECS E3 ligase complex. *PLoS Pathog* 2009;5(7).
- [195] Meek DW. Tumour suppression by p53: A role for the DNA damage response? *Nat Rev Cancer* 2009;9(10):714-723.
- [196] Meek DW, Anderson CW. Posttranslational modification of p53: cooperative integrators of function. *Cold Spring Harb Perspect Biol* 2009;1(6).
- [197] Jones RG, Plas DR, Kubek S, Buzzai M, Mu J, Xu Y, et al. AMP-activated protein kinase induces a p53-dependent metabolic checkpoint. *Mol Cell* 2005;18(3):283-293.
- [198] Dumaz N, Meek DW. Serine 15 phosphorylation stimulates p53 transactivation but does not directly influence interaction with HDM2. *EMBO J* 1999;18(24):7002-7010.
- [199] Lambert PF, Kashanchi F, Radonovich MF, Shiekhattar R, Brady JN. Phosphorylation of p53 serine 15 increases interaction with CBP. *J Biol Chem* 1998;273(49):33048-33053.
- [200] Ito A, Kawaguchi Y, Lai C-, Kovacs JJ, Higashimoto Y, Appella E, et al. MDM2-HDAC1-mediated deacetylation of p53 is required for its degradation. *EMBO J* 2002;21(22):6236-6245.
- [201] Sakaguchi K, Herrera JE, Saito S, Miki T, Bustin M, Vassilev A, et al. DNA damage activates p53 through a phosphorylation-acetylation cascade. *Genes Dev* 1998;12(18):2831-2841.
- [202] Dumaz N, Milne DM, Meek DW. Protein kinase CK1 is a p53-threonine 18 kinase which requires prior phosphorylation of serine 15. *FEBS Lett* 1999;463(3):312-316.
- [203] Saito S, Yamaguchi H, Higashimoto Y, Chao C, Xu Y, Fornace Jr. AJ, et al. Phosphorylation site interdependence of human p53 post-translational modifications in response to stress. *J Biol Chem* 2003;278(39):37536-37544.
- [204] Sakaguchi K, Saito S, Higashimoto Y, Roy S, Anderson CW, Appella E. Damage-mediated phosphorylation of human p53 threonine 18 through a cascade mediated by a casein 1-like kinase. Effect on MDM2 binding. *J Biol Chem* 2000;275(13):9278-9283.
- [205] Loughery J, Cox M, Smith LM, Meek DW. Critical role for p53-serine 15 phosphorylation in stimulating transactivation at p53-responsive promoters. *Nucleic Acids Res* 2014;42(12):7666-7680.

- [206] Saito S, Goodarzi AA, Higashimoto Y, Noda Y, Lees-Miller SP, Appella E, et al. ATM mediates phosphorylation at multiple p53 sites, including Ser46, in response to ionizing radiation. *J Biol Chem* 2002;277(15):12491-12494.
- [207] Radhakrishnan SK, Gartel AL. CDK9 phosphorylates p53 on serine residues 33, 315 and 392. *Cell Cycle* 2006;5(5):519-521.
- [208] Keller DM, Zeng X, Wang Y, Zhang QH, Kapoor M, Shu H, et al. A DNA damage-induced p53 serine 392 kinase complex contains CK2, hSpt16, and SSRP1. *Mol Cell* 2001;7(2):283-292.
- [209] Hupp TR, Meek DW, Midgley CA, Lane DP. Regulation of the specific DNA binding function of p53. *Cell* 1992;71(5):875-886.
- [210] Sakaguchi K, Sakamoto H, Lewis MS, Anderson CW, Erickson JW, Appella E, et al. Phosphorylation of serine 392 stabilizes the tetramer formation of tumor suppressor protein p53. *BIOCHEMISTRY* 1997;36(33):10117-10124.
- [211] Milne DM, Palmer RH, Meek DW. Mutation of the casein kinase II phosphorylation site abolishes the anti-proliferative activity of p53. *Nucleic Acids Res* 1992;20(21):5565-5570.
- [212] Bruins W, Zwart E, Attardi LD, Iwakuma T, Hoogervorst EM, Beems RB, et al. Increased sensitivity to UV radiation in mice with a p53 point mutation at Ser389. *Mol Cell Biol* 2004;24(20):8884-8894.
- [213] Hoogervorst EM, Bruins W, Zwart E, Van Oostrom CTM, Van Den Aardweg GJ, Beems RB, et al. Lack of p53 Ser389 phosphorylation predisposes mice to develop 2-acetylaminofluorene-induced bladder tumors but not ionizing radiation-induced lymphomas. *Cancer Res* 2005;65(9):3610-3616.
- [214] Bruins W, Bruning O, Jonker MJ, Zwart E, Van Der Hoeven TV, Pennings JLA, et al. The absence of Ser389 phosphorylation in p53 affects the basal gene expression level of many p53-dependent genes and alters the biphasic response to UV exposure in mouse embryonic fibroblasts. *Mol Cell Biol* 2008;28(6):1974-1987.
- [215] Bruins W, Jonker MJ, Bruning O, Pennings JLA, Schaap MM, Hoogervorst EM, et al. Delayed expression of apoptotic and cell-cycle control genes in carcinogen-exposed bladders of mice lacking p53.S389 phosphorylation. *Carcinogenesis* 2007;28(8):1814-1823.
- [216] Dai C, Gu W. P53 post-translational modification: Deregulated in tumorigenesis. *Trends Mol Med* 2010;16(11):528-536.
- [217] O'Brate A, Giannakakou P. The importance of p53 location: Nuclear or cytoplasmic zip code? *Drug Resist Updates* 2003;6(6):313-322.
- [218] Bosari S, Viale G, Roncalli M, Graziani D, Borsani G, Lee AKC, et al. p53 Gene mutations, p53 protein accumulation and compartmentalization in colorectal adenocarcinoma. *Am J Pathol* 1995;147(3):790-798.

- [219] Moll UM, LaQuaglia M, Benard J, Riou G. Wild-type p53 protein undergoes cytoplasmic sequestration in undifferentiated neuroblastomas but not in differentiated tumors. *Proc Natl Acad Sci U S A* 1995;92(10):4407-4411.
- [220] Schlamp CL, Poulsen GL, Michael Nork T, Nickells RW. Nuclear exclusion of wild-type p53 in immortalized human retinoblastoma cells. *J Natl Cancer Inst* 1997;89(20):1530-1536.
- [221] Sembritzki O, Hagel C, Lamszus K, Deppert W, Bohn W. Cytoplasmic localization of wild-type p53 in glioblastomas correlates with expression of vimentin and glial fibrillary acidic protein. *Neuro-oncology* 2002;4(3):171-178.
- [222] Ueda H, Ullrich SJ, Gangemi JD, Kappel CA, Ngo L, Feitelson MA, et al. Functional inactivation but not structural mutation of p53 causes liver cancer. *Nat Genet* 1995;9(1):41-47.
- [223] Murray-Zmijewski F, Slee EA, Lu X. A complex barcode underlies the heterogeneous response of p53 to stress. *Nat Rev Mol Cell Biol* 2008;9(9):702-712.
- [224] Gretchen S Jimenez, Shireen H Khan, Jayne M Stommel and Geoffrey M Wahl. p53 regulation by post-translational modification and nuclear retention in response to diverse stresses. *Oncogene* 1999(18):7656-7665.
- [225] Roth J, Dobbstein M, Freedman DA, Shenk T, Levine AJ. Nucleo-cytoplasmic shuttling of the hdm2 oncoprotein regulates the levels of the p53 protein via a pathway used by the human immunodeficiency virus rev protein. *EMBO J* 1998;17(2):554-564.
- [226] Freedman DA, Levine AJ. Nuclear export is required for degradation of endogenous p53 by MDM2 and human papillomavirus E6. *Mol Cell Biol* 1998;18(12):7288-7293.
- [227] Tao W, Levine AJ. Nucleocytoplasmic shuttling of oncoprotein Hdm2 is required for Hdm2-mediated degradation of p53. *Proc Natl Acad Sci U S A* 1999;96(6):3077-3080.
- [228] Stommel JM, Marchenko ND, Jimenez GS, Moll UM, Hope TJ, Wahl GM. A leucine-rich nuclear export signal in the p53 tetramerization domain: Regulation of subcellular localization and p53 activity by NES masking. *EMBO J* 1999;18(6):1660-1672.
- [229] Kawai H, Wiederschain D, Yuan Z-. Critical contribution of the MDM2 acidic domain to p53 ubiquitination. *Mol Cell Biol* 2003;23(14):4939-4947.
- [230] Lohrum MAE, Woods DB, Ludwig RL, Bálint E, Vousden KH. C-terminal ubiquitination of p53 contributes to nuclear export. *Mol Cell Biol* 2001;21(24):8521-8532.
- [231] Boyd SD, Tsai KY, Jacks T. An intact HDM2 RING-finger domain is required for nuclear exclusion of p53. *Nature Cell Biol* 2000;2(9):563-568.
- [232] Geyer RK, Yu ZK, Maki CG. The MDM2 RING-finger domain is required to promote p53 nuclear export. *Nature Cell Biol* 2000;2(9):569-573.
- [233] Labome VAD. Available at: <https://www.labome.com/method/Subcellular-Fractionation.html>, 2017.

[234] Drissi R, Dubois M, Boisvert F. Proteomics methods for subcellular proteome analysis. *Febs J* 2013 Nov;280(22):5626-5634.

[235] Stadler C, Rexhepaj E, Singan VR, Murphy RF, Pepperkok R, Uhlen M, et al. Immunofluorescence and fluorescent-protein tagging show high correlation for protein localization in mammalian cells. *Nat Methods* 2013 Apr;10(4):315-323.

[236] Giepmans BNG. Bridging fluorescence microscopy and electron microscopy. *Histochem Cell Biol* 2008 Aug;130(2):211-217.

[237] Ward Y. Fluorescence and Confocal Microscopy. Available at: <https://home.ccr.cancer.gov/Fluorescence> and Confocal Microscopy.ppt.